Protein-Protein Interactions in the Mammalian Heme Degradation Pathway: Heme Oxygenase-2, Cytochrome P450 Reductase and Biliverdin Reductase

by

Andrea L. M. Spencer

A dissertation submitted in partial fulfillment
of the requirements for the degree of
Doctor of Philosophy
(Cellular and Molecular Biology)
in the University of Michigan
2014

Doctoral Committee:

Professor Stephen W. Ragsdale, Chair
Professor Robert S. Fuller
Professor Ursula H. Jakob
Professor Janet L. Smith
Professor Joel A. Swanson

Acknowledgements

I am grateful for the support I received from so many people throughout my graduate studies; members of my lab, thesis committee, the Cellular and Molecular Biology training program, my friends and family.

First, I would especially like to thank my advisor Dr. Stephen Ragsdale for his guidance and mentorship during past five years. His depth of knowledge, encouragement, curiosity and advice were invaluable throughout the development and implementation of my thesis project.

I would also like to thank the past and present members of my thesis committee; Dr. Robert S. Fuller, Dr. Ursula H. Jakob, Dr. Jeffery R. Martens, Dr. Janet L. Smith, and Dr. Joel A. Swanson for providing suggestions, technical advice, and critical evaluation of my work.

The Cellular and Molecular Biology training program provided support and encouragement throughout my time at the University of Michigan, and I would particularly like to thank Dr. Jessica Schwartz, Dr. Robert S. Fuller and Cathy Mitchell for all of their help and hard work and dedication to making CMB a great training program.

I am grateful to past and present members of the Ragsdale lab for their assistance, encouragement and for creating a vibrant and creative research environment. I would particularly like to thank Dr. Eric Carter and Dr. Angela Fleischhacker for many fruitful discussions regarding hemoproteins, Christopher Walters, an undergraduate researcher who assisted with my BVR substrate inhibition studies and Dr. Ireena Bagai, Dr. Gunes Bender, Dr. Mehmet Can, Dr. Joe Darty, Dr. Nirupama Gupta, Dr. Xianghui Li, Dr. Elizabeth Pierce, Dr. Dariusz Sliwa, Dr. Thanyaporn Wongnate, Dr. Yi Li, Dr. Yuzhen Zhou, Heather Aman, Erika Martinez-Nieves, and Katherine Rush.

Over the years I have received assistance and technical support from many others. I would like to thank Dr. Erik Zuiderweg for his expertise and assistance in the NMR binding studies and Dr. Donald Becker (University of Nebraska, Lincoln) for collaboration on the analytical ultracentrifugation studies. I am grateful to Dr. Anne Vojtek, who generously allowed me to conduct my cell culture studies using her tissue culture space and Dr. Holoshitz for permitting me to use the Biacore2000 for SPR experiments.

I have also been fortunate to have the support of my parents and many friends throughout my graduate studies. An extra special thanks goes out to my husband, Collin, who had been unflagging in his support and encouragement.

Table of Contents

List of Figures

List of Tables

List of Abbreviations

ALA: Aminolevininate acid
AP-1: Activator protein
BiFC: Bifluorescent recombination
BR: Bilirubin
BSA:Bovine serum albumin
BV: Biliverdin
BVR: Biliverdin Reductase
CODH: Carbon monoxide dehydrogenase
COPRO III: Coproporphyrinogen III
CPM: 7-Diethylamino-3-(4'-maleimidylphenyl)-4-methylcourmarin
CPR: Cytochrome P450 reductase
DMSO: Dimethyl sulfoxide
EDC: 1-Ethyl-3-[3-dimethylaminopropyl]cabodiimide hydrochloride
EDTA: Ethylenediaminetetraacetic acid
ER: Endoplasmic reticulum
ERK: Extracellular signal-regulated kinase
FAD: Flavin adenine dinucleotide
FMN: Flavin mononucleotide
GFP: Green fluorescent protein
GFPR: Green fluorescent protein reassembly
GST: Glutaghione S-transferase
HEPES: 4-(2-hydroxyethyl)-1-piperazineethanesulfonic acid
HO: Heme oxygenase
HRM: Heme regulatory motif
HSP32: Heat shock protein 32
HSQC: Heteronuclear single quantum coherence
IPTG: isopropyl-β-D-thiogalactopyranoside
LB: Luria broth
LC-SPDP: Succinimidyl 6-(3[2-pyridyldithio]-propionamido)hexanoate
LIC: Ligation independent cloning
MAPK: Mitogen-activated protein kinase
NADH: Nicotinamide adenine dinucleotide
NADPH: Nicotinamide adenine dinucleotide phosphate
NHS: N-hydroxysuccinimide
NMR: Nuclear magnetic resonance
Nrf2: Nuclear factor (erythroid-derived 2)-like 2

NTA: Ni-nitrilotriacetic acid
PBS: Phosphate buffered saline
PCR: Polymerase chain reaction
SDS PAGE: Sodium dodecyl sulfate polyacrylamide gel electrophoresis
SPR: Surface plasmon resonance
STAT: Signal transducer and activation of transcription binding sites
TEV: Tobacco etch virus
TROSY: Transverse relaxation-optimized spectroscopy

Abstract

Protein-Protein Interactions in the Mammalian Heme Degradation Pathway: Heme Oxygenase-2, Cytochrome P450 Reductase and Biliverdin Reductase

by

Andrea L. M. Spencer

Chair: Stephen W. Ragsdale

Heme oxygenase (HO) catalyzes the rate-limiting step in the degradation of heme to biliverdin, CO and Fe, and requires electrons delivered from NADPH via cytochrome P450 reductase (CPR). Biliverdin reductase (BVR) then catalyzes conversion of biliverdin to bilirubin. The HO pathway is important for many cellular processes, including the maintenance of heme levels below toxic concentrations, iron homeostasis, carbon monoxide production, and antioxidant protection. Understanding protein-protein interactions of the heme degradation pathway will provide insight into potential regulatory mechanisms for the pathway. While the more well-studied HO isoform, HO-1, is reported to form complexes with CPR and BVR, little is known regarding the ability of HO-2 to bind either protein.

In this thesis I describe various *in vitro* studies aimed at evaluating interactions of soluble HO-2 with CPR and BVR. The ^{1}H-^{15}N TROSY NMR spectrum of HO-2 reveals specific residues, including L201, near the heme face of HO-2 that are affected by the addition of CPR, implicating this residue at the HO/CPR interface. Alanine substitutions at HO-2 residues L201 and K169 cause a respective 3- and 22-fold increase in K_m for CPR, consistent with a role for these residues in CPR binding. Sedimentation velocity experiments confirm the transient nature of the HO-2/CPR complex (K_d = 15.1 μM). Our results also indicate that HO-2 and BVR form a very weak complex that is only observed by cross-linking. Fluorescence quenching experiments suggest that the

previously reported high affinity of BVR for HO is artifactual, resulting from the effects of free heme (dissociated from HO) on BVR fluorescence.

Studies were also performed to evaluate the role of cysteine residues in catalytic activity and substrate inhibition for human BVR. Alanine substitution of C74 reduced catalytic activity by ~80% and this variant is less sensitive to substrate inhibition. Alanine substitution of C281, C292, C293 or C292/C293 had little effect on either catalytic activity or substrate inhibition.

The studies described herein elucidate mechanisms which may be important features of regulation for the HO system in the cell, and thus have implications for regulating the cellular processes affected by HO and BVR.

Chapter 1 General introduction to the heme degradation system

1.1 Heme biology and iron homeostasis

Heme is required as a prosthetic group for many biologically important processes including oxygen transport, electron transport, oxidation reactions, and transcriptional regulation. As such, it is crucial for aerobic life. A familiar role of the heme cofactor is to bind gases, such as for the oxygen transport and storage proteins hemoglobin and myoglobin (1,2). Furthermore, heme is required for electron transport in various proteins, e.g, cytochrome *c* in the respiratory chain of the mitochondria (3). Heme is required as a cofactor in oxygenases, such as monooxygenases like cytochrome P450, which insert oxygen atoms from O_2 to metabolize xenobiotic compounds (4). Finally, heme is an important regulator of transcription factors and signaling pathways (5).

The basic structure of heme consists of protoporphyrin IX with ferrous iron inserted into the tetrapyrrole macrocycle (Figure 1.1). There are several forms of the heme cofactor, which differ at the methyl and vinyl side chains of the tetrapyrrole. B-type heme, in which the molecule is noncovalently bound to the protein, is the most common form of the cofactor, while many cytochromes contain c-type heme in which thioester bonds covalently link the heme vinyl side chains to the protein. Less common forms of heme, such as a-type heme, found in cytochrome c oxidase, and d_1-type heme, which is found in nitrite reductase, also exist (6).

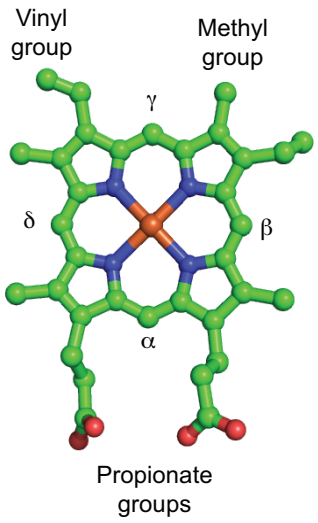

Figure 1.1. **Ball and stick representation of b-type heme.** Heme consists of four pyrrole rings linked by methylene bridges (α, β, γ, δ). Oxygens on the propionate groups are shown in red and can interact with the protein environment via electrostatic interactions. Nitrogens of the pyrrole rings (blue) coordinate ferric (3^+) or ferrous (2^+) iron, shown in orange.

Heme biosynthesis in mammals is initiated in the mitochondria. The first and rate-limiting step of heme synthesis is the synthesis of aminolevininate acid (ALA) which occurs in the mitochondria and is mediated by ALA synthase. This step is negatively regulated by both heme and glucose (7). ALA is then transferred to the cytosol where the next four steps of heme synthesis occur to produce coproporphyrinogen III (COPRO III), which is transported back into the mitochondria where the last three steps of heme synthesis occur. In the final step, ferrochelatase inserts iron into protoporphyrin IX, forming heme. Heme is then transported out of the mitochondria via an unknown transporter and is incorporated into hemoproteins in the cytosol. Unincorporated heme is either transported out of the cell, degraded by heme oxygenases, or may act as a regulator of biological events (8).

Iron and heme homeostasis are closely linked, as in humans approximately 70% of the iron in the body exists as heme iron and the majority of the dialy iron requirement is fulfilled by the recycling of heme iron from erythrocytes (9). Iron is crucial for most prokaryotic and eukaryotic life, as a constituent of heme and hemoproteins (as described above), for iron-sulfur (Fe-S) containing proteins such as ferredoxins and carbon monoxide dehydrogenase (CODH), and other iron containing enzymes

important for DNA synthesis, replication and repair such as ribonucleotide reductase (9). While iron deficiency can lead to cell death, free iron is also toxic due to its ability to generate reactive hydroxyl radicals via Fenton chemistry.

1.2 Heme degradation and its importance in biology

As described above, hemoproteins mediate crucial cellular and organismal functions such as oxygen transport, electron transport, and are required for numerous catalytic functions. Therefore, it is important that sufficient heme is available to be incorporated into hemoproteins. However, high heme levels (concentrations above 1 μM) are cytotoxic due to the ability of heme to generate hydroxyl radicals via Fenton chemistry and to intercalate into cellular membranes (10). Thus, heme levels must be tightly regulated to provide sufficient heme for cellular processes while avoiding toxicity.

Two major points of regulation exist for heme levels in the cell. ALA synthase is the major site of regulation for heme synthesis, while heme oxygenase (HO), NADPH-cytochrome P450 reductase (CPR) and biliverdin reductase (BVR) regulate heme degradation.

The HO pathway is the major enzymatic process through which cellular heme is degraded in the cell (Figure 1.2). HO converts heme to biliverdin (BV), requiring 7 electrons from CPR, and $3O_2$ [Equation 1]. Subsequently, BVR converts biliverdin (BV) to bilirubin (BR) utilizing 2 electrons from NADPH [Equation 2] (11,12).

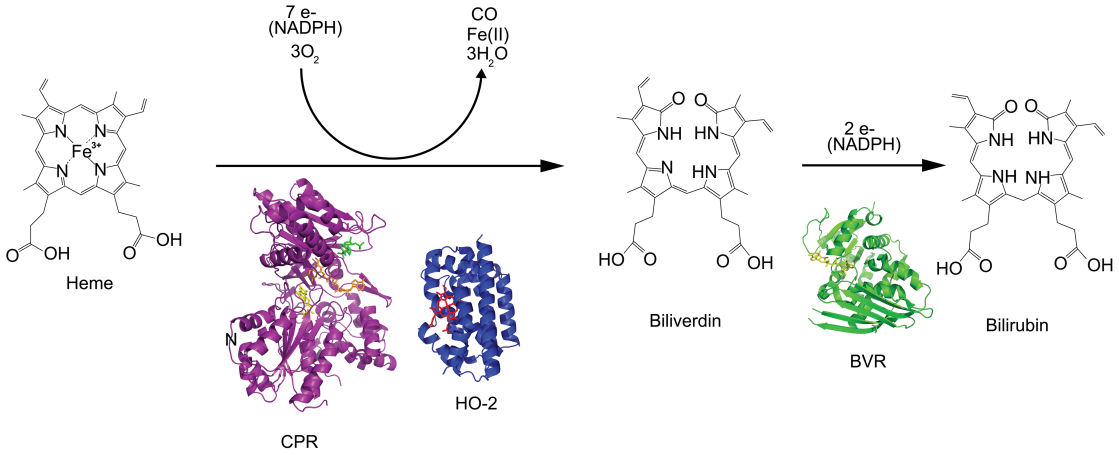

Figure 1.2. **The heme degradation pathway.** The two enzymatic steps of heme degradation mediated by HO, CPR and BVR. HO converts heme to biliverdin and BVR converts biliverdin to bilirubin. The HO reaction requires electrons transferred from NADPH via CPR. (PDB 1AMO, 2QPP, and 2H63)

$$\text{Heme} + 7e^- + 3O_2 \rightarrow \text{biliverdin} + CO + Fe(II) + 3H_2O \qquad \text{[Equation 1]}$$

$$\text{Biliverdin} + 2e^- \rightarrow \text{Bilirubin} \qquad \text{[Equation 2]}$$

In addition to maintaining heme homeostasis, the heme degradation pathway impacts cellular health through its products. The release and recycling of iron from heme is an important aspect of iron homeostasis as less than 3% of the daily requirement for iron is consumed in the diet (13). The heme degradation system not only prevents the accumulation of free heme, it also is protective against oxidative stress via its end product, bilirubin, which is a potent antioxidant (14). Finally, HO is the major physiologic source of CO, which is thought to be a signaling molecule akin to NO (15).

1.3 Enzymes of the heme degradation pathway

1.3.1 Heme oxygenase

HO mediates the first and rate limiting enzymatic step of heme degradation, and the HO reaction is comprised of four major steps. Initially, molecular oxygen (O_2) and electrons from NADPH-CPR are used to oxidize heme to α-*meso*-hydroxyheme (16). α-

verdoheme is then formed and the hydroxylated α-*meso* carbon is released as CO. The third step requires reducing equivalents from CPR and O_2 to convert α-verdoheme to biliverdin-iron. Finally, the biliverdin-iron complex is reduced, which results in the release of ferrous iron and biliverdin. In the absence of BVR, the limiting step in the HO reaction is the release of BV (17,18).

There are two major HO isoforms: HO-1 and HO-2. While HO-3 has also been described, the transcript is not enzymatically active and its biological relevance is uncertain (19). HO-1 and HO-2 share high sequence homology (55% identity and 76% similarity) and structural similarity (20). Both isoforms contain related hydrophobic C-terminal regions of approximately 20 amino acids that anchor the proteins to the microsomal membrane (21). HO-1 is a 288 amino acid protein with a molecular weight of approximately 32 kDa while HO-2 is slightly larger, with 316 amino acids and a molecular weight of 36 kDa. As shown in Figure 1.3, HO-1 and HO-2 are structurally similar and the crystal structures of the core catalytic regions of the two HOs overlay closely.

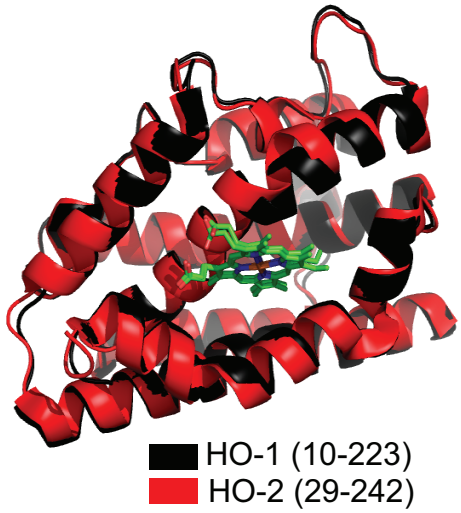

Figure 1.3. **HO-1 and HO-2 are structurally similar.** An overlay of the crystal structures of the catalytic cores of HO-1 (residues 10-233; black) and HO-2 (residues 29-242; red). (PDB files 1DVE and 2QPP).

While structurally similar, the expression patterns and regulation of HO-1 and HO-2 are distinct. HO-1 is expressed in most tissues and is transcriptionally regulated, while HO-2 is constitutively expressed in a narrow range of tissues, primarily the brain and testes (4,22).

HO-1, also known as heat shock protein 32 (HSP32), is induced by a variety of factors including heme (23), hypoxia (24), and oxidative stress (25). Both heme and hypoxia induce expression of HO-1 through transcriptional regulatory elements in the 5'-flanking region of the HO-2 promoter; activator protein (AP-1) DNA binding sites (23). Signal transducer and activation of transcription (STAT) DNA binding sites at the HO-1 promoter are also important for HO-1 induction under hypoxia (26). HO-1 induction by oxidative stress is mediated via nuclear factor (erythroid-derived 2)-like 2 (Nrf2), which is a transcription factor that regulates numerous genes involved in antioxidant protection (25,27).

The regulation of constitutively expressed HO-2 is not fully understood, however HO-2 contains three Cys-Pro heme regulatory motifs (HRMs) while HO-1 completely lacks cysteines. The C-terminal HRMs of HO-2 form a disulfide bond in response to the redox state of the cell, and the disulfide state of the HRMs modulates the ability of HO-2 to bind heme (28). Under oxidizing conditions the affinity of HO-2 for heme is increased 10-fold compared to the reduced protein (K_d values of 0.033 μM and 0.348 μM respectively) (28,29). This represents one regulatory mechanism for HO-2 distinct from HO-1, however it is not clear why the two major HO isoforms exist.

1.3.2 Cytochrome P450 reductase

As stated earlier, the heme oxygenase reaction requires 7 electrons transferred from NADPH via CPR. CPR is a 78 kDa protein which is tethered to the microsomal membrane through an N-terminal membrane spanning region and transfers electrons to many hemoproteins including heme oxygenase (30), cytochromes p450 (31), cytochrome b5 (32), and cytochrome c (33); and also the flavoprotein squalene monooxygenase (34,35). CPR is highly expressed in the liver, and is also found in many extrahepatic tissues. Regulation of CPR occurs primarily at the transcriptional level by the thyroid hormone T3, which stimulates CPR expression (36,37).

The crystal structure of soluble rat CPR, which lacks the N-terminal membrane spanning region, has been determined and shows that CPR consists of four structural domains; the FMN-binding domain, the connecting domain, and the FAD- and NADPH-binding domains (Figure 1.4) (38). To transfer electrons, CPR requires equimolar quantities of the bound cofactors FAD and FMN (31). The electron transfer path is typically from NADPH through FAD to FMN, then to the redox acceptor (HO, P450, etc) (39,40). CPR associates closely with many of its redox partners to mediate electron transport.

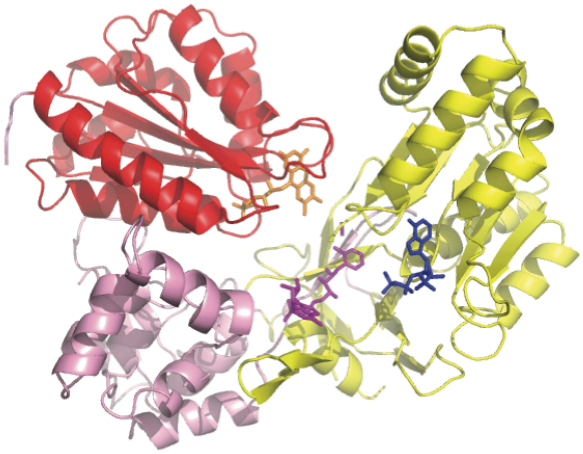

Figure 1.4. **Structural domains of CPR.** The FMN-binding domain is shown in red, the connecting domain in pink, the FAD and NADP(H) domains are shown in yellow. Cofactors are: $NADP^+$ (blue), FAD (purple), FMN (orange). PDB 1AMO

The interaction of CPR with members of the cytochrome p450 family has been well studied and may exemplify CPR's interaction with other electron acceptor proteins. Binding of CPR and p450 requires membrane association of both proteins, and complex formation occurs through a combination of electrostatic and hydrophobic interactions (41-44). The molecular surface of CPR surrounding FMN is predominately electronegative, while the surface of p450 surrounding the heme moiety is primarily electropositive (45). It is thought that charge coupling between the two proteins is a major factor in binding, however hydrophobic residues are also involved (41).

While the membrane-spanning region of CPR is required for electron transfer to cytochrome p450, other redox partners such as HO-1 and cytochrome c are reduced using soluble forms of both CPR and redox partner (46); however membrane association can enhance complex formation and electron transfer, for example with HO-1 (47).

A complex between the soluble forms of CPR and HO-1 (lacking their membrane-spanning regions) has been characterized by a variety of methods and suggests a relatively high affinity electron transfer complex is formed, with K_d values ranging from 0.4 ± 0.1 μM to 2.4 ± 0.6 μM (45,48). Like CPR and cytochrome P450, charge interactions are important for HO-1/CPR binding and an interface for CPR on HO-1 involving specific lysine residues has been proposed (48,49). While the HO-1/CPR complex is relatively well described, the HO-2/CPR complex remains uncharacterized.

1.3.3 Biliverdin reductase

BVR is a 33 kDa protein that mediates the second step in heme degradation, the conversion of biliverdin to bilirubin (Figure 1.2). BVR or BVR-like genes are found in life forms ranging from cyanobacteria to humans, and in humans BVR is present in most tissues (12). For some time the importance of converting non-toxic biliverdin to potentially toxic bilirubin was not understood, however a role for bilirubin as a powerful antioxidant has been proposed (50).

Mutagenesis studies using rat BVR suggest that cysteines may be required for BVR function, however there are conflicting reports regarding the specific residues that are required (51,52). The BVR reaction requires two electrons from NADPH (or NADH) [Equation 2] and BVR is unique in its duel cofactor specificity; the enzyme favors NADPH at high pH (8.7), however at pH ranges 6.7-6.9 BVR prefers NADH (53). NADPH is thought to be the physiologic cofactor, however, as at physiologic pH the K_m for NADPH is ~100-fold lower compared with NADH (54).

BVR is also unique in its diverse functions. In addition to catalyzing the conversion of biliverdin to bilirubin, BVR serves as a heme-sensitive transcriptional

regulator, a kinase that participates in insulin and AKT signaling pathways, and is thought to be important in the protection against oxidative stress (55). As a transcriptional regulator, BVR regulates genes involved in the oxidative stress response, including HO-1 (56,57). BVR contains a bZip motif that is commonly involved in homodimerization. The dimeric form of BVR, but not the monomeric form, is capable of binding DNA regulatory sequences and is likely responsible for BVR mediated transcriptional regulation (57). The kinase activity of BVR, including its autophosphorylation, facilitates its enzymatic activity and the phosphorylation of other proteins, enabling BVR to act as a signaling molecule in various pathways (55,58-61).

Regulation of the BVR product bilirubin is essential because, while at low levels bilirubin is protective against oxidative stress, high levels of bilirubin result in neurotoxicity (14,62-65). Under normal conditions bilirubin is glucuronidated to enhance solubility and excreted from the body. However, impaired glucoronidation or excessive BVR activity results in the accumulation of bilirubin causing hyperbilirubinemia, a common neonatal condition that can cause severe brain damage (66).

At the transcriptional level, BVR expression is upregulated by hypoxia, and inhibited by both biliverdin and NF-κB (67). Early studies characterizing rat BVR also show that the enzyme is strongly substrate inhibited, which may be an important aspect of regulating the production of bilirubin post transcriptionally (54). Two major mechanisms for substrate inhibition are the formation of a non-productive enzyme-substrate complex, or the presence of a second, regulatory substrate-binding site. An inhibitory complex of BVR bound to biliverdin and NADP+ has been proposed as the inhibitory complex responsible for BVR substrate inhibition (68).

1.4 Protein-protein interactions in the heme degradation pathway

Recent experiments addressing protein-protein interactions in the heme degradation pathway focus on soluble HO-1 and its interactions with CPR or BVR. Methods such as surface plasmon resonance (48), fluorescence quenching (45), and acetylation protection assays (49) demonstrate that soluble HO-1 and soluble CPR (lacking their membrane spanning regions) form an electron transfer complex. Furthermore, NADP+ increases the affinity of HO-1 for CPR by ~5 fold (48).

The interaction between HO-1 and CPR is mediated in part through charge interactions. The surface of CPR is predominately negatively charged, while the surface of HO-1 near the d-meso edge of heme is positively charged (38,45). Two groups have addressed the importance of specific HO-1 residues in binding CPR by evaluating the effect of alanine substitutions on the K_d value for HO-1 and CPR using fluorescence quenching or surface plasmon resonance methods (45,48). These studies both demonstrate that mutations disrupting the charge distribution on the heme binding face of HO-1 (in which the heme biding picket and surrounding residues are visible) can also disrupt HO-1/CPR binding, however the HO-1 residues identified as important for CPR binding are not consistent between the two studies (Figure 1.5*A* and *B*). Fluorescence quenching studies identify CPR K18, K22, K179, R185, E19, E127, E190, and R198 as important for binding to CPR (45). The fluorescence quenching studies also show that alanine substitution of additional residues, including K149 or K153, does not increase the K_d value of HO-1 and CPR (45). In contrast, surface plasmon resonance experiments, identify K149, K153, and R185 of HO-1 as important for CPR binding (48). Mass spectroscopy studies further support the location of K149 and K153 at the HO-1/CPR interface by demonstrating that both the lysine residues are protected from chemical modification in the presence of CPR, and therefore are likely at the interface of the two proteins (49).

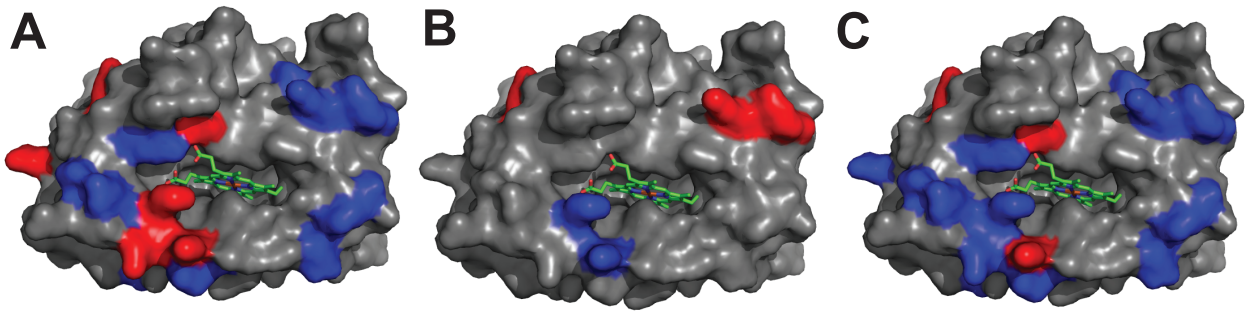

Figure 1.5. **HO-1 residues important for binding CPR.** Alanine substitution of HO-1 residues that increase the K_d are shown in *red* while residues that do not increase the K_d value are shown in *blue*. **(A)** Residues identified by fluorescence quenching studies for CPR and HO-1 (Wang *et al*, 2003). **(B)** Residues identified by SPR studies for HO-1 and CPR (Higashimoto *et al.* 2005). **(C)** Residues identified by fluorescence quenching studies for HO-1 and BVR (Wang *et al*, 2003). (PDB 1DVE)

The majority of studies addressing HO-1/CPR interactions were conducted *in vitro* using soluble forms of the proteins, as catalytic activity is retained in the truncated soluble enzymes and the soluble forms are more tractable than full-length proteins with intact membrane anchors. More recent studies using full length HO-1 and CPR establish that the membrane spanning regions and/or the membrane environment facilitates complex formation between HO-1 and CPR (69,70).

In addition to facilitating electron transport, CPR binding HO-1 may influence the oligomeric state of HO-1 (70). In mammalian cells under hypoxic conditions, HO-1 is rapidly cleaved from its membrane spanning region and translocated to the nucleus. If, however, CPR is coexpressed with HO-1, HO-1 is protected from proteolysis and is retained at the endoplasmic reticulum (70).

Studies similar to those used to characterize the HO-1/CPR complex also address the nature of an HO-1/BVR complex. Surface plasmon resonance studies demonstrate that BVR can compete for HO-1 binding to immobilized CPR (48), while fluorescence quenching studies demonstrate that HO-1 binds BVR with similar affinity as compared to CPR and identifies some HO-1 residues that may be important in binding BVR (Figure 1.5*C*) (45). However, while CPR and BVR are proposed to share an overlapping binding site on HO-1, acetylation protection studies with BVR do not identify any residues on HO-1 that are protected by BVR (49).

1.5 Unresolved questions

As described above, the heme degradation pathway plays a role in numerous cell processes; detoxification, iron and heme homeostasis, cell signaling and protection against oxidative stress. Understanding the mechanisms that regulate the HO pathway and its various processes is crucial to our understanding of cellular health, and is the first step in our ability to manipulate this pathway therapeutically.

It is not fully understood why two the major HO isoforms (HO-1 and HO-2) exist. Understanding the similarities and differences for these isoforms may shed light on distinct roles for the enzymes. While an HO-1/CPR complex has been well described for the soluble proteins (45,48,49,71), little is known regarding the ability of HO-2 to form a complex with CPR. Also, the nature of the membrane bound HO/CPR electron transfer complex in the cell is not known. Soluble HO-1 has also been reported to bind BVR, however while some evidence supports an HO-1/BVR complex, other challenges it (45,49) and the ability of BVR to form a complex with HO-2 has not been determined.

Understanding the ability of HO-1 and HO-2 to form complexes with the other proteins in the heme degradation pathway (CPR and BVR) will provide insight into mechanisms that are important for the regulation of the HO pathway in the cell, and is therefore important for understanding the cellular regulation of iron and heme homeostasis, and the defense against oxidative stress.

1.6 References

1. Kendrew, J. C., Bodo, G., Dintzis, H. M., Parrish, R. G., Wyckoff, H., and Phillips, D. C. (1958) A three-dimensional model of the myoglobin molecule obtained by x-ray analysis. *Nature* **181**, 662-666
2. Paoli, M., Marles-Wright, J., and Smith, A. (2002) Structure-function relationships in heme-proteins. *DNA Cell Biol* **21**, 271-280
3. Paine, M. J., Scrutton, N. S., Munro, A. W., Gutierrez, A., Roberts, G. C., and Wolf, C.R. (2005) Electron transfer partners of cytochrome p450. in *Cytochrome p450* (Ortiz De Montellano, P. R. ed.), 3rd Ed., Kluwer Academic/Plenum Publishers, New York. pp 115-148
4. Maines, M. D. (1997) The heme oxygenase system: a regulator of second messenger gases. *Annu Rev Pharmacol Toxicol* **37**, 517-554
5. Mense, S. M., and Zhang, L. (2006) Heme: a versatile signaling molecule controlling the activities of diverse regulators ranging from transcription factors to MAP kinases. *Cell Res* **16**, 681-692
6. Allen, J. W., Barker, P. D., Daltrop, O., Stevens, J. M., Tomlinson, E. J., Sinha, N., Sambongi, Y., and Ferguson, S. J. (2005) Why isn't 'standard' heme good enough for c-type and d1-type cytochromes? *Dalton Trans*, 3410-3418
7. Doss, M., Sixel-Dietrich, F., and Verspohl, F. (1985) "Glucose effect" and rate limiting function of uroporphyrinogen synthase on porphyrin metabolism in hepatocyte culture: relationship with human acute hepatic porphyrias. *Journal of clinical chemistry and clinical biochemistry. Zeitschrift fur klinische Chemie und klinische Biochemie* **23**, 505-513
8. Furuyama, K., Kaneko, K., and Vargas, P. D. (2007) Heme as a magnificent molecule with multiple missions: heme determines its own fate and governs cellular homeostasis. *Tohoku J Exp Med* **213**, 1-16
9. Li, C., and Stocker, R. (2009) Heme oxygenase and iron: from bacteria to humans. *Redox Rep* **14**, 95-101
10. Sassa, S. (2004) Why heme needs to be degraded to iron, biliverdin IXalpha, and carbon monoxide? *Antioxid Redox Signal* **6**, 819-824
11. Maines, M. D. (2004) The heme oxygenase system: past, present, and future. *Antioxid Redox Signal* **6**, 797-801
12. Maines, M. D. (2005) New insights into biliverdin reductase functions: linking heme metabolism to cell signaling. *Physiology (Bethesda)* **20**, 382-389
13. Sassa, S. (2006) Modern diagnosis and management of the porphyrias. *Br J Haematol* **135**, 281-292
14. Baranano, D. E., Rao, M., Ferris, C. D., and Snyder, S. H. (2002) Biliverdin reductase: a major physiologic cytoprotectant. *Proc Natl Acad Sci U S A* **99**, 16093-16098
15. Baranano, D. E., and Snyder, S. H. (2001) Neural roles for heme oxygenase: contrasts to nitric oxide synthase. *Proc Natl Acad Sci U S A* **98**, 10996-11002

16. Montellano, P. R. (2000) The mechanism of heme oxygenase. *Current opinion in chemical biology* **4**, 221-227
17. Liu, Y., and Ortiz de Montellano, P. R. (2000) Reaction intermediates and single turnover rate constants for the oxidation of heme by human heme oxygenase-1. *J. Biol. Chem.* **275**, 5297-5307
18. Higashimoto, Y., Sato, H., Sakamoto, H., Takahashi, K., Palmer, G., and Noguchi, M. (2006) The reactions of heme- and verdoheme-heme oxygenase-1 complexes with FMN-depleted NADPH-cytochrome P450 reductase. Electrons required for verdoheme oxidation can be transferred through a pathway not involving FMN. *J. Biol. Chem.* **281**, 31659-31667
19. McCoubrey, W. K., Jr., Huang, T. J., and Maines, M. D. (1997) Isolation and characterization of a cDNA from the rat brain that encodes hemoprotein heme oxygenase-3. *Eur J Biochem* **247**, 725-732
20. Bianchetti, C. M., Yi, L., Ragsdale, S. W., and Phillips, G. N., Jr. (2007) Comparison of apo- and heme-bound crystal structures of a truncated human heme oxygenase-2. *J. Biol. Chem.* **282**, 37624-37631
21. Maines, M. D., Ibrahim, N. G., and Kappas, A. (1977) Solubilization and partial purification of heme oxygenase from rat liver. *J. Biol. Chem.* **252**, 5900-5903
22. Ewing, J. F., and Maines, M. D. (1997) Histochemical localization of heme oxygenase-2 protein and mRNA expression in rat brain. *Brain Res Brain Res Protoc* **1**, 165-174
23. Prawan, A., Kundu, J. K., and Surh, Y. J. (2005) Molecular basis of heme oxygenase-1 induction: implications for chemoprevention and chemoprotection. *Antioxid Redox Signal* **7**, 1688-1703
24. Borger, D. R., and Essig, D. A. (1998) Induction of HSP 32 gene in hypoxic cardiomyocytes is attenuated by treatment with N-acetyl-L-cysteine. *Am J Physiol* **274**, H965-973
25. Ishii, T., Itoh, K., Takahashi, S., Sato, H., Yanagawa, T., Katoh, Y., Bannai, S., and Yamamoto, M. (2000) Transcription factor Nrf2 coordinately regulates a group of oxidative stress-inducible genes in macrophages. *J. Biol. Chem.* **275**, 16023-16029
26. Lee, P. J., Camhi, S. L., Chin, B. Y., Alam, J., and Choi, A. M. (2000) AP-1 and STAT mediate hyperoxia-induced gene transcription of heme oxygenase-1. *Am J Physiol Lung Cell Mol Physiol* **279**, L175-182
27. Shelton, P., and Jaiswal, A. K. (2013) The transcription factor NF-E2-related factor 2 (Nrf2): a protooncogene? *FASEB J* **27**, 414-423
28. Yi, L., and Ragsdale, S. W. (2007) Evidence that the heme regulatory motifs in heme oxygenase-2 serve as a thiol/disulfide redox switch regulating heme binding. *J. Biol. Chem.* **282**, 21056-21067
29. Yi, L., Jenkins, P. M., Leichert, L. I., Jakob, U., Martens, J. R., and Ragsdale, S. W. (2009) Heme regulatory motifs in heme oxygenase-2 form a thiol/disulfide redox switch that responds to the cellular redox state. *J. Biol. Chem.* **284**, 20556-20561
30. Kikuchi, G., Yoshida, T., and Noguchi, M. (2005) Heme oxygenase and heme degradation. *Biochem Biophys Res Commun* **338**, 558-567

31. Strobel, H. W., A. V. Hodgson, and S. Shen. . (1995) NADPH cytochrome P450 reductase and its structural and functional domains. *Cytochrome P 450*, 225-244
32. Enoch, H. G., and Strittmatter, P. (1979) Cytochrome b5 reduction by NADPH-cytochrome P-450 reductase. *J. Biol. Chem.* **254**, 8976-8981
33. Williams, C. H., Jr., and Kamin, H. (1962) Microsomal triphosphopyridine nucleotide-cytochrome c reductase of liver. *J. Biol. Chem.* **237**, 587-595
34. Ono, T., and Bloch, K. (1975) Solubilization and partial characterization of rat liver squalene epoxidase. *J. Biol. Chem.* **250**, 1571-1579
35. Marohnic, C. C., Huber Iii, W. J., Patrick Connick, J., Reed, J. R., McCammon, K., Panda, S. P., Martasek, P., Backes, W. L., and Masters, B. S. (2011) Mutations of human cytochrome P450 reductase differentially modulate heme oxygenase-1 activity and oligomerization. *Arch Biochem Biophys* **513**, 42-50
36. Li, H. C., Liu, D., and Waxman, D. J. (2001) Transcriptional induction of hepatic NADPH: cytochrome P450 oxidoreductase by thyroid hormone. *Mol Pharmacol* **59**, 987-995
37. Ram, P. A., and Waxman, D. J. (1992) Thyroid hormone stimulation of NADPH P450 reductase expression in liver and extrahepatic tissues. Regulation by multiple mechanisms. *J. Biol. Chem.* **267**, 3294-3301
38. Wang, M., Roberts, D. L., Paschke, R., Shea, T. M., Masters, B. S., and Kim, J. J. (1997) Three-dimensional structure of NADPH-cytochrome P450 reductase: prototype for FMN- and FAD-containing enzymes. *Proc Natl Acad Sci U S A* **94**, 8411-8416
39. Murataliev, M. B., Feyereisen, R., and Walker, F. A. (2004) Electron transfer by diflavin reductases. *Biochim Biophys Acta* **1698**, 1-26
40. Iyanagi, T. (2005) Structure and function of NADPH-cytochrome P450 reductase and nitric oxide synthase reductase domain. *Biochem Biophys Res Commun* **338**, 520-528
41. Kenaan, C., Zhang, H., Shea, E. V., and Hollenberg, P. F. Uncovering the role of hydrophobic residues in cytochrome P450-cytochrome P450 reductase interactions. *Biochemistry* **50**, 3957-3967
42. Hamdane, D., Xia, C., Im, S. C., Zhang, H., Kim, J. J., and Waskell, L. (2009) Structure and function of an NADPH-cytochrome P450 oxidoreductase in an open conformation capable of reducing cytochrome P450. *J. Biol. Chem.* **284**, 11374-11384
43. Jang, H. H., Jamakhandi, A. P., Sullivan, S. Z., Yun, C. H., Hollenberg, P. F., and Miller, G. P. (2010) Beta sheet 2-alpha helix C loop of cytochrome P450 reductase serves as a docking site for redox partners. *Biochim Biophys Acta* **1804**, 1285-1293
44. Shen, A. L., and Kasper, C. B. (1995) Role of acidic residues in the interaction of NADPH-cytochrome P450 oxidoreductase with cytochrome P450 and cytochrome c. *J. Biol. Chem.* **270**, 27475-27480
45. Wang, J., and de Montellano, P. R. (2003) The binding sites on human heme oxygenase-1 for cytochrome p450 reductase and biliverdin reductase. *J. Biol. Chem.* **278**, 20069-20076

46. Hayashi, S., Omata, Y., Sakamoto, H., Hara, T., and Noguchi, M. (2003) Purification and characterization of a soluble form of rat liver NADPH-cytochrome P-450 reductase highly expressed in Escherichia coli. *Protein Expr Purif* **29**, 1-7
47. Huber, W. J., 3rd, and Backes, W. L. (2007) Expression and characterization of full-length human heme oxygenase-1: the presence of intact membrane-binding region leads to increased binding affinity for NADPH cytochrome P450 reductase. *Biochemistry* **46**, 12212-12219
48. Higashimoto, Y., Sakamoto, H., Hayashi, S., Sugishima, M., Fukuyama, K., Palmer, G., and Noguchi, M. (2005) Involvement of NADPH in the interaction between heme oxygenase-1 and cytochrome P450 reductase. *J. Biol. Chem.* **280**, 729-737
49. Higashimoto, Y., Sugishima, M., Sato, H., Sakamoto, H., Fukuyama, K., Palmer, G., and Noguchi, M. (2008) Mass spectrometric identification of lysine residues of heme oxygenase-1 that are involved in its interaction with NADPH-cytochrome P450 reductase. *Biochem Biophys Res Commun* **367**, 852-858
50. Stocker, R., Glazer, A. N., and Ames, B. N. (1987) Antioxidant activity of albumin-bound bilirubin. *Proc Natl Acad Sci U S A* **84**, 5918-5922
51. McCoubrey, W. K., Jr., and Maines, M. D. (1994) Site-directed mutagenesis of cysteine residues in biliverdin reductase. Roles in substrate and cofactor binding. *Eur J Biochem* **222**, 597-603
52. Kikuchi, A., Park, S. Y., Miyatake, H., Sun, D., Sato, M., Yoshida, T., and Shiro, Y. (2001) Crystal structure of rat biliverdin reductase. *Nat Struct Biol* **8**, 221-225
53. Kutty, R. K., and Maines, M. D. (1981) Purification and characterization of biliverdin reductase from rat liver. *J. Biol. Chem.* **256**, 3956-3962
54. Noguchi, M., Yoshida, T., and Kikuchi, G. (1979) Purification and properties of biliverdin reductases from pig spleen and rat liver. *J Biochem* **86**, 833-848
55. Kapitulnik, J., and Maines, M. D. (2009) Pleiotropic functions of biliverdin reductase: cellular signaling and generation of cytoprotective and cytotoxic bilirubin. *Trends Pharmacol Sci* **30**, 129-137
56. Tudor, C., Lerner-Marmarosh, N., Engelborghs, Y., Gibbs, P. E., and Maines, M. D. (2008) Biliverdin reductase is a transporter of haem into the nucleus and is essential for regulation of HO-1 gene expression by haematin. *Biochem J* **413**, 405-416
57. Ahmad, Z., Salim, M., and Maines, M. D. (2002) Human biliverdin reductase is a leucine zipper-like DNA-binding protein and functions in transcriptional activation of heme oxygenase-1 by oxidative stress. *J. Biol. Chem.* **277**, 9226-9232
58. Salim, M., Brown-Kipphut, B. A., and Maines, M. D. (2001) Human biliverdin reductase is autophosphorylated, and phosphorylation is required for bilirubin formation. *J. Biol. Chem.* **276**, 10929-10934
59. Lerner-Marmarosh, N., Shen, J., Torno, M. D., Kravets, A., Hu, Z., and Maines, M. D. (2005) Human biliverdin reductase: a member of the insulin receptor substrate family with serine/threonine/tyrosine kinase activity. *Proc Natl Acad Sci U S A* **102**, 7109-7114
60. Pachori, A. S., Smith, A., McDonald, P., Zhang, L., Dzau, V. J., and Melo, L. G. (2007) Heme-oxygenase-1-induced protection against hypoxia/reoxygenation is

dependent on biliverdin reductase and its interaction with PI3K/Akt pathway. *J Mol Cell Cardiol* **43**, 580-592
61. Wegiel, B., Baty, C. J., Gallo, D., Csizmadia, E., Scott, J. R., Akhavan, A., Chin, B. Y., Kaczmarek, E., Alam, J., Bach, F. H., Zuckerbraun, B. S., and Otterbein, L. E. (2009) Cell surface biliverdin reductase mediates biliverdin-induced anti-inflammatory effects via phosphatidylinositol 3-kinase and Akt. *J. Biol. Chem.* **284**, 21369-21378
62. Dore, S., and Snyder, S. H. (1999) Neuroprotective action of bilirubin against oxidative stress in primary hippocampal cultures. *Ann N Y Acad Sci* **890**, 167-172
63. Dore, S., Takahashi, M., Ferris, C. D., Zakhary, R., Hester, L. D., Guastella, D., and Snyder, S. H. (1999) Bilirubin, formed by activation of heme oxygenase-2, protects neurons against oxidative stress injury. *Proc Natl Acad Sci U S A* **96**, 2445-2450
64. Jansen, T., Hortmann, M., Oelze, M., Opitz, B., Steven, S., Schell, R., Knorr, M., Karbach, S., Schuhmacher, S., Wenzel, P., Munzel, T., and Daiber, A. (2010) Conversion of biliverdin to bilirubin by biliverdin reductase contributes to endothelial cell protection by heme oxygenase-1-evidence for direct and indirect antioxidant actions of bilirubin. *J Mol Cell Cardiol* **49**, 186-195
65. Kapitulnik, J. (2004) Bilirubin: an endogenous product of heme degradation with both cytotoxic and cytoprotective properties. *Mol Pharmacol* **66**, 773-779
66. Fevery, J. (2008) Bilirubin in clinical practice: a review. *Liver international : official journal of the International Association for the Study of the Liver* **28**, 592-605
67. Gibbs, P. E., Miralem, T., and Maines, M. D. (2010) Characterization of the human biliverdin reductase gene structure and regulatory elements: promoter activity is enhanced by hypoxia and suppressed by TNF-alpha-activated NF-kappaB. *FASEB J* **24**, 3239-3254
68. Bell, J. E., and Maines, M. D. (1988) Kinetic properties and regulation of biliverdin reductase. *Arch Biochem Biophys* **263**, 1-9
69. Huber Iii, W. J., Scruggs, B. A., and Backes, W. L. (2009) C-Terminal membrane spanning region of human heme oxygenase-1 mediates a time-dependent complex formation with cytochrome P450 reductase. *Biochemistry* **48**, 190-197
70. Linnenbaum, M., Busker, M., Kraehling, J. R., and Behrends, S. Heme oxygenase isoforms differ in their subcellular trafficking during hypoxia and are differentially modulated by cytochrome P450 reductase. *PLoS One* **7**, e35483
71. Sugishima, M., Sato, H., Higashimoto, Y., Harada, J., Wada, K., Fukuyama, K., and Noguchi, M. (2014) Structural basis for the electron transfer from an open form of NADPH-cytochrome P450 oxidoreductase to heme oxygenase. *Proc Natl Acad Sci U S A* **111**, 2524-2529

Chapter 2 Protein-Protein Interactions in the Mammalian Heme Degradation Pathway: Heme Oxygenase-2, Cytochrome P450 Reductase and Biliverdin Reductase

This project was in collaboration with Dr. Erik Zuiderweg and Dr. Ireena Bagai at the University of Michigan, Ann Arbor and Dr. Donald Becker at the University of Nebraska, Lincoln. The results from this chapter have been submitted to *J. Biol. Chem* for publication: **Spencer AM, Bagai I, Becker DF, Zuiderweg ERP, and Ragsdale, SW.** "Protein-Protein Interactions in the Mammalian Heme Degradation Pathway: Heme Oxygenase-2, Cytochrome P450 Reductase and Biliverdin Reductase".

In this chapter Dr. Bagai and Dr. Zuiderweg collected NMR TROSY spectra and Dr. Zuiderweg conducted an analyzed the NMR relaxation studies. Dr. Becker performed and analyzed the analytical the ultracentrifugation experiments. Andrea Spencer performed the sample preparation for all experiments, and both conducted and analyzed the studies utilizing mutagenesis, gel filtration, surface plasmon resonance, chemical cross linking, fluorescence quenching, and optical absorbance, and performed data analysis for the NMR binding experiments.

2.1 Abstract

Heme oxygenase (HO) catalyzes the rate-limiting step in the O_2-dependent degradation of heme to biliverdin, CO and Fe with electrons delivered from NADPH via cytochrome P450 reductase (CPR). Biliverdin reductase (BVR) then catalyzes conversion of biliverdin to bilirubin. We describe mutagenesis combined with kinetic, spectroscopic (fluorescence and NMR), surface plasmon resonance, cross-linking, gel filtration and analytical ultracentrifugation studies aimed at evaluating interactions of HO-2 with CPR and BVR. Based on these results, we propose a model in which HO-2 and CPR form a dynamic ensemble of complex(es) that precede formation of the productive electron transfer complex. The ^{1}H-^{15}N TROSY NMR spectrum of HO-2 reveals specific residues, including L201, near the heme face of HO-2 that are affected by the addition of CPR, implicating this residue at the HO/CPR interface. Alanine substitutions at HO-2 residues L201 and K169 cause a respective 3- and 22-fold increase in K_m for CPR, consistent with a role for these residues in CPR binding. Sedimentation velocity experiments confirm the transient nature of the HO-2/CPR complex (K_d = 15.1 μM). Our results also indicate that HO-2 and BVR form a very weak complex that is only captured by cross-linking. For example, under conditions that CPR affects the ^{1}H-^{15}N TROSY NMR spectrum of HO-2, BVR has no effect. Fluorescence quenching experiments also suggest that BVR binds HO-2 weakly, if at all, and that the previously reported high affinity of BVR for HO is artifactual, resulting from the effects of free heme (dissociated from HO) on BVR fluorescence.

2.2 Introduction

Precise regulation of heme metabolism is crucial for the cell. Heme is an active catalyst for generating reactive oxygen species by Fenton chemistry and is cytotoxic at elevated levels (above ~1μM) (1). Heme is also a required prosthetic group for many proteins involved in electron transfer, oxygen transport and redox enzymology (e.g., oxidases) (2). The mammalian heme degradation pathway consists of two enzymatic steps, which are mediated by heme oxygenase (HO) and biliverdin reductase (BVR) (Figure 2.1). Cytochrome P450 reductase (CPR) is required as an electron donor for HO catalysis. HO is the only known catalyst in the mammalian cell that degrades heme [Equation 1]. HO catalyzes the conversion of heme to biliverdin in a reaction that requires O_2, NADPH, and CPR, which transfers seven electrons as shown in Equation 1 (3,4). BVR then converts biliverdin to bilirubin [Equation 2], which undergoes conjugation with glucuronate and is excreted from the body.

$$\text{Heme} + 7e^- + 3O_2 \rightarrow \text{biliverdin} + CO + Fe(II) + 3H_2O \qquad \text{[Equation 1]}$$

$$\text{Biliverdin} + 2e^- \rightarrow \text{Bilirubin} \qquad \text{[Equation 2]}$$

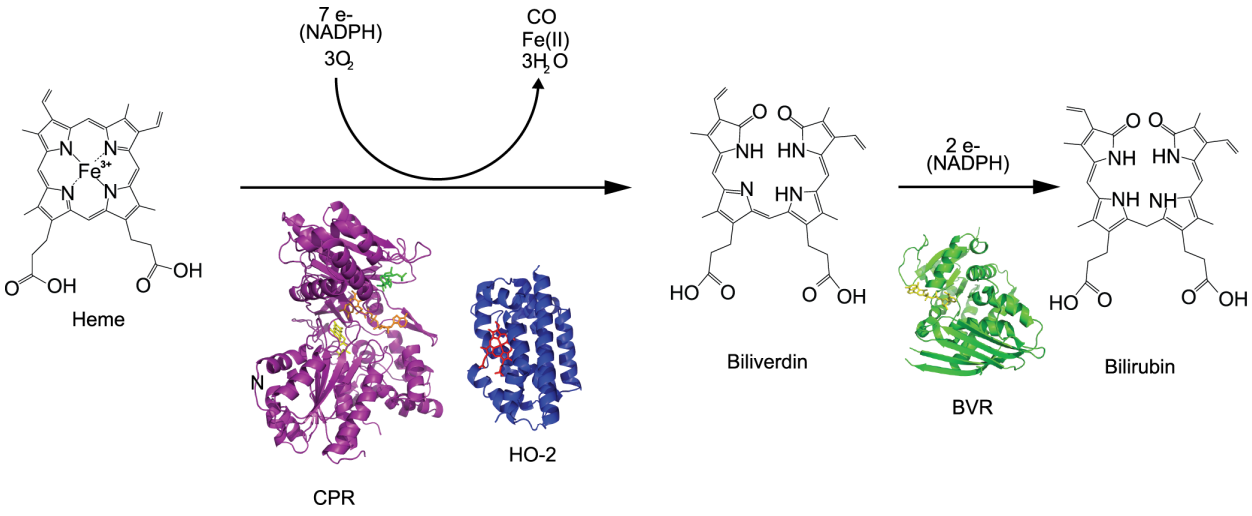

Figure 2.1. **The heme degradation pathway.** The two enzymatic steps of heme degradation mediated by heme oxygenase and biliverdin reductase. HO converts heme to biliverdin and BVR converts biliverdin to bilirubin. The HO reaction requires electrons transferred from NADPH via cytochrome P450 reductase. (PDB 1AMO, 2QPP, and 2H63)

In addition to protecting the cell from the toxicity of free heme, the heme degradation pathway generates biologically important products. The HO reaction is the only cellular source of CO and, while high levels of CO are toxic (>500 ppm), at low levels, CO acts as a signaling molecule akin to NO (5,6) and is cytoprotective (7). The release and recycling of iron from heme is critical for iron homeostasis as most of the iron required for the synthesis of new ferroproteins and heme comes from recycled iron, with less than 3% of the daily iron requirement deriving from the diet (2,8). Finally, the HO system protects cells against oxidative stress, both by controlling free heme levels and by producing bilirubin, a potent antioxidant (9-11).

The heme degradation pathway affects many areas of cellular health; heme and iron homeostasis, antioxidant protection, and gaseous signaling. As such, it is crucial to understand the mechanisms that regulate the activity of HO.

HO exists as two major isoforms: HO-1 and HO-2. HO-3 has also been described, however it has low catalytic activity and its biological role and relevance are uncertain (12,13). HO-1 and HO-2 share a high degree of homology (55% identity and 76% similarity) and display similar enzymatic activity (14). The two isoforms, however, have distinct patterns of expression and regulation. HO-1 is transcriptionally regulated and is expressed in most tissues, while HO-2 is constitutively expressed in a narrow range of tissues, primarily the brain and testes (15). Both HOs possess C-terminal membrane-spanning regions that tether them to the endoplasmic reticulum. However, due to poor solubility of the full-length protein, most enzymatic studies (as those described in this paper) have been conducted with a stable soluble form of HO lacking the C-terminal region. A major difference between the two HOs is that HO-2 contains three heme regulatory motifs (HRMs), consisting of a Cys-Pro dyad, while HO-1 completely lacks cysteines (16). Two of these HRMs are at the C-terminus of HO-2, just preceding the membrane-spanning section. When these are in the dithiol state, the affinity of HO-2 for heme (relative to the disulfide state) decreases significantly, suggesting that the HRMs act as a redox switch that controls activity in response to changes in cellular redox poise (17-19).

Electrons are transferred to HO from NADPH via the ~77-kDa dual flavin enzyme

CPR through a pathway that involves its bound cofactors, FAD and FMN (20-23). In the cell, CPR is tethered to the ER by an N-terminal membrane-spanning region. Protein-protein interactions between the soluble forms of HO-1 and CPR and between HO-1 and BVR have been described *in vitro* (24-27) and are an aspect of regulation that has not been addressed for HO-2. CPR also forms electron-transfer complexes with the cytochromes P450, cytochrome b_5, cytochrome *c*, and squalene monoxygenase (23,28-31). Interactions with CPR may help define distinct roles for the HO isoforms. For example, recent reports suggest that binding of HO-1 and CPR regulates HO-1 nuclear translocation and the transcriptional regulatory response under hypoxia by stabilizing the ER-tethered form of HO-1 in the cell (32). On the other hand, HO-2 appears to remain stably associated at the ER irrespective of hypoxic challenge (32).

The complex between the soluble forms of CPR and HO-1 (lacking their membrane-spanning regions) has been characterized by fluorescence quenching (27), surface plasmon resonance (SPR) (24), and acetylation protection assays (25). These reports provide K_d values for the HO-1/CPR complex that range from 0.4 ± 0.1 μM to 2.4 ± 0.6 μM. CPR protects lysine residues 149 and 153 in HO-1 from chemical modification, suggesting that these basic residues are at the interface of the HO-1/CPR complex (25). Additionally, SPR studies indicate that the K149A substitution results in an ~10-fold increase in K_d for the HO-1/CPR complex (24). While the HO-1/CPR complex has been relatively well characterized, the HO-2/CPR complex has not.

BVR catalyzes the second step in heme degradation: the reduction of biliverdin to bilirubin [Eq 2]. BVR is a soluble ~33 kDa protein that utilizes two electrons from either NADH or NADPH making it unique in having dual cofactor specificity at distinct pH values (33). In addition to its canonical enzymatic function, BVR has also been shown to bind and traffic heme to the nucleus where it regulates HO-1 expression (34-37). Also, BVR is a dual specificity (Ser/Thr and Tyr) kinase, and as such is implicated in MAPK (mitogen-activated protein kinase) cell signaling pathways (38,39).

Two groups have reported interactions between HO-1 and BVR via fluorescence quenching studies and surface plasmon resonance studies (SPR) (24,27). The fluorescence quenching studies suggest a high affinity HO-1/BVR complex (K_d = 0.2 μM) is formed while SPR studies report that BVR competes with CPR for binding to HO-

1. However, studies that identified the HO-1/CPR interface via lysine acetylation protection assays failed to find evidence for an HO-1/BVR interaction (25). Under single turnover conditions, the rate-limiting step of the HO-1 reaction is the release of biliverdin; however, in the presence of BVR, this step is accelerated (40), which indicates kinetic coupling between these two enzymes. Thus, while some evidence supports the formation of a high-affinity complex between HO-1 and BVR, other challenges it. Furthermore, to our knowledge, the extent to which HO-2 is able to interact with BVR has not been addressed. Protein-protein interactions between HO and its reaction partners may play an important role in regulating its various properties, including cellular localization and enzymatic activity. Furthermore, given that they exhibit different modes of transcriptional regulation, HO-1 and constitutive HO-2 may differ in their affinity for BVR and CPR.

In order to gain insight into the protein-level mode of regulating HO-2 activity, and to resolve some of the discrepancies related to measured interactions (or lack thereof) of HO-1 and HO-2 with their binding partners, we have performed nuclear magnetic resonance (NMR), kinetic, analytical ultracentrifugation, gel filtration, cross-linking, SPR and fluorescence quenching studies. Our experiments indicate that both HO-1 and HO-2 form complexes with CPR. The interaction between HO-2 and BVR, however, is weak as compared to CPR, and can only be detected by irreversible methods such as cross-linking. Our results allow us to propose an interface for the HO-2/CPR complex near the heme-binding face of HO-2 that includes residues L201 and K169. Furthermore, our studies demonstrate that the HO/CPR interface includes both hydrophobic and charge interactions. Our studies suggest a reinterpretation of protein-protein interactions in the heme degradation pathway. We demonstrate that both HO-1 and HO-2 bind CPR in a transient electron-transfer complex that is required for HO activity. On the other hand, interactions between BVR and HO-2 are weak to undetectable and may not play a significant role in the physiologic context of a cell.

2.3 Materials and methods

2.3.1 Materials

Ampicillin, isopropyl-β-D-thio-galactopyranoside, kanamycin, NADPH, $NADP^+$, riboflavin, and hemin were purchased from Sigma (St Louis, MO). 7-Diethylamino-3-(4'-maleimidylphenyl)-4-methylcoumarin (CPM) was purchased from Molecular probes, Inc. (Eugene, OR). OneShot® BL21(DE3) chemically competent cells were purchased from Invitrogen/Life Technologies (Grand Island, NY). Ni-nitrilotriacetic acid (NTA) resin is from Qiagen (Valencia, CA). Glutathione Sepharose was purchased from GE Healthcare (Piscataway, NJ).

2.3.2 Enzyme purification

Truncated versions of human HO-1_{265} containing residues 1-265, and human HO-2_{288} containing residues 1-288, and variants of these enzymes, were used in these studies. These enzymes lack the C-terminal amino acids that comprise their membrane anchors and will be referred to as HO-1 and HO-2. To facilitate expression, solubility and ease of purification, HO-1 was cloned into the expression vector pMCSG10 by ligation independent cloning (LIC) (41). HO-2 was expressed and purified from the pET28a(+) vector. HO-1 and HO-2 were purified via an N-terminal 6xHis tag using Ni-NTA affinity chromatography according to the manufacturer's guidelines (Qiagen, Valencia, CA).

Human $CPR_{\Delta 66}$ lacking the N-terminal membrane anchor was expressed from the pET28a(+) vector and is referred to as CPR for all studies described herein. CPR was expressed in BL21(DE3) cells and purified according to published methods (42). Human BVR was expressed from the pGEX-4T-2 vector and purified via Glutathione Sepharose affinity resin according to the manufacturer's instructions (GE Healthcare, Piscataway, NJ).

Unless stated otherwise, affinity purification tags were removed from all proteins by proteolysis before use in these experiments. Tobacco Etch Virus (TEV) protease (expressed in *E. coli* from pRK793, a derivate of BL21(DE3)-RIL, generously supplied by Dr. David S. Waugh at the Center for Cancer Research at the National Cancer Institute) was used for HO-1 and thrombin was used for HO-2, CPR, and BVR. The

affinity tags were separated from the protein by chromatography with the appropriate affinity resin (Ni-NTA for HO-1, HO-2 and CPR; Glutathione Sepharose for BVR). All purification steps were performed at 4°C.

The cDNA for human full-length HO-1 was graciously supplied by Dr. Ortiz de Montellano (University of California, San Francisco, CA). The LIC expression vector pMCSG10 was donated by Dr. William Clay Brown (University of Michigan, Ann Arbor, MI). Human full-length HO-2 cDNA in a pGEX-4T-2 vector was generously contributed by Dr. Mahin D. Maines (University of Rochester, School of Medicine, Rochester, NY) and was subcloned into the pET28a(+) expression vector. CPR was kindly donated by Dr. Bettie Sue Masters (University of Texas Health Sciences Center, Arlington, TX). The *BVR* gene was purchased from American Type Culture Collection (Manassas, VA) and subcloned into the pGEX-4T-2 plasmid.

2.3.3 Site-directed mutageneisis of HO-1 and HO-2

Single-site substitutions of HO-1 and HO-2 were constructed using the QuickChange site-directed mutagenesis protocol (Stratagene, La Jolla, CA). Oligonucleotides were synthesized by Integrated DNA Technologies (Coralville, Iowa). Positive transformants were enriched by antibiotic selection and confirmed using sequence analysis. All of the variants were purified exactly as described above for the wild type enzymes.

2.3.4 Preparation of NMR samples

BL21(DE3) cells containing the pET28a(+)/HO-2 plasmid were cultured in M9 minimal media with 1.0 g/L $^{15}NH_4Cl$ (Cambridge Isotopes, Tewksbury, MA, USA) to achieve ^{15}N labeling of the soluble HO-2 protein. HO-2 was purified as described above and loaded with heme by titration of freshly prepared hemin. Hemin stocks were prepared by solubilizing hemin in 15% dimethyl sulfoxide (DMSO), 0.1 M NaOH, 50 mM Tris pH 7.0. Hemin stocks were centrifuged at 17,000 x g for 10 min at 4°C and the supernatant was then passed through a 0.22 micron filter (Millipore, Billerica, MA) to remove insoluble matter. Hemin concentration was determined using an Σ_{385nm} of 58.44 mM^{-1}(43). HO-2 was loaded with hemin by titrating in small amounts of hemin and monitoring the Soret peak at 404 nm until saturating levels of heme binding were

achieved. NMR samples were prepared with 150 μM heme-bound HO-2 in 50 mM Tris-HCl pH 7.0, 50 mM KCl with 10% D_2O in a total volume of 350 μl and placed in a Shigemi NMR tube. Experiments testing the ability of CPR or BVR to bind HO-2 were conducted with 150 μM HO-2 and the binding partner (BVR or CPR) at the indicated concentration.

^{1}H-^{15}N apoHO-2 NMR TROSY samples were prepared identically to those described for hHO-2, however heme was absent from the samples.

For perdeuterated ^{15}N-HO-2, samples were prepared as described above, however BL21(DE3) cells were grown and induced in $^{2}H_2O$-M9 minimal media. Electrospray ionization mass spectrometry analysis revealed label incorporation to be 99.8%.

2.3.5 ^{1}H-^{15}N TROSY NMR measurements

Two-dimensional ^{1}H-^{15}N HSQC TROSY spectra were acquired on an Agilent/Varian 800 MHz spectrometer equipped with a triple resonance gradient (PFG) cryo probe operating at 30°C. Spectra were acquired using an array of 2404 x 300 complex points and with the spectral widths of 12019.2 Hz and 2999.9 Hz for ^{1}H and ^{15}N respectively. All spectra were processed with NMRPipe software (44) and visualized using Sparky 3.114 (45). Intensity analysis was conducted as described (46); the peak heights of chemical shifts were derived from Sparky and used to calculate the ratio of resonance height for the ^{1}H- ^{15}N HO-2 spectrum with and without CPR or BVR. The chemical shift perturbation (CSP) for the assigned crosspeaks was measured between the 0 μM CPR spectrum and the 75 or 150 μM CPR spectrum for the perdeuterated ^{15}N-hHO-2 TROSY spectrum. CSPs were calculated from the square root of the sum of the squared $N^{1}H$ and ^{15}N CSPs for each assigned cross peak.

2.3.6 Determination of HO-2 molecular mass by NMR relaxation experiments

The experiments for studying the ^{15}N NMR relaxation of HO-2 were carried out using a 40 μM HO-2 sample that was ^{15}N labeled, in 50 mM Tris-HCl, 50 mM KCl pH 7.0, recorded at 30 °C on a Agilent/Varian 800 MHz NMR System, using a cryo probe.

1D versions of the standard ^{15}N R_1 and ^{15}N R_2 HSQC experiments (with cross correlation, but with without R_{ex} suppression) were carried out (47). In these experiments, amide proton magnetization is transferred to the amide ^{15}N, where it is allowed to decay according to ^{15}N R_1 or R_2 relaxation mechanisms, and transferred back to the amide proton for observation. R_2 relaxation is faster for larger than for smaller molecules; R_1 relaxation is slower for larger than for smaller molecules. From the ratio one may calculate the rotational correlation time. For spherical, rigid proteins, the rotational correlation time is proportional to the molecular weight. The data was processed in NMR pipe, and exported in text format using the Pipe2txt.tcl routine. The data were then imported into Microsoft Excel. For each spectrum, the ranges 8.7-9.0 ppm (structured core residues) were integrated and the data were fit to a single exponential decay curve using in-house written non-linear least square fit code with jackknife error estimation (48).

2.3.7 Steady-state kinetic analysis of HO-1, HO-2 and variants

The HO enzymatic assay was modified from previously described methods (49,50). Recent studies establish that catalase enhances the linearity of the membrane-bound HO-1-catalyzed reaction (50). In our soluble system, we found a similar benefit of catalase for both HO-1 and HO-2 and therefore included it in the enzymatic assays. The 200 μl reaction contained 0.1 μM HO, 15 μM heme, 0.35 μM BVR, 0.25 μg/μl BSA, 20 U/μl catalase and varying concentrations of CPR in reaction buffer (50 mM Tris-HCl, pH 8.0, 50 mM KCl). The reaction was incubated at 37°C for 2 minutes and then initiated with the addition of 8 μl of 10mM NADPH. Activity was monitored using a Shimadzu UV-2600 spectrophotometer by following the increase in bilirubin absorbance at 468 nm. The difference extinction coefficient between heme and bilirubin at 468 nm of 43 mM^{-1} cm^{-1} was used.

2.3.8 Size exclusion chromatography analysis of HO-1, HO-2, and CPR

For gel filtration experiments, proteins were dialyzed into buffer containing 50 mM Tris-HCl, pH 7.0, 50 mM KCl. After recovery from the dialysis tubing, samples were prepared with 50 μM of the indicated protein, 150 μM heme and 150 μM $NADP^+$. Gel

filtration was conducted with a Shimadzu HPLC with an LC-10AT pump system using a Shodex KW-803 column (Shodex, Torrance, CA). The column was calibrated using gel filtration standards (BioRad, Hercules, CA) and the void volume was determined using blue dextran (2,000 kDa, Sigma, St Louis, MO).

2.3.9 Surface Plasmon Resonance with HO-1, HO-2, and CPR

SPR binding experiments were conducted using a BIAcore 2000 (GE Healthcare, Pittsburgh, PA) at 25°C in 50 mM Tris pH 7.0, 50 mM KCl with 0.005% surfactant p20. HO-1 or HO-2 was immobilized directly to the dextran matrix of a research grade CM5 sensor chip by amine coupling according to the manufacturers instructions (GE Healthcare, Pittsburgh, PA). The sensor chip surface was activated with NHS/EDC for 7 minutes. Immobilized proteins were diluted to 0.001 μg/μl with 10 mM sodium acetate pH 4.5 and injected over the sensor chip surface. To minimize nonspecific binding and mass transfer immobilization levels were kept below 1000 RU. HO-1 and HO-2 were immobilized to 900 and 300 RU, respectively.

For kinetic analysis of CPR and HO, 45 μl of varying concentrations of CPR were injected at a flow rate of 20 μl/min. Chip regeneration was conducted with a 5 μl injection of 0.5 mM NaCl. A blank reference cell was subtracted from the experimental data. To determine kinetic parameters, three independent experiments were initially analyzed using BIAevaluation software (GE Healthcare) and fit to a 1:1 Langmuir binding model or a bivalent analyte model. Because these models fit the data poorly, the association phase of CPR binding to HO was analyzed using single exponential fits (GraphPad 6.0). Kinetic constants were determined from the linear regression of k_{obs} values plotted against CPR concentration.

For experiments with immobilized CPR, human CPR was immobilized to the CM5 chip according to previously described methods for immobilization of rat CPR (24). Briefly, CPR was immobilized via thiol groups of cysteine residues with the coupling reagent 2-(2-pyridinyldithio)ethaneamine). To stabilize the enzyme and protect residues near the NADPH binding site, NADPH was included during the immobilization of CPR. CPR was immobilized to ~2000 response units. Others have reported that modification of CPR by 2-(2-pyridinyldithio)ethaneamine) does not affect enzyme activity (24).

Binding analysis with immobilized CPR was performed identically to those described above, with freshly prepared hemin as the soluble analyte.

2.3.10 Sedimentation velocity analysis of HO-2 and CPR

Binding interactions between HO-2 and CPR were analyzed by sedimentation velocity experiments using a method described previously (51). Sedimentation velocity experiments were performed on an Optima XL-I analytical ultracentrifuge (Beckman coulter, Inc.) equipped with an eight-hole An50Ti rotor. Prior to analysis, HO-2 and CPR were dialyzed against 50 mM Tris pH 8.0 containing 150 mM NaCl. CPR (20.5 μM) was then mixed with increasing concentrations of HO-2 (0-55 μM) and the resulting protein mixtures (400 μl) were loaded into the sample compartment of a double-sector cell. The reference compartment was filled with 430 μl of the dialysate buffer. Sample cells were then incubated at 20^{o}C in the rotor chamber for 2 h under vacuum. After 2 h of incubation, samples were sedimented at 40,000 rpm. A total of 180 absorbance scans (450 nm) at 3 min intervals were collected. Absorbance values ranged from 0.2-0.8 for the different samples. The data were analyzed by SEDFIT version 10.58d (52) using the continuous *c*(*s*) distribution model and allowing the frictional ratio to float. CPR-/HO-2 interactions were monitored by integrating the *c*(*s*) distribution between 4 and 7 S to determine the weight-average *s*-value of the new observed boundary component (51). A K_d value for the CPR/HO-2 complex was estimated by plotting the weight-average *s*-value as a function of HO-2 and fitting the data to a single-site binding isotherm.

2.3.11 Chemical cross-linking of HO-1 and HO-2 with CPR, BVR or RNase

The reducible, heterobifunctional cross-linker (succinimidyl 6-(3-[2-pyridyldithio]-propionamido)hexanoate) (LC-SPDP) was used in a two-step reaction according to the manufacturer's instructions (Thermo Scientific/Pierce, Rockford, IL). HO-1 or HO-2 was activated as follows: a fresh 3 mM solution of LC-SPDP was prepared in DMSO. 10 μM HO-1 or HO-2 was prepared in conjugation buffer (0.1 M 4-(2-hydroxyethyl)-1-piperazineethanesulfonic acid (HEPES), pH 7.5, 30 mM ethylenediaminetetraacetic acid (EDTA), 150 mM NaCl) and incubated with 0.1 mM LC-SPDP for 30 min at room temperature. Unconjugated cross-linker was then removed by 3 rounds of buffer exchange using 10,000 MWCO Amicon microconcentrators (Millipore, Billerica, MA). 10

μM BVR, CPR, or RNase was then added to the activated protein and the reaction was incubated at 4°C overnight. Cross-linking reactions were analyzed by 5-15% gradient sodium dodecyl sulfate polyacrylamide gel electrophoresis (SDS PAGE) (BioRad, Berkeley, CA) and visualized by staining the gel with Coomassie blue (53).

2.3.12 Co-purification of BVR with HO-2

For the co-purification of BVR with HO-2, the cross-linking reaction was performed exactly as described above, however HO-2 contained an N-terminal 6xHis tag (hisHO-2) that was absent in the other reactions. By SDS-PAGE, the cross-linked products of the reaction containing hisHO-2 and BVR migrated to identical positions as those in which the 6xHis tag had been removed from HO-2. Samples of hisHO-2 alone, BVR alone, or cross-linked hisHO-2/BVR were incubated with 100 μl of Ni NTA resin (50% slurry) for 2 hours at 4°C. Samples were rotated on a Boekel variable speed mini-tube rotator (Fisher Scientific, Pittsburgh, PA). Affinity resin and associated proteins were harvested by centrifugation for 5 minutes at a setting of 2,400 x g at 4°C with an accuSpin Micro 17R refrigerated microcentrifuge (Fisher Scientific, Pittsburgh, PA) and washed three times with 1 ml of wash buffer (50 mM Tris-HCl pH 8.0, 30 mM NaCl, 20 mM imidazole). Protein bound to the resin was eluted with 50 mM Tris-HCl, pH 8.0, 30 mM NaCl, 300 mM imidazole. Eluted fractions were boiled for 5 minutes in SDS-PAGE loading buffer (50 mM Tris-HCL, pH 6.8, 2% (w/v) SDS, 0.1% (w/v) bromophenol blue, 10% (v/v) glycerol, and 100 mM dithiothreitol) and separated by 10% SDS PAGE (53). Proteins were then transferred to a nitrocellulose membrane and detected using antibodies against either HO-2 (18) or BVR (Abcam, Cambridge, MA).

2.3.13 Modification of BVR with CPM

Human BVR was modified with 7-diethylamino-3-(4'-maleimidylphenyl)-4-methylcoumarin (CPM) according to methods used to modify rat BVR (27). A 20 mM solution of CPM was prepared in dimethyl sulfoxide. 10 μM BVR with 1 mM NADPH was incubated in the dark with 100 μM CPM at 4°C for 16 h. Free CPM was removed using a PD-10 desalting column (Amersham, Buckinghamshire, England). Labeled BVR

was then frozen and stored in the dark at -80°C. BVR-CPM was analyzed by LC MS/MS to determine the location of the CPM modification.

2.3.14 Fluorescence resonance energy transfer (FRET): Analysis of the interaction of HO-1 or HO-2 with BVR

FRET experiments to examine HO-1 or HO-2 binding to human BVR were conducted according to previously described methods for rat BVR (27). Briefly, because the UV-visible spectra of heme-bound HO-1 and HO-2 overlap the fluorescence emission spectrum of the fluorescent probe CPM, binding of heme bound HO should result in fluorescence quenching of BVR-CPM. BVR-CPM (0.05 μM) was titrated with various concentrations of heme-bound HO-1, heme-bound HO-2, or heme, and fluorescence was monitored at 450 nm with excitation at 350 nm. These experiments were performed in 0.1 M potassium phosphate buffer at pH 7.4 on a Shimadzu FR-5301PC spectrofluorophotometer.

2.3.15 Heme binding BVR by optical absorbance

To obtain the absorbance spectrum of heme BVR, the difference spectra between 350 and 700 nm was recorded for 2.5 μM BVR with 2.0 μM heme, while the reference cuvette contained 2.5 μM BVR alone. To determine binding affinity of heme for BVR, 10 μM hemin was titrated with increasing amounts of BVR (0.5 - 5.0 μM) with 10 μM heme alone in the reference cuvette. Absorbance at 415 nm vs BVR concentration was fit to a single site binding model using GraphPad Prism 6.0. To asses the ability of BVR to bind heme from hHO-2, 5 μM of hHO-2 was incubated with varying concentrations of BVR (1.0 – 20.0 μM) and the absorbance spectra from 250 - 700 nm was collected, with the reference cuvette containing 5 μM hHO-2. hHO-2 was prepared by incubating apoHO-2 with a 5-fold excess of freshly prepared hemin for 1 h at 4°C. Unbound heme was removed using a PD 10 desalting colum according to the manufacturers instructions (GE healthcare). For all experiments fresh hemin was used, prepared as described above. All spectra were collected on a Shimadzu UV-2600 spectrophotometer.

2.4 Experimental results

Various forms of HO and CPR lacking their transmembrane segments were used in these studies. These are HO-1(1-265) containing residues 1-265, HO-2(1-288) and CPR(66-680). For clarity, these proteins will be referred to simply as HO-1, HO-2 or CPR. In experiments that use heme-bound HO, we refer to the protein as hHO-1 or hHO-2.

2.4.1 NMR analysis of the interaction between hHO-2 and CPR

Nuclear magnetic resonance (NMR) is a highly sensitive method to probe protein-protein interactions. Binding of an NMR-silent protein to an NMR-visible protein can perturb the spectrum in several ways: it can change the chemical shift, alter the line width of a resonance, or affect both chemical shift and line width. If resonances within the NMR spectrum have been assigned, these spectral changes can provide residue-specific information regarding the interface between the two proteins.

We recently assigned 70% of the backbone chemical shifts of the hHO-2 (heme bound) NMR spectrum by 3D NMR experiments using a highly concentrated sample (1 mM) (Bagai, Ragsdale & Zuiderweg, in preparation). To avoid potential non-specific interaction effects that could arise with highly concentrated protein, in the binding studies described here, we used 150 μM ^{15}N hHO-2 samples. Because large proteins such as HO-2 (~33 kDa) tend to exhibit faster transverse relaxation that reduces signal intensity of the NMR spectrum, we utilized transverse relaxation-optimized spectroscopy (TROSY). TROSY is a method that reduces the ^{1}H and ^{15}N resonance linewidths to enhance the spectra of larger proteins (>30 kDa) (54). By applying TROSY, we observe 211 cross peaks in the ^{1}H-^{15}N TROSY spectrum of perdeuterated ^{15}N-hHO-2, which accounts for resonances arising from ~70% of the hHO-2 residues (Figure 2.2). The hHO-2 spectrum consists of resonances arising from both ordered and disordered regions of the protein. Amide proton resonances arising from disordered regions of HO-2 occur in the 7.7-8.6 ppm range, which has a high density of overlapping peaks characteristic of poorly structured regions (46). This region of the spectrum corresponds to the flexible N- and C- terminal domains of hHO-2; residues 1–28 and 243-288. The well-dispersed peaks outside of the disordered region arise from the core of hHO-2, as

highlighted by the annotated spectra (Figure 2.2) (Bagai, Ragsdale & Zuiderweg, in preparation). Also, in the crystal structure of HO-2 (PDB 2QPP) only the catalytic core of the protein (residues 29-242) is visible, and both the N- and C- termini are not observed, further supporting the flexibility of the N- and C- termini (55).

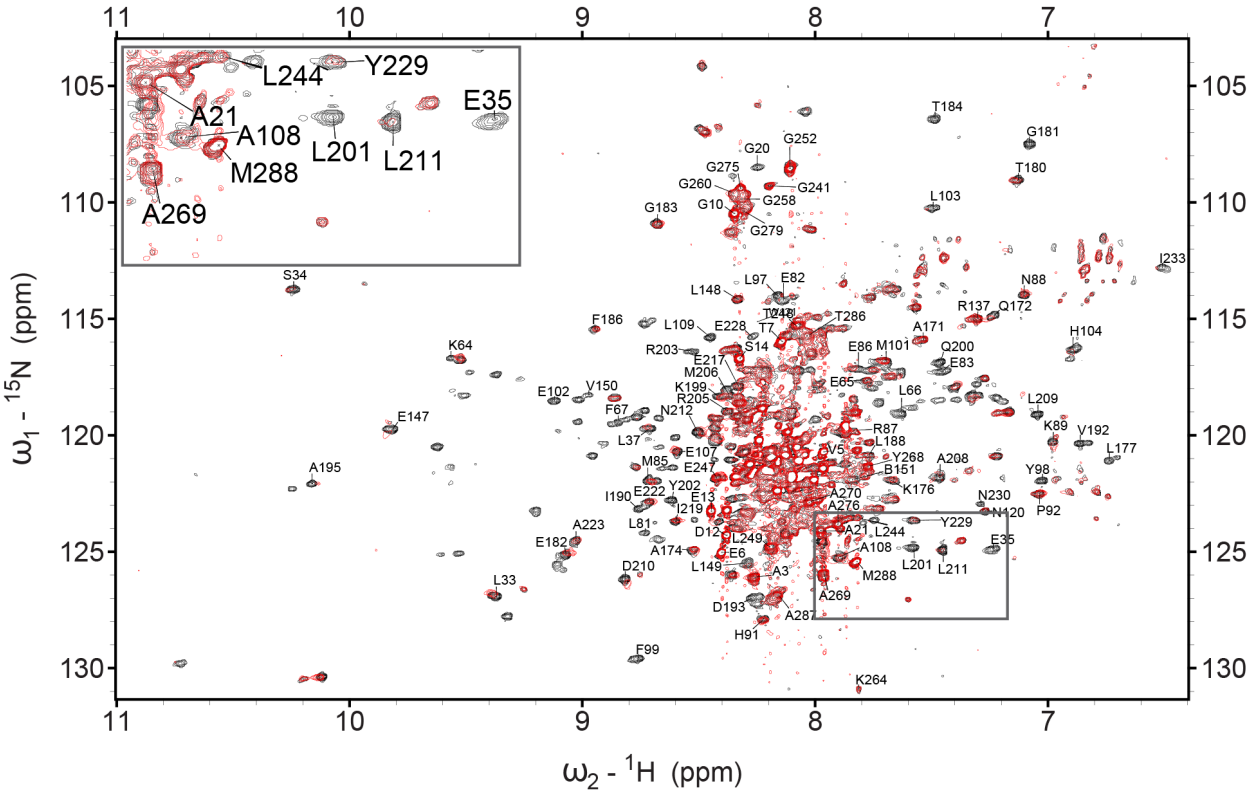

Figure 2.2. **NMR analysis of CPR binding hHO-2.** ^{1}H-^{15}N TROSY spectra of 150 μM perdeuterated ^{15}N-hHO-2 collected in the absence (black) or presence (red) of equimolar CPR.

To probe the interface between hHO-2 and CPR, we collected the spectrum of perdeuterated ^{15}N-hHO-2 in the presence or absence of natural abundance CPR (lacking any label). As noted above, we used a lower concentration of hHO-2 (150 μM) than was used earlier to make the assignments in order to minimize the potential for non-specific effects such as aggregation. We overlayed the assigned HO-2 spectrum with that collected in the binding studies to determine assignments for the spectrum in the binding studies. Using this method, ~50% of the 288 HO-2 residues in the binding

study could be assigned. Analysis of the HO-2 spectrum described below will focus on the assigned region of the protein.

We measured the chemical shift and peak height for resonances in the hHO-2 TROSY spectrum in the presence and absence of CPR. To identify hHO-2 residues that are affected by CPR, we compared the ^{1}H- ^{15}N TROSY spectrum of hHO-2 in the presence of equimolar unlabeled CPR to that of hHO-2 alone. The addition of CPR to hHO-2 causes changes in hHO-2 chemical shifts and also decreases in peak intensities for a number of hHO-2 residues (Figure 2.2). This peak intensity loss is consistent with an increase in molecular weight and concomitant reduction of TROSY intensity that we would expect to occur as hHO-2 molecular weight increases with the binding of a 70 kDa protein such as CPR (46,56).

The addition of CPR to hHO-2 also results in chemical shift perturbations (CSPs) for some hHO-2 cross peaks (Figure 2.3). This demonstrates that the kinetics of binding is in the fast or intermediate fast exchange for which the resonance position ω_i^{obs} of a certain residue *i* is given by (57)

$$\omega_i^{obs} = f_{free}\omega_i^{free} + f_{bound}\omega_i^{bound} \qquad \text{[Equation 3]}$$

where f_{free} and f_{bound} are the molar fractions of free and complexed HO-2 and where ω_i^{free} and ω_i^{bound} bound are the chemical shifts in radians of that resonance in those states. The equation holds for both ^{1}H and ^{15}N dimensions in the TROSY spectrum.

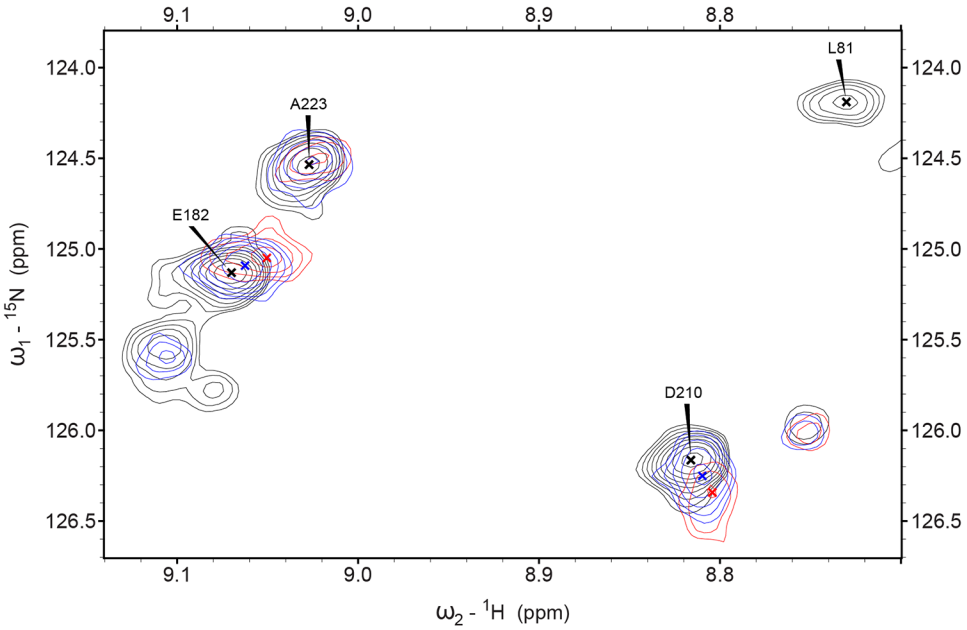

Figure 2.3. **The effect of CPR on hHO-2 chemical shifts.** Detail of the ^{1}H-^{15}N hHO-2 spectrum with 0, 75, or 150 μM CPR (black, blue, and red respectively) highlighting cross peaks that experience significant perturbations of the chemical shift or significant intensity loss. E182 and D210 show highly significant change in chemical shifts, while L81 is broadened beyond detection with the addition of CPR. "x" represents the center of the indicated cross peak. Highly significant changes in CSP are greater than 2 standard deviations from the mean CSP for assigned residues.

To quantify CSPs, the ^{1}H and ^{15}N chemical shift difference was calculated by comparing the chemical shifts of hHO-2 alone to those with CPR. The combined $^{15}N/NH$ chemical shift change was calculated as the chemical shift change vector as described in the Experimental Methods. Of the 47 assigned cross peaks in the N- and C- termini, non exhibit significant CSPs with the addition of equimolar CPR; however 28 residues of the 96 assigned residues from the HO-2 core exhibit significant CSPs (~30%) (Figure 2.4). Mapping the residues with significant CSPs onto the hHO-2 crystal structure highlights contiguous patches of residues on HO-2 that are likely involved in binding CPR or experience allosteric effects upon CPR binding (Figure 2.5) Equally important, there are also many assigned resonances that do not shift, and they also form contiguous patches.

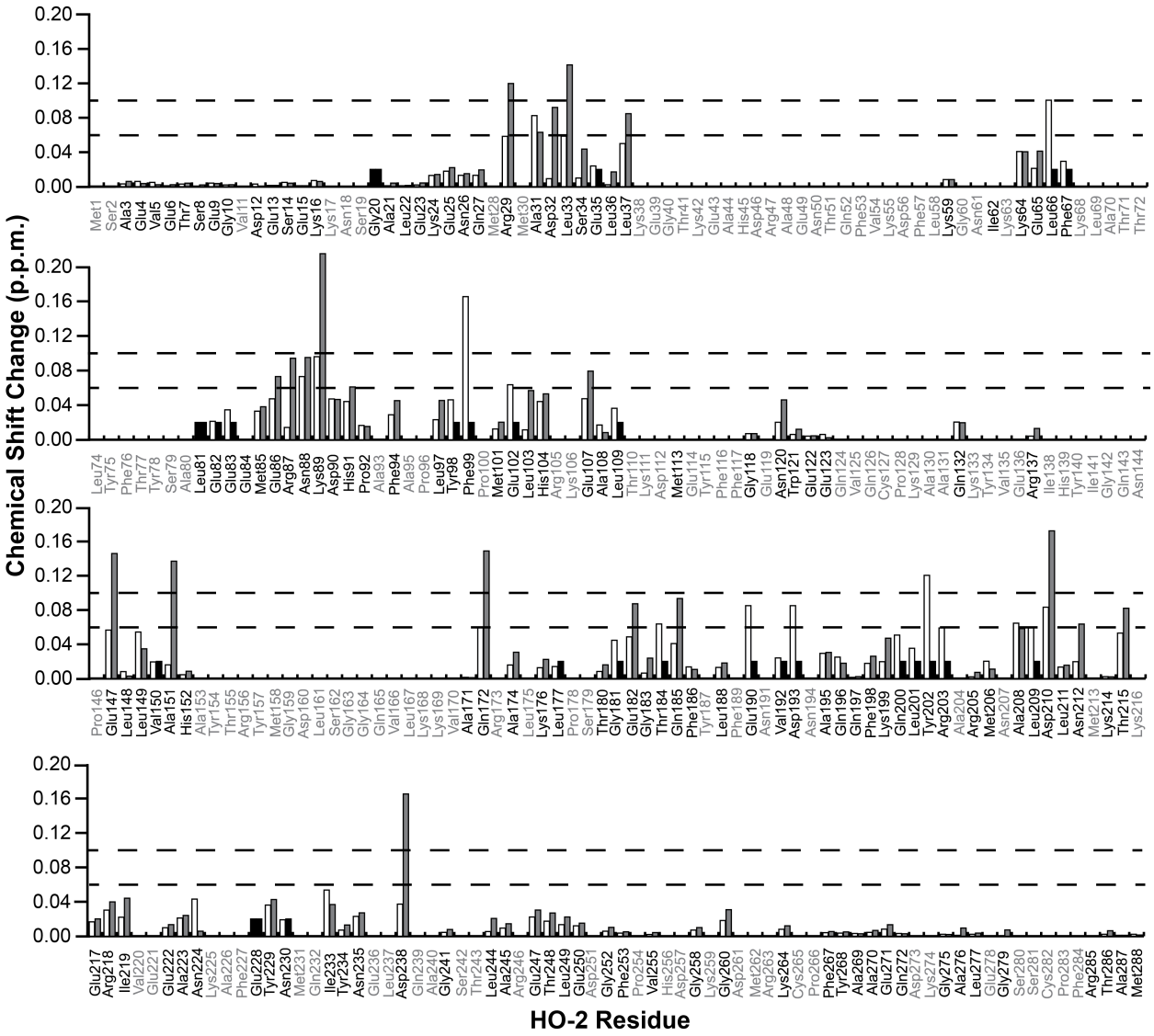

Figure 2.4. **The effect of CPR on hHO-2 chemical shifts.** Histogram bars represent the combined ^{15}N/NH chemical shift perturbation (CSP) for assigned residues in the hHO-2 spectrum in the presence of 75 μM or 150 μM CPR (white or grey respectively). The CSP for the assigned cross peaks, measured between the 0 μM CPR spectrum and the 75 or 150 μM CPR spectrum, was calculated from the square root of the sum of the squared N^1H and ^{15}N CSPs. Cross peaks that have broadened beyond detection with the addition of CPR are shown as black bars of uniform height. Dotted lines indicate CSPs that are significant (1 standard deviation from the mean) or very significant (2 standard deviations from the mean). Bars with greyed labels represent resonances that are unassigned, while assigned residues are in black.

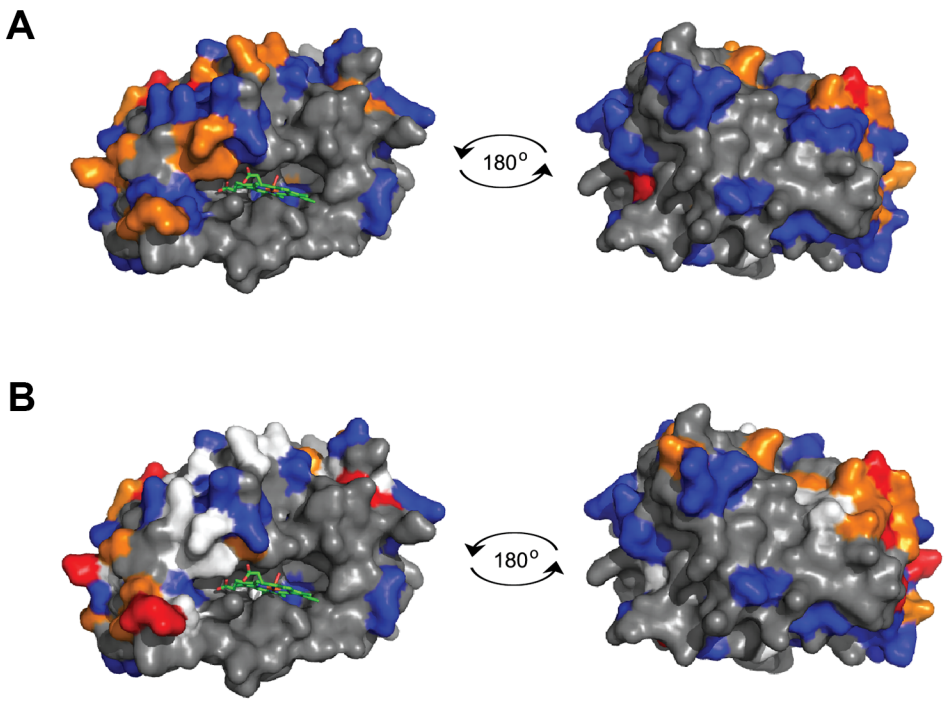

Figure 2.5. **CPR induced CSPs on the hHO-2 spectrum mapped onto the crystal structure.** The effect of 75 or 150 μM CPR (**(A)**, and **(B)** respectively) on hHO-2 CSPs as determined in Figure 2.4 mapped on to the crystal structure of hHO-2 (PDB 2QPP). The color of the residue reflects the degree of CSP effect by CPR. Red: residues with highly significant CSPs (more than two standard deviations from the mean); Orange: residues with significant CSPs (at least one standard deviation from the mean); Blue: residues with no significant CSP; White: residues that are broadened beyond detection; Grey: residues that are unassigned.

For the range 0.1 < f_{free} or f_{bound} < 0.9, the linewidth LW_i^{obs} for a resonance *i* in the fast/ intermediate exchange regime is given by Equation 4 (57).

$$LW_i^{obs} = f_{free} LW_i^{free} + f_{bound} LW_i^{bound} + f_{free}\, f_{bound} \frac{(\omega_i^{free} - \omega_i^{bound})^2}{(1 + f_{bound}/f_{free}) k_{off}} \qquad \text{[Equation 4]}$$

Here, the first two terms represent the increase in linewidth due to a change in the time-averaged molecular weight of HO-2, while the latter term, called exchange broadening, is excess broadening due to the kinetics of binding.

The increase in linewidth causes a loss in TROSY cross peak height by two processes: the first is a linear effect and occurs because a broader line in the *spectrum*

has a lower peak height; the second is a strongly non-linear effect due to a decrease in the coherence transfer efficiencies in the TROSY *experiment* itself. For large proteins that bind to other large proteins, the second effect is dominant.

To quantify the peak intensity loss in the hHO-2 spectrum upon CPR binding, the peak intensity ratio was determined by dividing the cross peak intensity in the presence of CPR by the cross peak intensity from the hHO-2 alone spectrum (+CPR/-CPR) (Figure 2.6). A ratio of 1 indicates no effect, while a decreased ratio indicates line broadening for that resonance. Cross peaks deriving from residues located at the HO-2 N- and C-termini (residues 1-28 and 243-288) are largely unaffected by the addition of equimolar CPR; of the 47 assigned cross peaks, only 4 exhibit chemical shift intensity ratios of less than 0.8 (G20, A245, and E247). This is in contrast to the 96 assigned cross peaks located at the core of HO-2 (residues 29-242); 88 resonances exhibit an intensity ratio of less than 0.8 and 23 have disappeared likely due to broadening beyond detection (Figure 2.6). Mapping the intensity ratios onto the hHO-2 crystal structure shows the residues that are most strongly affected by CPR are on the heme binding face of hHO-2 (in which the heme binding pocket and surrounding residues are visible), while residues on the opposite face (180° rotation) of hHO-2 are less affected (Figure 2.7).

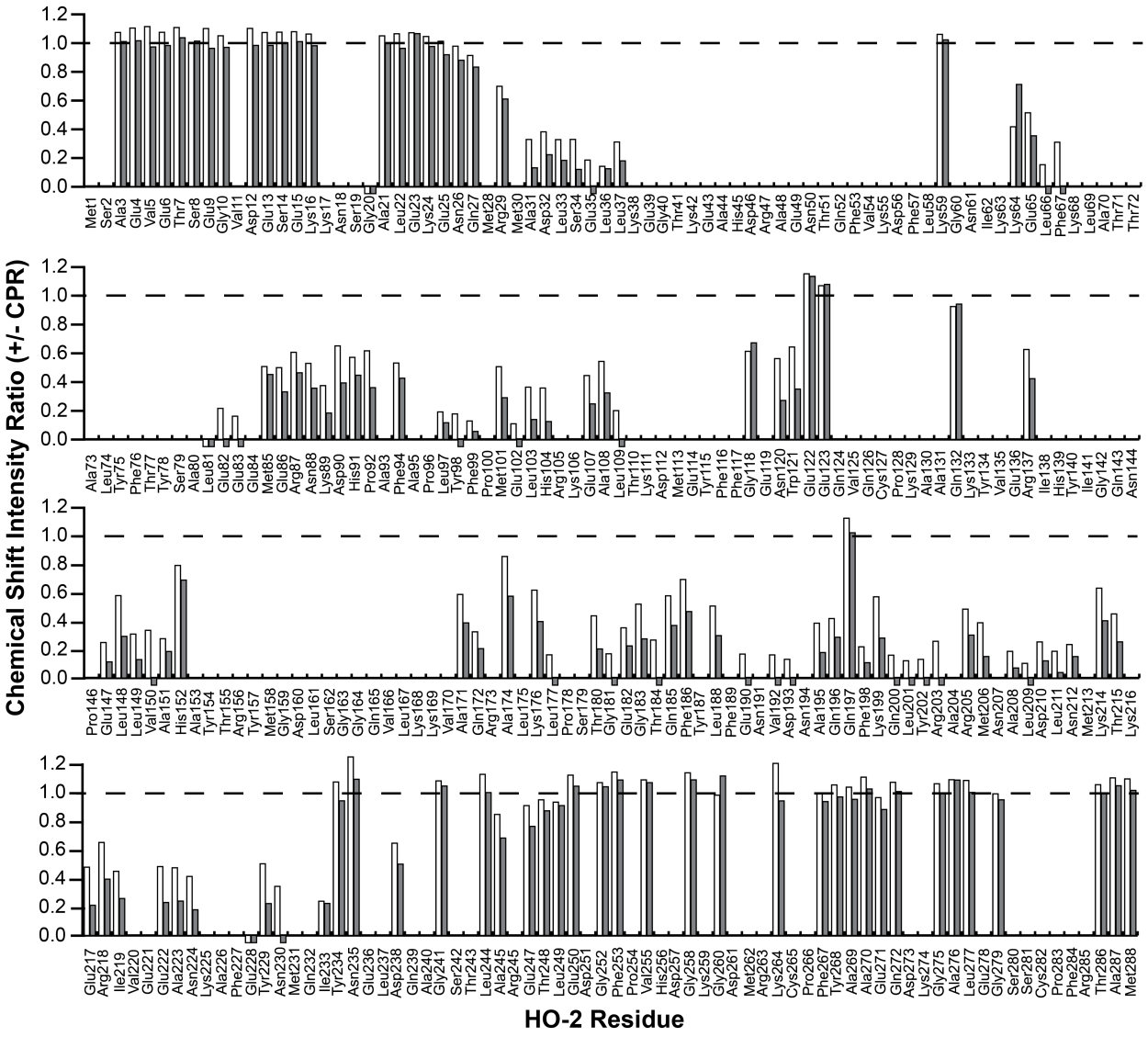

Figure 2.6. **The effect of CPR on perdeuterated hHO-2 chemical shift intensities.** Histogram bars represent the ratio of peak height in the absence or presence of CPR (+CPR/-CPR). Ratios with 75, and 150 μM CPR are shown (white and grey, respectively). A ratio of 1 (dotted line) indicates no change for that residue. Negative bars represent cross peaks that are broadened beyond detection with the addition of CPR. Bars that are absent represent residues that are unassigned in the spectrum.

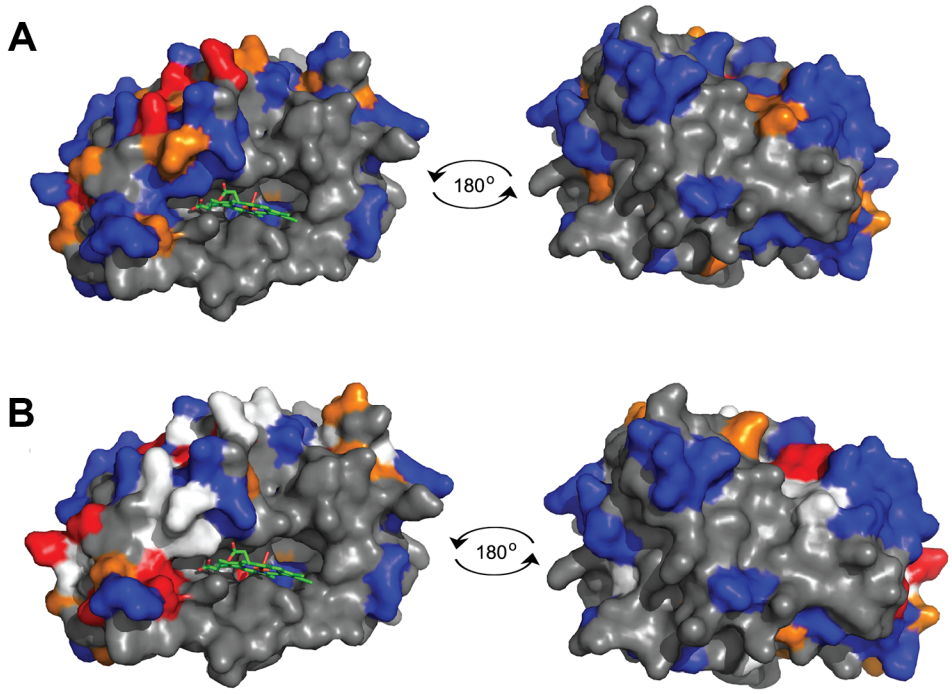

Figure 2.7. CPR induced changes for hHO-2 cross peak intensities mapped onto the crystal structure. The effect of 75 or 150 μM CPR (**(A)**, and **(B)** respectively) on hHO-2 cross peak heights mapped on to the crystal structure of hHO-2 (PDB 2QPP). Cross peak intensity ratios are as determined in Figure 2.6. The color of the residue reflects the degree of effect by CPR. Red: ratio of 0 < 0.2; Orange: ratio of 0.2 < 0.3; Blue: ratio > 0.3; White: residues that are broadened beyond detection; Grey: residues that are unassigned.

The interaction areas determined from intensity changes (Figure 2.5) and chemical shift changes (Figure 2.7) do overlap in general, suggesting the main binding area is identified by both observables. However, the intensity changes and chemical shifts do not correlate per residue. The most compelling case occurs for the resonance of L201, which completely disappears while large changes in chemical shift are not observed. As discussed below, this discrepancy indicates a complex binding mechanism.

2.4.2 A titration of CPR into hHO-2 by NMR

If the effects of CPR on the hHO-2 spectrum are due to CPR binding, changes induced by CPR should be titratable. Thus, additional experiments were conducted with 50 μM, 150 μM, 200 μM, and 300 μM CPR and the resonance height ratio calculated as

described above (Figure 2.8 and Figure 2.9). Under these conditions, using hHO-2 that was not perdeuterated, we observe 165 cross peaks in the ^{1}H- ^{15}N hHO-2 spectrum, which accounts for resonances arising from ~60% of the hHO-2 residues. Comparison of these spectra with the assigned spectrum allows for assignment of 36% of 288 HO-2 residues (Figure 2.9).

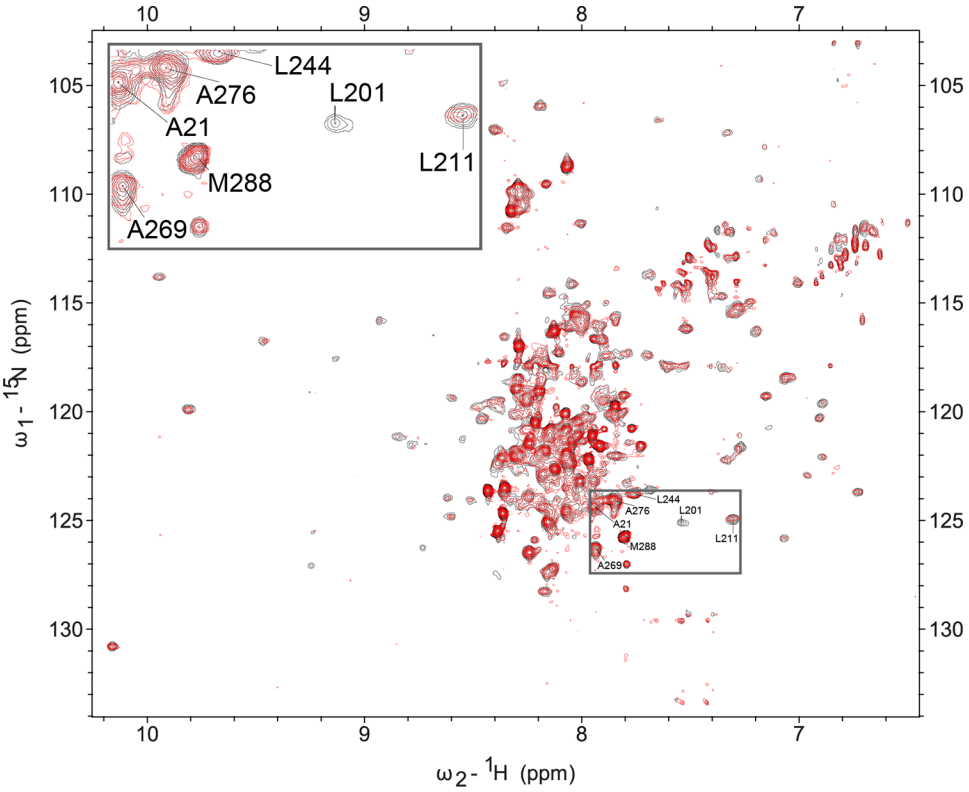

Figure 2.8. **NMR analysis of CPR binding non-perdeuterated ^{15}N hHO-2.** ^{1}H- ^{15}N TROSY spectra of 150 μM non-perdeuterated ^{15}N-hHO-2 collected in the absence (black) or presence (red) of equimolar CPR.

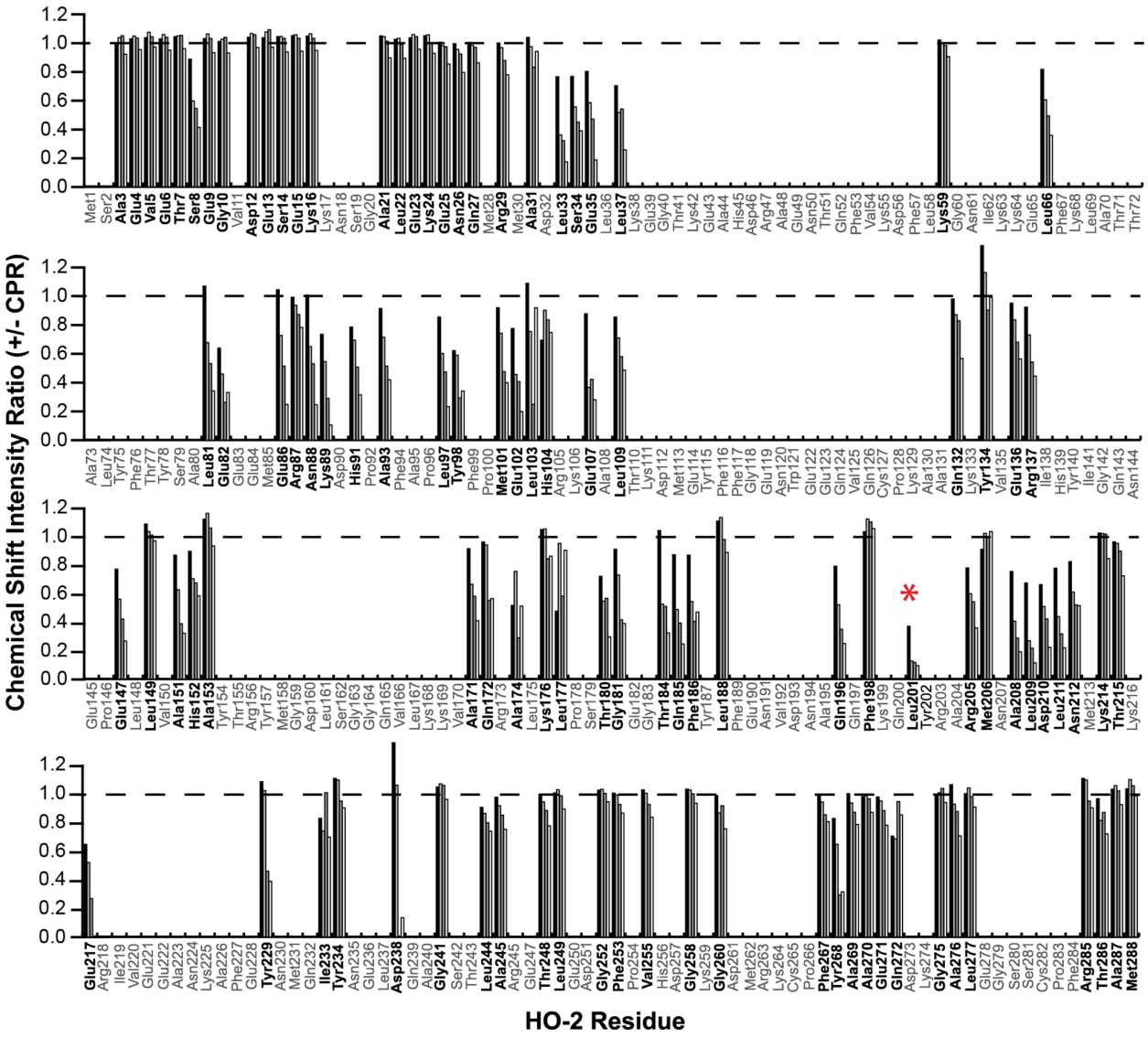

Figure 2.9. **The effect of various concentrations of CPR on non-perdeuterated ^{15}N-hHO-2 resonances.** Histogram bars represent the ratio of resonance height in the absence or presence of CPR (+CPR/-CPR). Ratios with 50, 150, 200 and 300 μM CPR are shown (black, light grey, dark grey and white bars respectively). A ratio of 1 (dotted line) indicates no change for that residue. Bars that are absent (greyed label) represent resonances that are unassigned, while assigned residues are in bold. The asterisk highlights L201 as the cross peak that is most sensitive to the addition of CPR.

To quantify the effects of CPR on hHO-2 residues, we compared the ^{1}H- ^{15}N TROSY spectrum of hHO-2 in the presence of CPR to that of hHO-2 alone. While the addition of CPR to hHO-2 does not cause observable changes in hHO-2 chemical shifts in the TROSY spectrum for non-perdeuterated hHO-2, a decrease in peak intensity for a

number of hHO-2 residues proportional to the concentration of CPR is observed (Figure 2.9). Although titratable changes in the HO-2 spectrum could conceivably result from CPR-dependent catalytic activity of HO-2, this is unlikely to be the cause of the observed intensity changes because NADPH in not present in the NMR experiment and HO-2 is inactive in its absence. Furthermore, CPR causes similar peak height reduction for the apoHO-2 spectrum – here substrate and reducing equivalents are both absent, preventing any catalytic turnover.

Of the assigned residues in the hHO-2 spectrum, the residue that is most affected by the addition of equimolar concentrations of CPR is L201; cross peak hight is most strongly affected by CPR even at the lowest concentration of CPR (50 μM). E107, A208, L209, L211 and L33 are also strongly affected. While in our 150 μM NMR sample we do not have consecutive assignments for these residues, in the more concentrated multi-dimensional experiments used for assigning the hHO-2 spectrum L201, A208, L209, and L211 are part of a consecutively assigned region E190-N212. L33 is part of a consecutively assigned region from R29-L37 and E107 is part of a consecutively assigned region from E107-L109, so the assignments are quite secure.

We also conducted ^{15}N T_2 and T_1 relaxation experiments to estimate the molecular mass of hHO-2 under the NMR conditions. The rotational correlation time of a protein is linearly related to its molecular weight; therefore, ^{15}N spin relaxation rates can be used to determine the molecular weight of a protein in solution (58). The molecular mass estimate for the hHO-2 core is found to be 55 kDa. The mass of monomeric hHO-2 (1-288) is 33 kDa and that of the hHO-2 core (29-242) is 25 kDa. Thus, the NMR relaxation experiments indicate that hHO-2 is a dimer under the present conditions (> 40 μM protein).

2.4.3 NMR analysis of the interaction between apoHO-2 and CPR

To test the ability of CPR to bind apoHO-2, the ^{1}H- ^{15}N spectrum of 500 μM non-perdeuterated ^{15}N-apoHO-2 was collected in the presence or absence of 100 μM CPR, as described for hHO-2. The addition of CPR to apoHO-2 causes a loss of intensity for apoHO-2 cross peaks similar to what is observed in the hHO-2 spectrum (Figure 2.10). In the apoHO-2 spectrum, 121 distinct cross peaks are visible, representing ~40% of

HO-2 residues. While assignments for the apoHO-2 spectrum have not been determined, changes in chemical shift intensity were quantified by calculating the chemical shift height ratio (+CPR/-CPR) for each of the cross peaks. Of the 121 distinct cross peaks analyzed in the apoHO-2 spectrum, 19 exhibit a chemical shift height ratio of less than 0.8, indicating a loss of cross peak height for the corresponding HO-2 residues. Changes in chemical shift are not observed for any cross peaks in the non-perdeuterated spectra. These data indicate that CPR is capable of binding apoHO-2 as well as hHO-2.

Assignments have not been independently determined for the apoHO-2 TROSY spectrum and the spectrum is distinct from that of hHO-2 (Figure 2.11). However, some isolated cross peaks of the hHO-2 spectrum have identical chemical shifts as in the apoHO-2 spectrum, allowing for a reasonable assignment of the apoHO-2 cross peak from the hHO-2 spectrum, notably L201 (Figure 2.11). Strikingly, of the 121 cross peaks analyzed, the cross peak at the location of L201 in the apoHO-2 spectrum is the most sensitive to the addition of CPR, similar to what is observed for the hHO-2 spectrum.

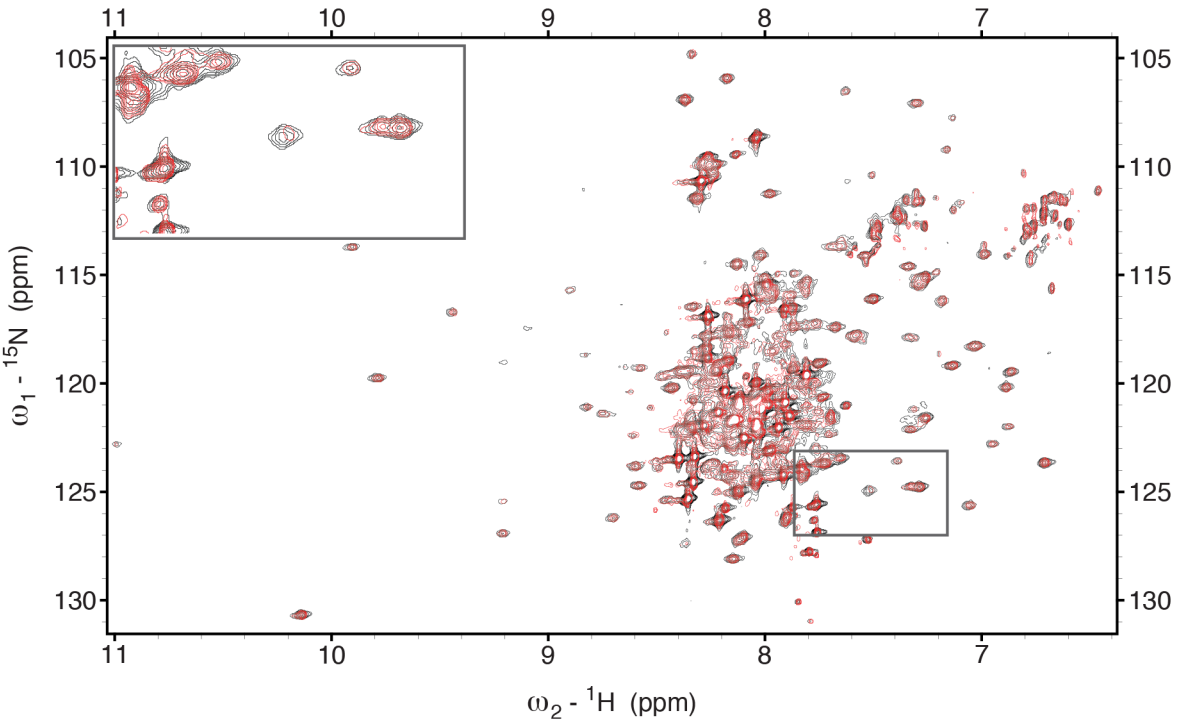

Figure 2.10. **NMR analysis of CPR binding apoHO-2.** ^{1}H-^{15}N TROSY spectra of 500 μM non-perdeuterated ^{15}N-apoHO-2 collected in the absence (black) or presence (red) of 100 μM CPR.

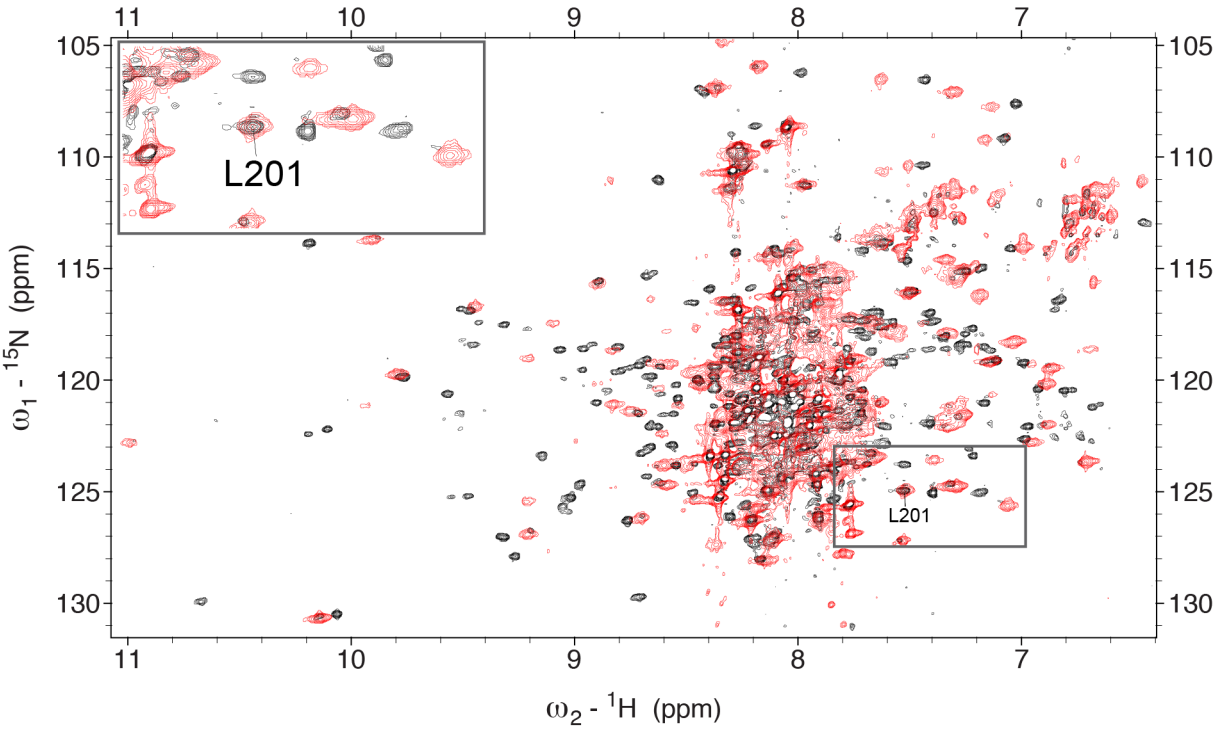

Figure 2.11. **TROSY spectra of hHO-2 (black) and apoHO-2 (red).** ^{1}H-^{15}N TROSY spectra of 150 μM non-perdeuterated^{15}N-hHO-2 (black) or 500 μM non-perdeuterated apoHO-2 (red). The cross peak assigned as L201 for the hHO-2 spectrum is identified.

2.4.4 Steady-state kinetic analysis of HO-1 and HO-2 mutants

Residues that exhibit large changes in the hHO-2 NMR spectrum upon binding CPR could be present at the interface of HO-2 and CPR, or alternatively, they could change their chemical environment due to long-range conformational changes in HO-2 induced by CPR binding at a distant site. In the CPR titration experiments using non-perdueterated HO-2, at all CPR concentrations L201 exhibits the greatest loss of cross peak height compared with the other assigned cross peaks (e.g. a low cross peak height ratio). In the apoHO-2/CPR binding studies L201 is also exhibits the largest loss of cross peak height. Therefore, of the assigned residues in the HO-2 spectrum, we consider L201 to be the most sensitive to the addition of CPR.

Based on the hypothesis that mutation of residues at the HO-2/CPR interface would lead to an increase in K_d for the HO-2/CPR complex and, thus, an increased K_m

value for CPR, we tested the effect of alanine substitutions on steady-state kinetic parameters for L201 and K169, which were expected to exhibit higher K_m values, and R87, which was used as a control. If a residue exhibits changes in the NMR spectrum by indirect effects (e.g., due to a conformational change), making a conservative mutation of that residue is unlikely to affect the K_d or K_m values. Also, we note that HO-2 is likely a homodimer in the NMR binding studies. If a resonance is affected by a change in HO-2 dimerization state, a mutation of that residue would be unlikely to effect the kinetic parameters of HO-2 and CPR.

Alanine substitution of the HO-2 residue with the cross peak intensity that is most strongly affected by equimolar CPR in the non-perdeuterated NMR binding studies (Figure 2.9), L201A, results in a 3-fold increase in the K_m for CPR and no change in k_{cat} compared to wild-type protein (Figure 2.12*B*, Table 2.1). On the other hand, the R87A variant of HO-2, whose NMR cross peak height is not strongly affected by the addition of CPR, exhibits no change in the k_{cat} or K_m for CPR (Figure 2.12*B*, Table 2.1). These results are consistent with a role for L201 at the binding interface for CPR.

We also studied the K169A variant of HO-2 because alanine substitution of K149, the analogous residue in HO-1, exhibits a 7-10-fold increase in K_d of the HO-1/CPR complex (24,27). K169 is present on the heme binding face of HO-2. We observe a ~20-fold increase in the K_m of the K169A variant of HO-2 for CPR and a 40-fold increase in the K_m value for the K149A variant of HO-1 (Figure 2.12, Table 2.1). These results indicate that this lysine residue of HO-2 and HO-1 is involved in binding CPR.

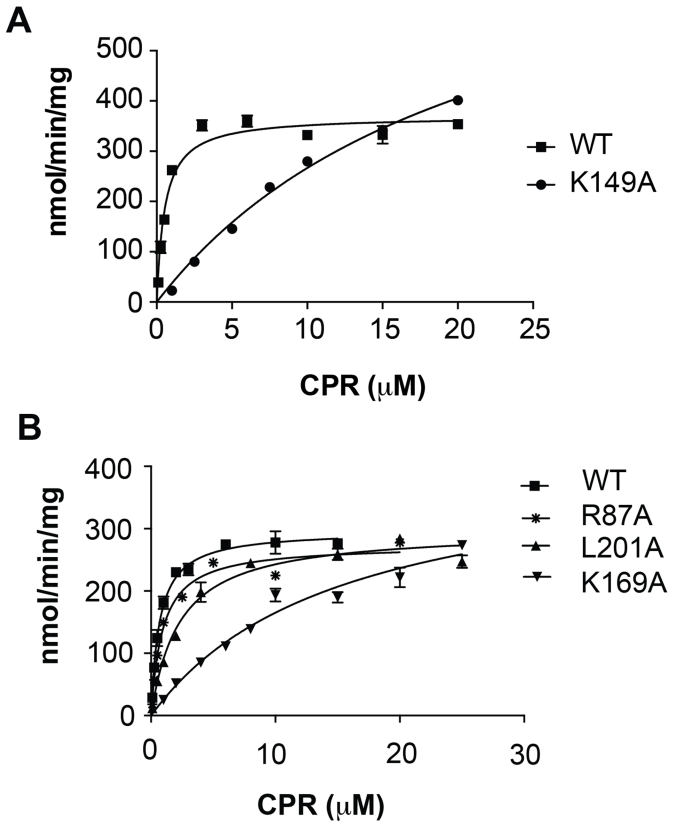

Figure 2.12. **HO mutants have an increased K_m for CPR.** Heme oxygenase activity for HO-1 **(A)** or HO-2 **(B)** and their respective mutants with varying amounts of CPR. Activity was monitored by observing the formation of bilirubin at 468 nm, as described in the methods.

Table 2.1. **Michaelis parameters for HO variants and CPR.** Heme oxygenase activity was monitored for HO-1 or HO-2 and the indicated mutants with varying amounts of CPR as shown in Figure 2.12. Specific activity is represented as nmol bilirubin/min/mg HO.

Construct	V_{max}	K_m	K_m
	(nmol·min^{-1}·mg^{-1})	(μM)	(Fold Change)
HO-1			
WT	370.1 ± 12.5	0.5 ± 0.1	1
K149A	847 ± 64	21.7 ± 2.6	42.4
HO-2			
WT	297 ± 5	0.7 ± 0.1	1
R87A	275 ± 11	0.9 ± 0.1	1.3
L201A	298.2 ± 8.0	2.3 ± 0.2	3.3
K169A	416.9 ± 36.9	15.2 ± 2.6	21.7

2.4.5 Gel filtration analysis of the binding of hHO-1, hHO-2, and CPR

In an attempt to observe the complex between CPR and HO-2 (and HO-1) by other methods, we performed gel filtration experiments. K_d values ranging from ~0.5-2.0 μM have been reported for hHO-1 and CPR, and $NADP^+$ is reported to enhance binding (24,27). We performed gel filtration experiments with 50 μM HO-1 or HO-2 and equimolar CPR in the presence of 150 μM $NADP^+$ and 150 μM hemin. For comparison, the elution of the individual proteins (HO-1, HO-2 and CPR) in the presence of heme and NADP+ was also determined. Because heme or $NADP^+$ could affect the migration of the individual proteins, they were included in 3-fold excess in all samples.

By gel filtration analyses, we did not observe any evidence for a complex between CPR and either hHO-1 or hHO-2 (Figure 2.13, Table 2.2). CPR migrates at position 1 (~70 kDa) in the absence (dashed line) or presence (red lines) of hHO-1 or hHO-2 (Figure 2.13). Peak 2, which marks the migration of hHO-2 or hHO-1, corresponds to ~60 kDa and 44 kDa, respectively, and shows up as a shoulder in Figure 2.13*A* in the HO-1/CPR sample. Consistent with the NMR relaxation studies, these results suggest that hHO-2 exists as a homodimer under these conditions. The difference in apparent mass between HO-1 and CPR is greater than that between HO-2 and CPR; therefore peaks 1 and 2 are slightly separated in Figure 2.13*A* and are overlapped in Figure 2.13*B*. The elution profile of CPR was unaffected by incubation with either HO-1 or HO-2; for example, a CPR/HO-2 complex, which would have eluted at a position corresponding to ~100 kDa, was not observed. Others have also failed to observe a complex between wild type HO-1 and CPR by gel filtration (26). The HO/CPR complex is undetected under these conditions, suggesting that the complex is weak and/or highly transient, consistent with the NMR and steady-state kinetic studies.

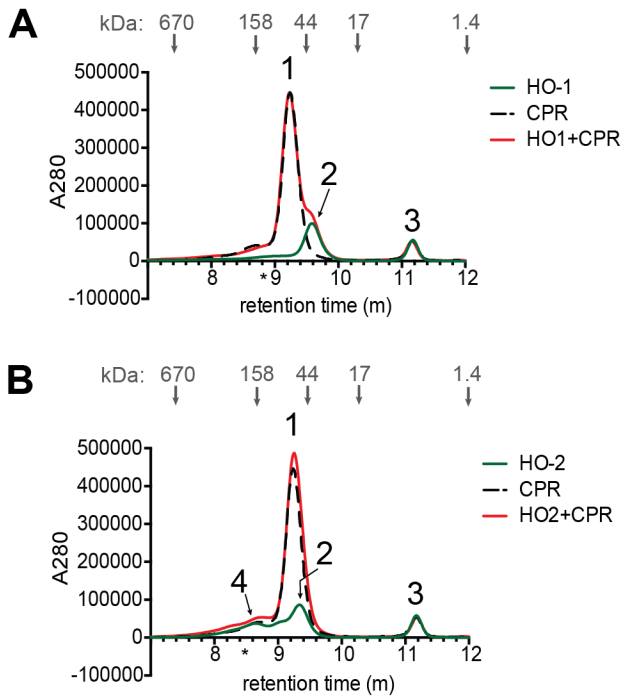

Figure 2.13. **HO and CPR analysis by size exclusion chromatography.** 50 μM CPR and HO-1 **(*A*)** or CPR and HO-2 **(*B*)** were loaded onto a Shodex KW-803 gel filtration column individually or in the indicated mixture in the presence of 150 μM heme and 150 μM NADP+ in running buffer (50 mM Tris, 50 mM KCl pH 7.0). The asterisk (*) represents the retention time for a 100 kDa protein and grey arrows mark the position of the molecular weight standards. Peak 1: CPR, peak 2: heme oxygenase, peak 3: $NADP^+$ and heme, peak 4: HO-2 aggregate.

Table 2.2. **Apparent molecular weight of HO-1, HO-2, and CPR by gel filtration.** V_e/V_o values for the indicated proteins, blue dextran (V_0), B12, and protein standards (BioRad) were measured and the apparent masses were determined as described in the Experimental Procedures section.

Protein	V_e/V_0	Apparent Mass (kDa)
HO-1	1.565 ± 0.005	44.02 ± 1.67
HO-2	1.525 ± 0.002	60.26 ± 1.15
CPR	1.509 ± 0.004	68.63 ± 1.99
CPR (with HO-1)	1.507 ± 0.004	69.60 ± 2.02
CPR (with HO-2)	1.506 ± 0.002	70.00 ± 1.33

2.4.6 Binding of CPR to HO-1 or HO-2 by surface plasmon resonance (SPR)

We also attempted to quantify CPR binding to HO-1 and HO-2 using SPR, with HO-1 or HO-2 immobilized on the dextran surface of the SPR chip through amine chemistry (Figure 2.14). Representative association and dissociation curves with various concentrations of CPR (1.25 - 20 μM) are shown in Figure 2.14*A*. The SPR sensorgrams show CPR-dependent association and CPR-independent dissociation phases, clearly demonstrating that CPR binds to both HO-1 and HO-2. To avoid potential artifacts, these experiments were performed in the absence of heme because heme itself produced a strong "binding" response (Figure 2.14*E)*. Use of the apoproteins is justified by our NMR experiments (above) using apoHO-2 and CPR, which clearly demonstrate that CPR can bind both apoHO-2 and hHO-2.

To derive binding kinetic constants from the SPR sensorgrams, the association and dissociation phases were fit individually because simultaneous global fitting analysis of CPR association and dissociation curves using the 1:1 Langmuir model (BiaEvaluation) produces a poor fit to the data. Single exponential fits of the association phase (GraphPad Prism6) of CPR and HO-1 or HO-2 were used to determine k_{on} values (0.0010 ± 0.0002 $s^{-1}\mu M^{-1}$ and 0.0014 ± 0.0002 $s^{-1}\mu M^{-1}$) and k_{off} values (0.020 ± 0.003 s^{-1} and 0.0230 ± 0.0003 s^{-1}) for CPR binding to HO-1 or HO-2 respectively (Figure 2.14*B* and *C*). From these k_{on} and k_{off} values, K_d values of 20.5 ± 7.6 μM and 16.7 ± 2.5 μM were determined for CPR and HO-1 or HO-2, respectively, indicating that these proteins form relatively weak (transient) complexes. Biexponental fits of the dissociation curves (Figure 2.14*D*) indicate a fast and slow dissociation phase, with k_{fast} values in reasonable agreement with the values determined by linear regression analysis of the binding data (k_{fast} = 0.026 ± 0.002 and 0.035 ± 0.008 s^{-1}; k_{slow} = 0.0030 ± 0.0015 and 0.0025 ± 0.0005 s^{-1} for HO-1 and HO-2 respectively).

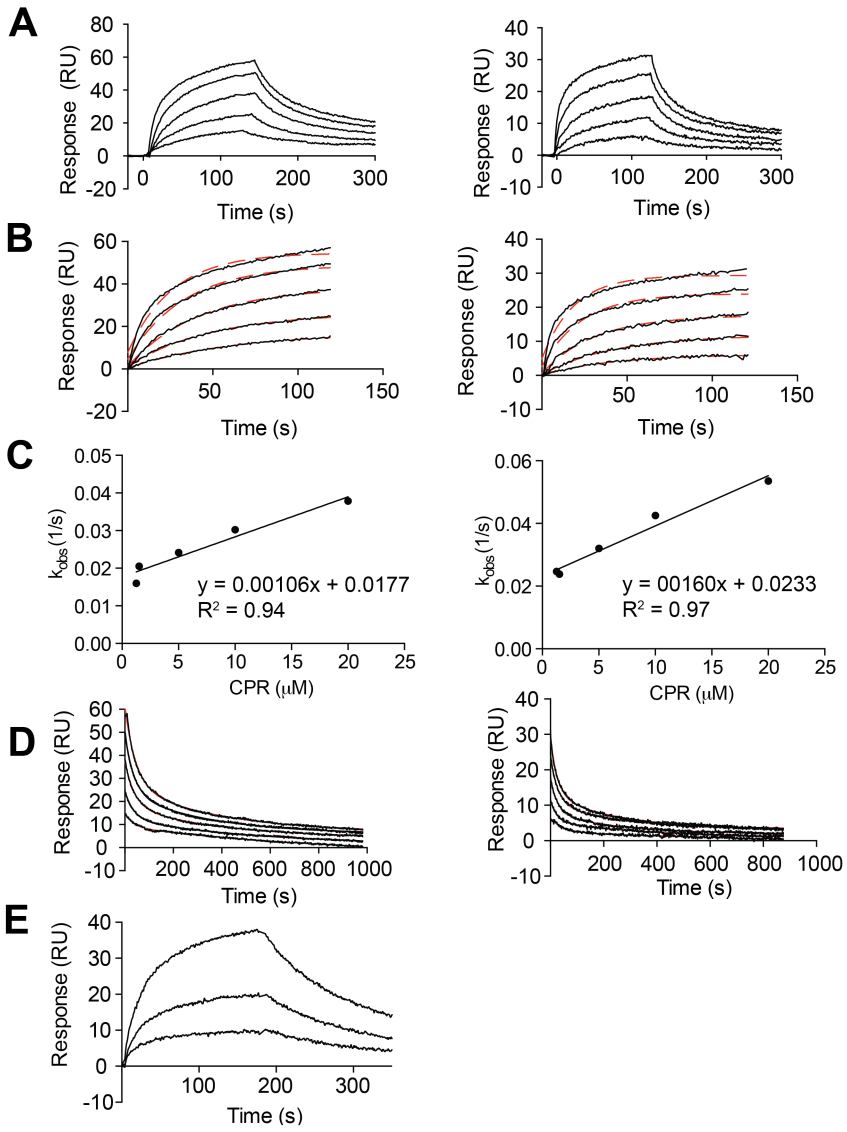

Figure 2.14. **SPR analysis of CPR binding HO-1 (left) and HO-2 (right). (*A*)** Various concentrations of CPR (1.25, 2.5, 5.0, 10.0 and 20.0 μM) were injected against immobilized HO-1 or HO-2. **(*B*)** Single exponential fits for the association phase of CPR binding HO-1 or HO-2 are shown in red. **(*C*)** Single exponential fits were used to determine k_{obs} for the association phase of CPR binding HO-1 or HO-2. k_{on} and k_{off} values are derived from the linear regression of k_{obs} (k_{on}= slope; k_{off}= y intercept). **(D)** Biexponential fits for the dissociation phase of CPR binding HO-1 or HO-2 are shown in red **(*E*)** Various concentrations of heme (0.125, 0.25, and 0.5 μM) were injected against immobilized CPR. Data are representative of three independent experiments.

2.4.7 Sedimentation velocity analysis of HO-2 and CPR

Binding interactions between CPR and HO-2 were also analyzed by sedimentation velocity ultracentrifugation, a method that is less sensitive to heme artifacts than SPR. As described in the methods, 20.5 μM CPR was titrated with varying concentrations of heme bound HO-2 (0-55 μM). In these experiments, the sedimentation coefficient distribution of CPR was monitored in the presence of increasing concentrations of hHO-2. Figure 2.15*A* shows a sedimentation velocity profile obtained with a 2:1 molar ratio of hHO-2 to CPR. In the absence of hHO-2, CPR is characterized by a sedimentation coefficient centered at 4.5 S as shown in Figure 2.15*B*. hHO-2 alone shows two sedimentation coefficients with a major component (60%) centered at 2.8 S and a minor component (34%) at 4.2 S. Upon adding hHO-2, the shape of the CPR component changes with the boundary shifting to a higher sedimentation coefficient. The weight-average *s*-value of this fast boundary component was determined by integrating the *c*(*s*) distribution between 4 and 7 S. From these data, a K_d of 15.1 ± 6.5 μM was determined for hHO-2 and CPR. At the highest hHO-2 concentration, the CPR/HO-2 complex was characterized by a weight-average s-value of 5.2 S.

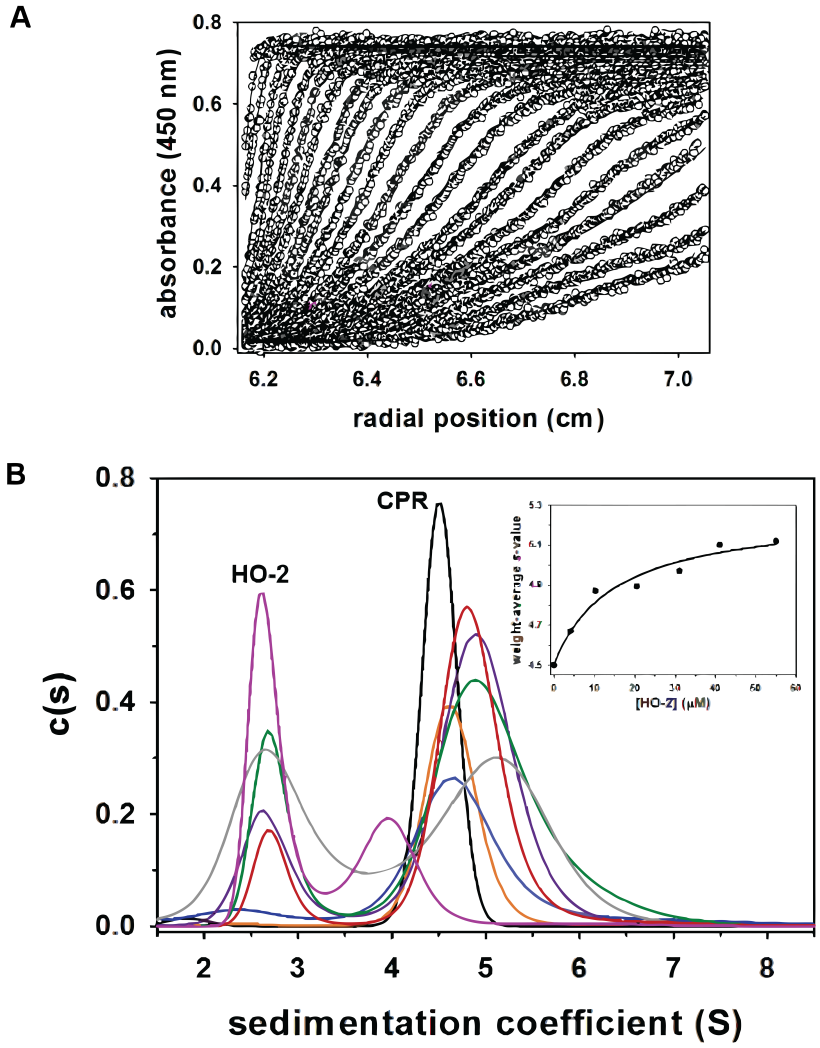

Figure 2.15. **Sedimentation velocity analysis of HO-2 and CPR interactions. (A)** Velocity scans selected from analysis of a 2:1 ratio of hHO-2 (41 μM) to CPR (20.5 μM). Shown are the absorbance data (open circles) fitted (solid lines) to the continuous c(s) distribution model. **(B)** Sedimentation coefficient distributions of CPR (20.5 μM) alone (black trace) and in the presence of 4.1 μM (orange trace), 10.25 μM (blue trace), 20.5 μM (red trace), 30.75 μM (purple trace), 41 μM (green trace), and 55 μM HO-2 (gray trace). hHO-2 alone (41 μM) is shown in magenta. The inset shows the weight-average s-value plotted versus HO-2 concentration. The data were fit to a single-site binding isotherm to yield a K_d value of 15.1 ± 6.5 μM.

2.4.8 Chemical cross-linking of CPR and HO-1 or HO-2

We conducted chemical cross-linking experiments to trap the complex between HO-2 and CPR. Because cross-linking is an irreversible reaction, even transient complexes can be detected. Because CPR has been reported to bind HO-1 (24-27), we used HO-1 and CPR as a positive control. According to the crystal structure (PDB 3QE2), human CPR possesses at least two surface cysteine residues, which should be available for cross-linking. Thus, we utilized the heterobifunctional cross-linker LC-SPDP, which contains both an amine and a thiol reactive group. As described in the Methods section, after activating HO-1 or HO-2 and removing unreacted cross-linker, CPR was added and the reaction was incubated overnight at 4°C. Stable complexes between CPR and HO-1 as well as CPR and HO-2 were formed (Figure 2.16). A small amount of HO-2 homodimer is visible in the HO-2 sample that lacks CPR, while, for activated HO-1 alone, no homodimeric complex was observed.

As a negative control, we activated the HOs as described above and incubated with a physiologically unrelated cysteine containing protein, RNase, instead of CPR. RNase (based on PDB 1RCA) contains eight cysteine residues, four of which are surface exposed. No high-molecular weight complex between RNaseA and either HO-1 or HO-2 was observed (Figure 2.16*B*).

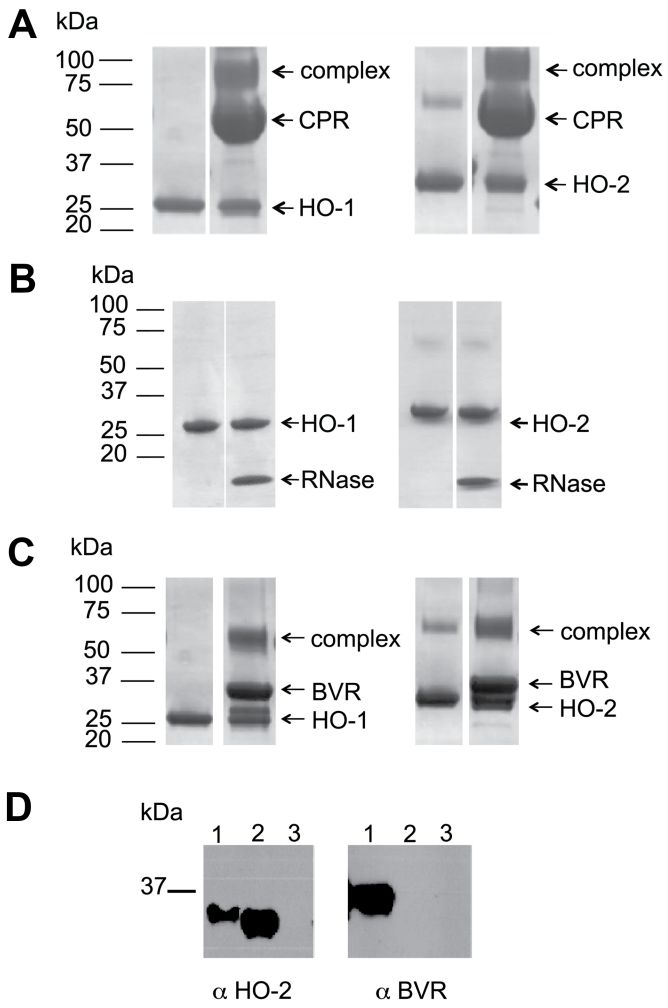

Figure 2.16. **Chemical crosslinking of HO-2 and CPR. (*A*)** The heterobifunctional cross linker LC-SPDP stabilizes a complex between HO-1 or HO-2 and CPR. **(*B*)** No complex is trapped for HO-1 or HO-2 with RNAse. **(*C*)** Chemical crosslinking also stabilizes a complex between HO-1 or HO-2 and BVR. **(*D*)** Reducing SDS-PAGE and Western blot of HO-2 pull down and associated BVR. Lane 1: crosslinking reaction, Lane 2: HO-2 only, Lane 3: BVR only. Crosslinking reactions contained 10 μM of the indicated protein. **A**, **B**, and **C** are Coomassie stained non-reducing SDS PAGE analyses of the indicated reaction.

2.4.9 NMR studies of HO-2 in the presence of BVR

BVR mediates the second step in heme degradation, the conversion of biliverdin to bilirubin. HO-1 and BVR are reported to form a complex with a K_d of 0.2 ± 0.1 μM (24,27). An overlapping binding site on HO-1 for CPR and BVR has been proposed, but

with the binding sites not identical (24,25,27). To our knowledge, binding of HO-2 and BVR has not been addressed.

To attempt to characterize the binding interface between HO-2 and BVR, we performed NMR experiments similar to those described for HO-2 and CPR. The ^{1}H- ^{15}N TROSY spectrum of 150 μM non-perdeuterated ^{15}N-hHO-2 was collected in the absence or presence of equimolar BVR (not labeled with ^{15}N). While CPR induced obvious changes in the hHO-2 spectrum (Figure 2.8), the spectrum of hHO-2 collected in the presence of BVR is almost identical to that of hHO-2 alone (Figure 2.17). No changes in the chemical shifts are apparent and the majority of assigned resonances exhibit a height ratio (+BVR/-BVR) close to 1, indicating no change (Figure 2.18). These results suggest that under the NMR conditions (150 μM), BVR binds hHO-2 very weakly, if at all. Experiments with ^{15}N-apoHO-2 and equimolar BVR also showed BVR has no effect on the apoHO-2 spectrum (data not shown).

Our NMR binding studies thus suggest that BVR has a significantly lower affinity for HO-2 compared with CPR. In contrast, others have reported nM K_d values for the BVR/hHO-1 complex (27). Because HO-1 and HO-2 are highly homologous, our results were unexpected. Thus, other experiments were performed to assess the interaction between the HO's and BVR.

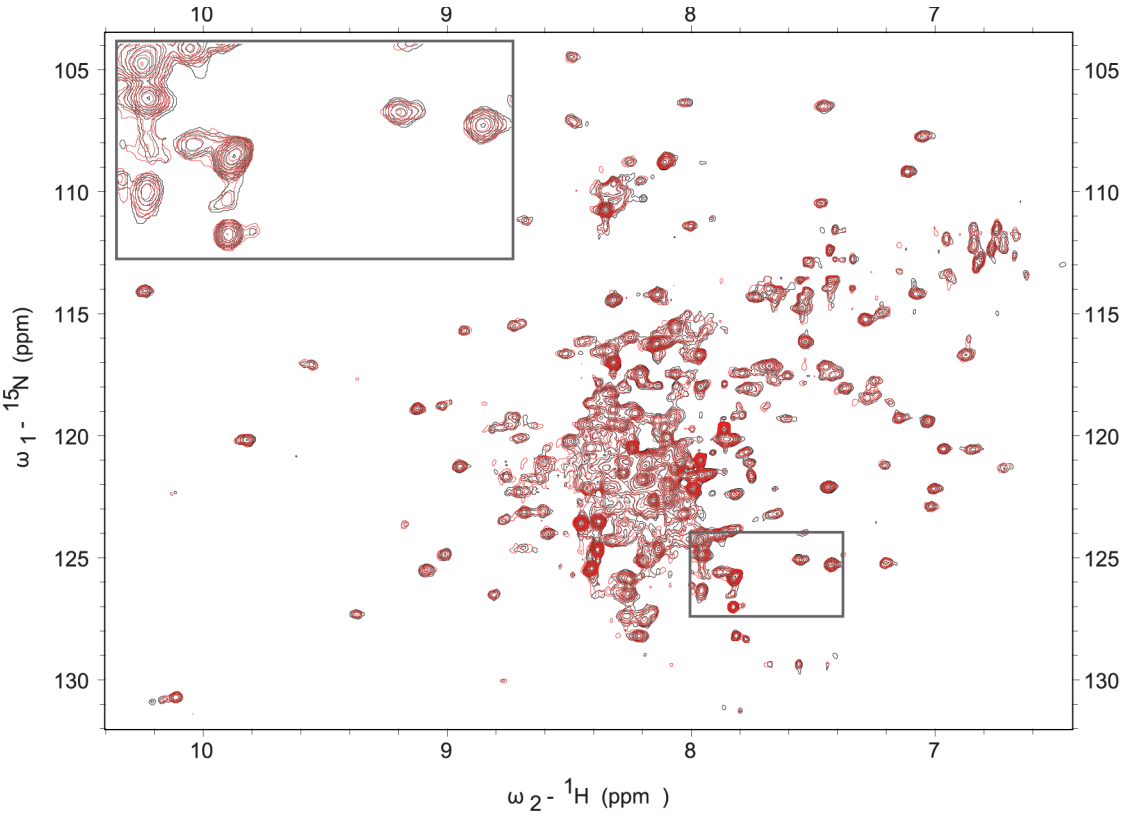

Figure 2.17. **NMR analysis of BVR binding HO-2.** ^{1}H- ^{15}N TROSY spectra of 150 μM non-perdeuterated ^{15}N-hHO-2 collected in the absence (black) or presence (red) of equimolar BVR.

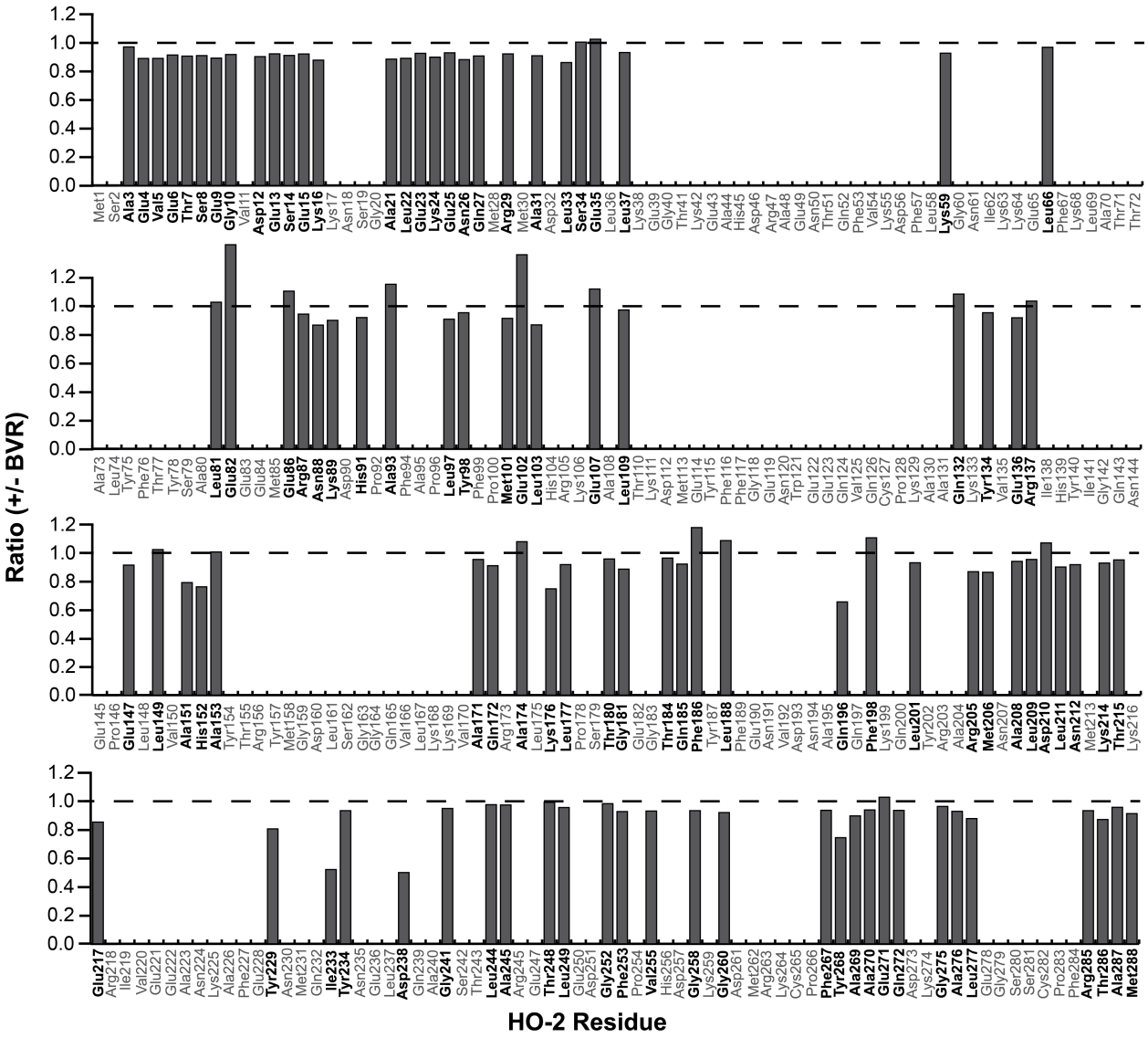

Figure 2.18. **The effect of BVR on HO-2 resonances.** The ratio of hHO-2 resonance height with and without equimolar BVR (+BVR/-BVR) is represented by the grey bars. A ratio of 1 (dotted line) indicates no change for that residue. Bars that are absent (greyed label) represent resonances that are unassigned while assigned residues are in bold.

2.4.10 Fluorescence quenching experiments with BVR-CPM and HO-1 or HO-2

One possible explanation for the lack of NMR evidence for an HO-2/BVR interaction is that HO-2 interacts differently with BVR compared to HO-1. To address this possibility, we repeated the published fluorescence quenching experiments for measuring interactions between HO-1 and BVR (27) and performed similar experiments to determine the binding affinity of HO-2 for BVR. In these studies, BVR was labeled

with the thiol-reactive dye CPM to produce fluorescent BVR upon excitation at 350 nm. Because the hHO-1 absorption spectrum overlaps with the emission spectrum of BVR-CPM, hHO-1 binding results in fluorescence quenching due to FRET processes. Because apoHO has no absorbance in the 350 nm region, this method can only be used to evaluate hHO binding. Plotting the % fluorescence quenching at 455 nm *versus* hHO-1 concentration produced a binding curve (Figure 2.19*A*) that fits to a one-site binding model with a K_d of 0.25 ± 0.09 μM, almost identical to the previously reported value of 0.22 ± 0.09 μM (27). Similar FRET experiments with hHO-2 and BVR (Figure 2.19*B*) provided concentration-dependent, saturable binding curves with a K_d of 0.27 ± 0.01 μM.

These results suggest that BVR binds both HO-1 and HO-2 with similar high affinity. Equation 5 can be used to estimate a K_d value in situations where the concentration of free ligand cannot be estimated due to high affinity and near stoichiometric binding. If HO-2 and BVR have a K_d of ~300 nM (as suggested by the fluorescence quenching results), Equation 5 predicts 70% of HO-2 should be complexed with BVR under the NMR conditions (with 150 μM HO-2 and 150 μM BVR). This is clearly inconsistent with the NMR results; therefore, we conducted additional experiments to interrogate the source of this apparent discrepancy between the NMR and FRET experiments.

$$EL = 0.5(E_0 + L_0 + K_d - ((E_0 + L_0 + K_d)^2 - 4E_0 \cdot L_0)^{1/2}) \qquad \text{[Equation 5]}$$

2.4.11 Fluorescence quenching of BVR-CPM by heme

To attempt to resolve the inconsistency between the NMR and fluorescence quenching results, we tested the hypothesis that free heme, dissociating from HO-2, may be responsible for the fluorescence quenching of BVR-CPM. When free heme was titrated into BVR-CPM under conditions identical to those used for hHO titrations, there was strong concentration-dependent and saturable quenching of BVR-CPM fluorescence (Figure 2.19*C*), indicating a K_d value of 0.037 ± 0.01 μM. These results suggest that the fluorescence quenching observed in the FRET experiments could be

due to the effects of heme binding to BVR, or the CPM fluorophore, rather than the HO protein. Assuming a K_d of 33 nM for HO-2 and heme (17), Equation 5 predicts that 1 μM hHO-2 will contain approximately 0.17 μM dissociated heme, which is well above the K_d value determined in these experiments. Thus, we suggest that the quenching of BVR-CPM fluorescence observed in the titration with hHO-1 or hHO-2 results from free heme, dissociated from HO, not the HO protein. We propose that the heme binds to BVR-CPM from solution and not through direct heme transfer from the heme-HO complex to BVR. In fact, our results demonstrate that these proteins do not form a complex, dispelling the possibility of a protein-to-protein heme transfer.

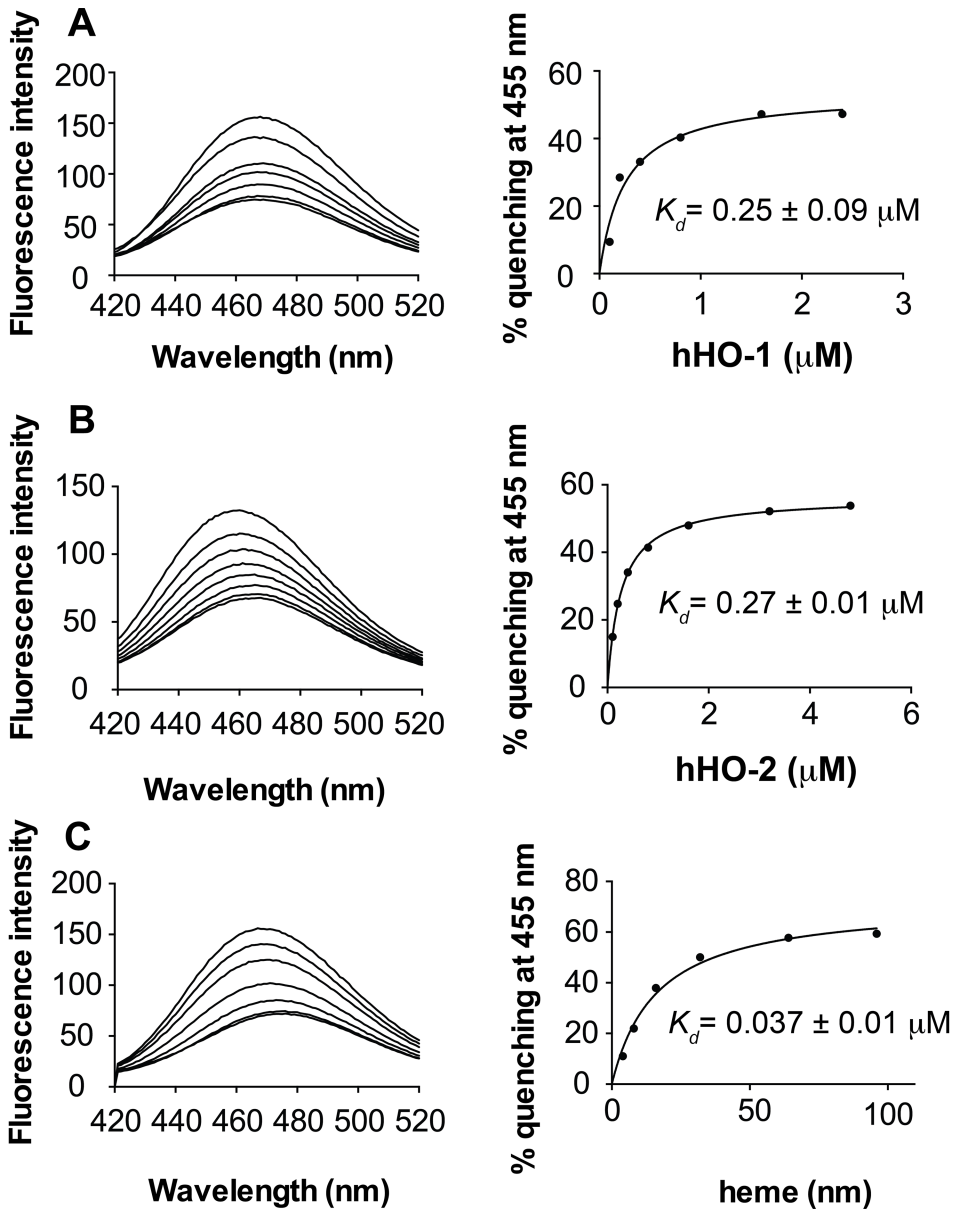

Figure 2.19. **Fluorescence Quenching of BVR-CPM by Heme Oxygenases and Heme.** Titration of heme-bound HO-1 **(*A*)**, HO-2 **(*B*)** or heme alone **(*C*)** into BVR-CPM. Percent fluorescence quenching plotted against the concentration of the titrant and fit to a single binding model to determine the K_d of binding using GraphPad Prism 6.0.

The effects of free heme on BVR-CPM fluorescence are consistent with the report that heme binds to BVR and to residues 290-296 of the BVR C-terminal peptide (KYCCSRK) (36). Furthermore, when we analyzed BVR-CPM by LC MS/MS to determine the location of the CPM label, we identified one CPM molecule attached to C204 and another to either C292 or C293 of BVR (Figure 2.20). Because C292 and

C293 are located on the same peptide in the LC MS/MS analysis, the two cysteines were not distinguished by this analysis.

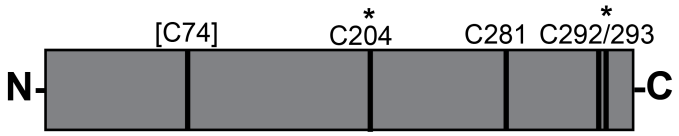

Figure 2.20. **Biliverdin reductase modified by CPM.** LC-MS/MS analysis of BVR-CPM identifies CPM modification (*) at C280 and either C292 or C293. C74 was not observed in this analysis.

While the other surface-exposed Cys (C74) is not observed in this analysis, it is most likely unmodified because BVR-CPM has enzymatic activity similar to that of the wild type protein (109%). We and others (59) find that mutation of C74 in human BVR, or its homolog C73 in rat BVR, ablates enzymatic activity. Additionally, CPM labeling was conducted in the presence of $NADP^+$, which is expected to protect the enzymatic cleft from modification.

2.4.12 BVR binding heme by optical absorbance

To further investigate the possibility that the fluorescence quenching of BVR-CPM by hHO-2 results from the binding of free heme by BVR, we titrated BVR with free heme and measured the absorbance spectrum. As observed by others (36), BVR alone shows no optical absorbance in the 350-700 nm range, however in the presence of heme, we observe the development of an absorbance band with a wavelength maximum at 415 nm, indicating that free heme binds BVR (Figure 2.21*A*). To determine the affinity of heme and BVR, 5 μM heme was titrated with BVR and the absorbance at 415 nm was measured and fit to a single-site binding model, yielding a K_d of 220 ± 50 nM (Figure 2.21*B*).

Titration of BVR-CPM with hHO-2 produces strong fluorescence quenching; however, because there is no evidence of HO-2/BVR binding by NMR, we hypothesize that heme, not HO, is responsible for a large part of the fluorescence quenching. To test if heme from hHO-2 can bind BVR, we incubated hHO-2 with BVR. Because the absorbance of hHO-2 is ~10-fold greater than that of heme-bound BVR and because

the absorbance spectra overlap, hHO-2 was included in the reference cuvette for these titrations. Under these conditions, with increasing concentrations of BVR titrated into hHO-2, absorbance at 415 nm also increases. This result supports that BVR is capable of binding heme from hHO-2 (Figure 2.21).

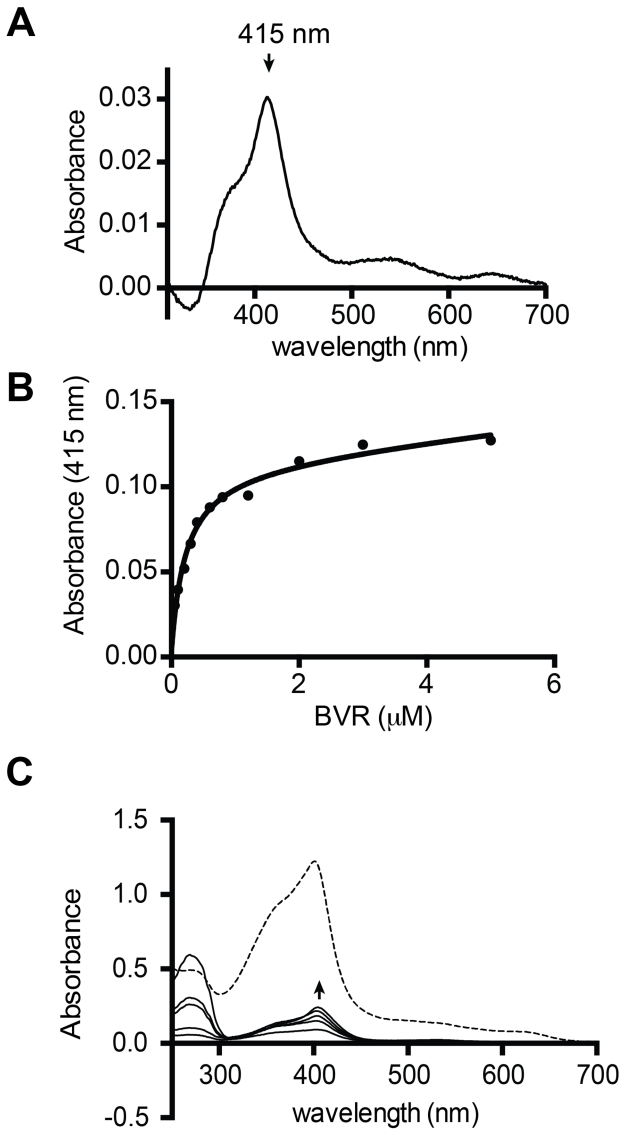

Figure 2.21. **Heme binds BVR by optical absorbance. (*A*)** The absorbance spectrum of 2.5 μM BVR with 2.0 μM heme. BVR alone shows no absorbance in the 350-700 nm range. **(B)** Absorbance at 415 nm for 10 μM heme titrated with varying concentrations of BVR (0.05, 0.1, 0.2, 0.3, 0.4, 0.6, 0.8, 1.2, 2.0, 3.0, and 5.0 μM BVR). Data are fit to a single binding model using GraphPad Prism 6.0. **(*C*)** 5 μM hHO-2 alone (dotted line) or titrated with various concentrations of BVR (1.0, 2.0, 8.0, 10.0, 20.0 μM). Samples for BVR titrations contain 5 μM hHO-2 in the reference cuvette because the absorbance of hHO-2 is ~10-fold that of heme BVR and the hHO-2 spectrum overwhelms the heme BVR spectrum if it is not subtracted.

2.4.13 Chemical cross-linking of HO-2 and BVR

The above results suggest that HO-2 and BVR either do not interact or that that they form a very weak complex. To determine if an HO-2/BVR complex can be trapped by chemical cross-linking, we incubated HO-2, which had been activated with LC-SPDP, with BVR, as described above for trapping the HO-2/CPR complex. Because HO-1 and BVR have been reported to form a complex (24,27), we also conducted the experiment with HO-1 as a positive control. Under conditions identical to those used to stabilize the HO-2/CPR complex, a high molecular weight complex of ~60 kDa was observed by SDS-PAGE for BVR and both HO-1 and HO-2 (Figure 2.16*C*).

Because HO-2 and BVR are similar in molecular mass, a heterodimer of HO-2 and BVR is not distinguishable from either homodimer by size alone. To determine if BVR is directly linked to HO-2 in the cross-linked product, we conducted the cross-linking reaction using HO-2 that retained an N-terminal 6xhis tag (hisHO-2). The cross-linked products with hisHO-2 were identical to those with HO-2 by SDS PAGE analysis (data not shown). We then isolated hisHO-2 from the cross-linking reaction using Ni-NTA resin and analyzed the proteins that associated with the affinity resin by reducing SDS-PAGE, which was subjected to Western blotting using antibodies against HO-2 or BVR. Under these conditions, the cross-linker undergoes reduction, allowing the proteins to migrate at their native size. BVR was found to copurify with HO-2 in the cross-linked product (Figure 2.16*D*). A control reaction demonstrated that BVR alone did not associate with the affinity resin (Figure 2.16*D*). These results demonstrate that an HO-2/BVR complex can be trapped by chemical cross-linking.

To identify the location of the cross-linker in the HO-2/BVR complex, we conducted a tryptic digest followed by LC-MS/MS analysis of the cross-linked product. This analysis identified the HO-2 peptide containing K264 (KCPFYAAEQKD) linked to the BVR peptide containing C292 and C293 of BVR (YCCSR) – the same peptide shown earlier to bind heme (36).

2.5 Discussion

In the HO reaction, seven electron-equivalents from NADPH are transferred to the HO-bound heme via CPR. For rapid and efficient electron transfer, the electron

donor (flavin on CPR) and acceptor (heme of HO-2) should be at optimal orientation and distance, implying that an electron-transfer complex is formed during the catalytic cycle. One of the issues we have addressed in this paper is the existence and nature of that electron transfer complex. One possibility is that HO and CPR form a stable complex within which multiple electrons transfer from NADPH through the bound flavins (FAD and FMN) on CPR to the HO-bound heme as it undergoes oxygenation and conversion to biliverdin and CO. The other possibility is that HO and CPR encounter each other only transiently and associate/dissociate multiple times during each catalytic cycle. Similarly, either HO and BVR form a stable complex, within which biliverdin is transferred (perhaps channeled) between the two proteins, or, as another alternative, remain completely unattached as the HO-product (biliverdin) is released into solution and captured by BVR to undergo conversion to bilirubin. Based on fluorescence quenching, SPR and acetylation-protection studies, a moderately tight HO-1/CPR complex with a K_d value in the ~1 μM range had been identified. However, SPR, fluorescence quenching, and acetylation protection assays with HO-1 have yielded inconsistent results regarding which residues form the HO-1/CPR binding interface (24,25,27).

2.5.1 Interactions between HO and CPR

Whether or not HO-2 and CPR form a complex has not been previously investigated. As a result of spectroscopic (NMR, fluorescence), steady-state kinetic and other biochemical (chromatographic, analytical centrifugation, SPR) studies, we have obtained novel information about the nature of the interactions between these two proteins.

Though our focus is on HO-2, we also analyzed CPR binding to HO-1, primarily as a positive control for the HO-2/CPR studies, as CPR binding HO-1 has been previously described (24-27). Consistent with previous reports, we observe CPR binding HO-1 by SPR and by chemical cross-linking.

By gel filtration experiments, under our experimental conditions (50 μM hHO, 50 μM CPR with $NADP^+$), HO-2 appears to form a homodimer. We do not observe any evidence for a complex between HO-2 and CPR. Gel filtration experiments occur under

non-equilibrium conditions in which the component proteins of any transient complex, once dissociated from the complex, are unable to reassociate once they are in a separate zone of the chromatographic column. On the other hand, SPR experiments clearly demonstrate CPR binding to HO-2 (Figure 2.14).

SPR is a valuable method for studying protein-protein interactions because the proteins remain in the same solution and reach equilibrium; furthermore, one can monitor both the rates of association and dissociation. Our SPR results clearly demonstrate that CPR binds to both HO-1 (K_d of 20.5 μM) and HO-2 (K_d of 16.7 μM) with CPR-dependent rates of association and CPR-independent dissociation rates. For HO-1, our results give a K_d value that is 10-fold larger than previously reported (24). The lower affinity of CPR for HO-1 observed in our studies could be due to differences in the experimental design; our studies were conducted in the absence of heme and utilized immobilized HO-1 with human CPR as the soluble analyte, whereas earlier studies were conducted with immobilized rat CPR with hHO-1 in solution. Although we also observe a binding response when we titrate either hHO-1 or hHO-2 against immobilized human CPR, we found that free heme also produces a strong 'binding' response with immobilized human CPR (Figure 2.14*E*) and with immobilized BVR (not shown). Thus, to avoid potential artifacts, these experiments were performed in the absence of heme. Our use of the apo-HOs is justified by our NMR experiments, which clearly demonstrate that CPR can bind both forms (apoHO-2 and heme-bound) of HO-2. We are unaware of any physiologic rationale for heme binding to CPR, so this is likely to be a nonspecific effect. However, as we discuss below, BVR has previously been shown to bind heme and to shuttle heme into the nucleus (36). While by SPR we observe no binding of apoHO to immobilized CPR, the conformation of CPR is critical for HO-1 binding (26) and it is possible that immobilization of CPR stabilizes a conformation that has a lower affinity for HO.

Sedimentation velocity experiments also provide evidence of a dynamic complex between HO-2 and CPR, with a K_d (15.1 μM) value that is similar to that calculated from the SPR data. The HO-2/CPR complex can also be captured by chemically cross-linking an amino group of HO-2 through a 15.7 Å tether to a surface-reactive Cys residue on

CPR. The latter is, of course, irreversible, and designed to capture even highly transient interactions.

The NMR experiments also show that an interaction between HO-2 and CPR occurs. The primary proof is the overall and large loss of peak intensity for the core resonances, due to broadening associated with the large increase in time-averaged molecular weight. In addition, excess peak intensity loss due to exchange broadening and chemical shift perturbations (CSP) occur for several but not all signals. The latter observations are compatible with specific binding, and with binding-kinetics that is on the fast/intermediate NMR shift time scale ($k_{off} \sim 100\ s^{-1}$). In turn, this is suggestive of a K_d in the low μM range, consistent with the values of 15 μM as found by analytical ultracentrifugation experiments, and 16.7 μM as found by SPR. Regretfully, the NMR experiments do not allow a precise determination of these values, because the NMR signals disappear at higher titration stoichiometries and saturation of binding cannot be observed.

Having assigned ~70% of the resonances in the HO-2 NMR spectrum, we used the CSPs to identify the HO-2/CPR interface. Titration of perdeuterated ^{15}N-hHO-2 with CPR altered the chemical shift of several residues in the hHO-2 NMR spectrum. At both 75 and 150 μM CPR, residues of the HO-2 catalytic core exhibit larger CSPs compared with the N- and C-termini (Figure 2.4). Residues that exhibit the largest CSPs with the addition of 75 μM CPR are F99, Y202, L66, K89, and E190.

Upon adding CPR, we also observed dramatic and titratable reductions in the intensities of some of the ^{1}H-^{15}N TROSY peaks of resonances from the catalytic core domain of HO-2 (Figure 2.6 and Figure 2.9). The majority of intensity changes due to exchange broadening of the TROSY peaks occur in the structured core region of HO-2, with few intensity changes originating from the dynamically unfolded N- or C-termini; only Ser8 and Tyr268 exhibit intensity changes in these region. Chemical shift perturbations induced by CPR titrations also affect the core residues of hHO-2, while the N- and C-termini are unaffected (Figure 2.4). These results indicate that CPR interacts with the catalytic core of the protein and has minimal interactions with the N- or C-terminal regions of HO-2.

Figure 2.22*A* highlights residues on hHO-2 that exhibit *both* significant CSPs and large intensity changes with the addition of 75 μM CPR; L66, F99, E102, D193, Q200, Y202, and L209. Strikingly, in the recent HO-1/CPR crystal structure, residues of HO-1 that are conserved with HO-2 residues F99, E102, Q200, and Y202 form a patch that is at the CPR interface (Figure 2.22*B*). The HO-1 residue conserved with D193 is also located at the CPR interface, as are HO-1 residues conserved with the HO-2 residues identified by mutagenesis, L201 and K169 (Figure 2.22). In the crystal structure, HO-1 is bound to a deletion variant of CPR (ΔTGEE) for which the deletion of four residues in the hinge region of CPR (residues TGEE) stabilizes an open conformation of CPR which has a 10-20-fold higher affinity for HO-1, allowing successful crystallization of the HO-1/CPR complex (26).

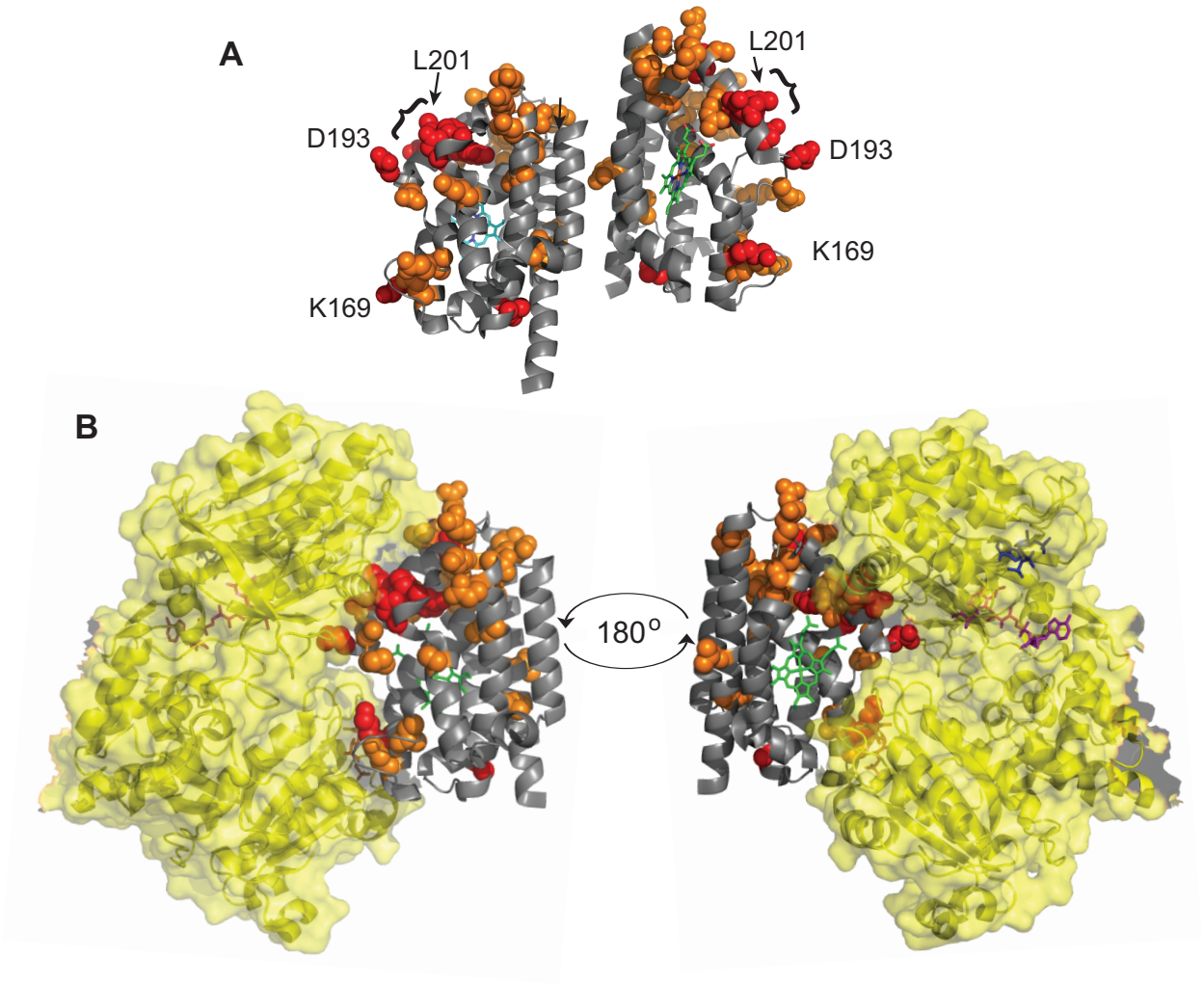

Figure 2.22. **The interface for CPR on HO-2 defined by NMR and mutagenesis. (*A*)** Residues in red have *both* significant CSPs and large intensity ratio changes with the addition of 75 μM CPR. Residues of HO-2 that are have significant CSPs *or* large changes in peak intensity ratio with the addition of 75 μM CPR are shown in orange. The bracket "{" identifies a patch of residues strongly affected by CPR (F99, E102, Q200, L201 and Y202). L201 and K169 were targeted by mutagenesis. Side chains are shown as spheres (PDB 2QPP) **(*B*)** Residues identified for HO-2 mapped onto the analogous residues of HO-1 in the published crystal structure of the complex of rat HO-1 (grey) and rat CPRΔTGEE (yellow) (PDB 3WKT). Cofactors are as indicated: heme (green), $NADP^+$ (blue), FAD (purple), FMN (orange).

Additional HO-2 residues show *either* significant CSPs without extra intensity change, *or* large changes in intensity without chemical shift changes. Especially the latter phenomenon is prevalent for the most affected residue, L201, and is theoretically incompatible with a canonical intermediate exchange binding process as described by

Equation 4. Rather, it is suggestive of additional, significantly populated bound states of CPR sensed by L201 that are in intermediate/fast exchange with each other and with L201 in the free state. It can be shown that the observed broadening without shift can occur if the CSP's of the different bound states approximately cancel (Zuiderweg, unpublished). The residues affected by this non-canonical mechanism are conserved in HO-1, where they are located at the interface for CPR (E86, D90, E190, L201, R203, A208, and D210) or in patches of residues adjacent to the interface in (A31, L33, L36, L37, L81, E107, K89, N88, L149, Q172, E182, Thr184, and T215). These residues also localize at and around the binding site for HO-2 as identified from CSPs alone. The extended nature of the interaction surface would also be compatible with multiple binding modes for CPR as implied from the non-canonical broadening. The existence of multiple bound states, or an ensemble of encounter complexes, has been suggested for other electron-transfer complexes as well {Crowley, 2003 #3581;Ubbink, 2009 #4146}.

NMR relaxation and gel filtration studies indicate that HO-2 exists as a homodimer in solution at the conditions used. Changes in the homodimerization state of HO-2 upon CPR binding could give rise to CPR-dependent changes in the TROSY spectrum, and these changes would be difficult to distinguish from changes induced by CPR binding HO-2 directly. However, HO-2 crystalizes as a homodimer, and the HO-2/HO-2 interface is distant from the majority of the CPR induced changes that occur in the HO-2 TROSY spectrum (Figure 2.22*A*). This supports that the CPR-induced changes observed in the HO-2 TROSY spectrum are not due to changes in the HO-2 dimerization state but rather CPR directly binding to HO-2.

There is a major difference between the k_{off} as suggested by NMR (~100 s^{-1}) and the value measured by SPR (~0.023 s^{-1}). The latter value would give rise to an extremely slow NMR shift time scale, and would not allow for any of the observed chemical shift changes. This contradictory situation is reminiscent of the binding of an organic phosphate molecule to hemoglobin, where, despite an off-rate of 0.01 s^{-1}, fast exchange dynamics were observed using ^{31}P NMR. Multiple binding sites for the small molecule on the hemoglobin surface were proposed to explain the apparent discrepancy and a mathematical model that recapitulated the experimental results was described (60,61). In the present case, we have evidence for the existence of multiple

bound states of CPR. Perhaps the observed rate of ~100 s^{-1} as indicated by NMR is reflective of the exchange kinetics between the various bound states. In contrast, the off-rate as measured by SPR monitors the complete dissociation.

While previous reports on the HO-1/CPR complex focus on charge-charge interactions (from residues that we were not able to assign in our NMR spectra), our results provide the first evidence that hydrophobic residues may be involved in HO/CPR binding. The majority of the residues highlighted in the NMR binding studies are involved in interacting with the FAD binding domain of CPR (Figure 2.22). Kinetic results discussed below concur with these NMR results.

Our steady-state kinetic analyses support the conclusion that the area near the exposed heme binding face in the catalytic core of HO-2 is involved in binding CPR. For example, HO-1 and HO-2, which share a high degree of structural similarity in their catalytic core region (55), exhibit similar K_m values for CPR (0.5 - 0.7 μM). Furthermore, alanine substitution of the core residues that are proposed to be at the HO/CPR interface, K169 (or K149 in HO-1) and L201, results in significant increases in the K_m for CPR. K149A, for example, exhibits a 40-fold increase in K_m for CPR, in agreement with prior SPR (24) and acetylation protection assays (25), but in contrast with earlier FRET measurements, which showed no effect of Ala substitution at that site (27). The K169A variant of HO-2 also exhibits a 1.4-fold increase in V_{max} and the K149A variant of HO-1 exhibits a 2.2-fold increase in V_{max} suggesting that lowering the affinity for CPR increases the steady-state rate under saturating substrate (NADPH, O_2, and CPR) concentrations. That the K149A variant binds heme with identical affinity as the wild type (24) and does not exhibit a decrease (instead a slight increase) in V_{max} supports our conclusion that its increase in K_m for CPR reflects disruption of a key interaction between CPR and HO-2, not some major disruption in the overall structure or at the active site of HO-1.

The HO reaction involves many steps, including heme binding, seven steps of electron transfer, three mol of oxygen binding, oxygen activation, biliverdin release, etc. It is accepted that the rate-limiting step in the HO-1 catalytic cycle when BVR is present is ring opening of Fe(II)-verdoheme (40,62). However, it is possible that this lysine variant is rate-limited by another step. The details of the catalytic cycle for HO-2 or for

this variant have not been characterized. However, given that K149A (HO-1) and K169A (HO-2) exhibit a 1.4-2.2-fold increase in V_{max} and a 20-40-fold increase in K_m for CPR, it seems reasonable to speculate that, at saturating concentrations of CPR, the rate-limiting step for the lysine variants is electron transfer from CPR to the heme.

Taken together, our results suggest that during the multi-step HO-2 reaction, a transient complex between HO-2 and CPR forms and dissociates rapidly and that the productive electron-transfer complex includes HO-2 residues L201 and K169. The transient nature of the interactions between HO-2 and CPR is likely to be an important catalytic feature, especially in this and other systems where multiple electrons must be passed during each catalytic cycle.

Our results indicate that a similar dynamic and transient binding scenario exists with HO-1. Our gel filtration and SPR results indicate that HO-1 (like HO-2) forms a rather weak complex with CPR. The transient nature of these interactions between HO and CPR is likely to be important in the HO mechanism, which requires seven electrons to be transferred from NADPH through the redox centers on CPR.

The catalytic core, shown clearly to be the domain of HO-2 that interacts with CPR, is highly homologous with HO-1. For example, catalytic core residues with NMR resonances most strongly affected by CPR that exhibit both CSPs and broadening (L66, F99, E102, D193, Q200, Y202, and L209), or with binding constants affected by mutagenesis (K169 and L201) are highly conserved between HO-1 and HO-2. All of those residues are strictly conserved except L66 (G46 in HO-1). Earlier reports identified K149 of HO-1 to be important in binding CPR (24,25). It was shown that CPR prevents acetylation of that Lys residue and that substitution of Ala at that position results in a 7-fold decrease in affinity for CPR. We found that the K149A substitution results in a 40-fold increase in K_m for CPR (20-fold for the analogous K169A mutation in HO-2). Thus, it appears that both HO's interact similarly with CPR.

Our results support that HO-2 forms a highly dynamic complex with CPR at an interface that includes HO-2 residues L201 and K169 and the CPR interface is likely highly conserved for both HO-1 and HO-2. As shown in Figure 2.22*B*, the homologous residues in HO-1 (L181 and K149) are located at the HO-1/CPR interface in the crystal structure of a complex between HO-1 and a deletion variant of CPR (CPR ΔTGEE) (26).

This CPR variant forms a stable complex with HO-1 that, unlike the wild-type protein, can be observed even by gel filtration (26). Given the high homology of the structures of the catalytic cores of HO-1 and HO-2 (55), we suggest that L201 and K169 of HO-2 participate in stabilizing the electron transfer complex between HO-2 and CPR.

2.5.2 Interactions between HO and BVR

Based on prior fluorescence quenching studies, HO-1 and BVR were proposed to form a high affinity complex (27); and our goal was to characterize the analogous HO-2/BVR complex using various biochemical and biophysical methods. However, addition of BVR to ^{15}N-labeled hHO-2 results in no chemical shift perturbation and, of the 104 assigned resonances in the hHO-2 spectrum, only five exhibit a BVR-dependent decrease in intensity. Of those residues that exhibit sensitivity to BVR, three are on the surface of the crystal structure and could reasonably be involved in binding BVR (K176, Q196 and Y229) (Figure 2.18). In contrast, under the same conditions with equimolar CPR, 48 of the assigned HO-2 resonances exhibit strong CPR dependent effects (Figure 2.9). These results suggest BVR binds hHO-2 with a weak affinity compared with CPR.

Because the TROSY experiments indicated that HO-2 does not bind BVR with high affinity (Figure 2.18), we repeated the original fluorescence quenching studies that described the hHO-1/BVR complex (27). Although our results with hHO-1 are nearly identical to those described in the original paper, additional controls indicate that free heme strongly quenches BVR-CPM fluorescence independently of HO. We also used optical absorbance methods to verify the ability of BVR to bind heme, as was reported previously (36). The K_d for the heme-BVR complex differs between the two experiments, with the absorbance data indicating binding of more than one heme to BVR. Furthermore, labeled BVR contains fluorophores at two specific sites (C292 or C293 and C204). We suggest that the fluorescence quenching studies may monitor binding of one heme to BVR at a high affinity site near one of these fluorophores, while the optical absorbance studies may reflect multiple heme binding events.

Thus, the fluorescence quenching studies aimed at studying interactions between HO-2 and BVR actually derive from binding of heme in solution that has

dissociated from hHO, rather than direct interactions between hHO and BVR. In fact, detection of an HO/BVR complex requires the use of methods like chemical cross-linking, where even transient complexes can be trapped.

This result describing the low affinity of HO for BVR is important because it clarifies the mechanism by which BVR couples to the HO reaction. It has been shown that BVR changes the rate limiting step of the HO-1 reaction from biliverdin release to the conversion of the Fe^{2+}-verdoheme intermediate to Fe^{3+}-biliverdin (40). We had taken this to indicate the possibility that biliverdin is channeled between the two proteins. However, it now appears that the effect of BVR on the HO rate limiting step occurs by kinetic coupling of the HO and BVR reactions, not substrate channeling. BVR binds HO-2 very weakly, therefore substrate channeling, which requires a stable complex, is unlikely. Thus, BVR simply binds the biliverdin upon release from its product complex with HO, enhancing the HO reaction by affecting the mass balance.

2.6 Conclusions

In conclusion, we show that protein-protein complexes between HO-2 and other proteins in the heme degradation pathway (CPR and BVR) are highly transient. HO-2 and CPR form a transient electron transfer complex and, like other electron transfer pairs, HO-2 and CPR may form an ensemble of complexes that is in equilibrium with the productive electron transfer complex. NMR binding studies and mutagenesis of HO-2 highlight an interface for CPR on HO-2, which is consistent with what has been described for CPR and HO-1. However, in contrast to studies with CPR and HO-1, our results suggest that CPR binding HO-2 in solution is dynamic. Gel filtration and ultracentrifugation studies support a weak/transient CPR/HO-2 complex. Complex formation between HO-2 and BVR is undetected, except via irreversible binding (cross-linking) methods. In the cell, CPR is an electron donor for many biologically important reactions. The dynamic interactions between CPR and HO-2 revealed in these studies may play an important role in the regulation of the HO system in a cellular context.

2.7 References

1. Sassa, S. (2004) Why heme needs to be degraded to iron, biliverdin IXalpha, and carbon monoxide? *Antioxid Redox Signal* **6**, 819-824
2. Furuyama, K., Kaneko, K., and Vargas, P. D. (2007) Heme as a magnificent molecule with multiple missions: heme determines its own fate and governs cellular homeostasis. *Tohoku J Exp Med* **213**, 1-16
3. Maines, M. D. (2004) The heme oxygenase system: past, present, and future. *Antioxid Redox Signal* **6**, 797-801
4. Maines, M. D. (2005) New insights into biliverdin reductase functions: linking heme metabolism to cell signaling. *Physiology (Bethesda)* **20**, 382-389
5. Maines, M. D. (1993) Carbon Monoxide: An Emerging Regulator of cGMP in the Brain. *Mol Cell Neurosci* **4**, 389-397
6. Kim, H. P., Ryter, S. W., and Choi, A. M. (2006) CO as a cellular signaling molecule. *Annu Rev Pharmacol Toxicol* **46**, 411-449
7. Hanafy, K. A., Oh, J., and Otterbein, L. E. (2013) Carbon Monoxide and the brain: time to rethink the dogma. *Current pharmaceutical design* **19**, 2771-2775
8. Andrews, N. C., and Schmidt, P. J. (2007) Iron homeostasis. *Annual review of physiology* **69**, 69-85
9. Jansen, T., Hortmann, M., Oelze, M., Opitz, B., Steven, S., Schell, R., Knorr, M., Karbach, S., Schuhmacher, S., Wenzel, P., Munzel, T., and Daiber, A. (2010) Conversion of biliverdin to bilirubin by biliverdin reductase contributes to endothelial cell protection by heme oxygenase-1-evidence for direct and indirect antioxidant actions of bilirubin. *J Mol Cell Cardiol* **49**, 186-195
10. Baranano, D. E., Rao, M., Ferris, C. D., and Snyder, S. H. (2002) Biliverdin reductase: a major physiologic cytoprotectant. *Proc Natl Acad Sci U S A* **99**, 16093-16098
11. Sedlak, T. W., Saleh, M., Higginson, D. S., Paul, B. D., Juluri, K. R., and Snyder, S. H. (2009) Bilirubin and glutathione have complementary antioxidant and cytoprotective roles. *Proc Natl Acad Sci U S A* **106**, 5171-5176
12. McCoubrey, W. K., Jr., Huang, T. J., and Maines, M. D. (1997) Isolation and characterization of a cDNA from the rat brain that encodes hemoprotein heme oxygenase-3. *Eur J Biochem* **247**, 725-732
13. Hayashi, S., Omata, Y., Sakamoto, H., Higashimoto, Y., Hara, T., Sagara, Y., and Noguchi, M. (2004) Characterization of rat heme oxygenase-3 gene. Implication of processed pseudogenes derived from heme oxygenase-2 gene. *Gene* **336**, 241-250
14. Ishikawa, K., Takeuchi, N., Takahashi, S., Matera, K. M., Sato, M., Shibahara, S., Rousseau, D. L., Ikeda-Saito, M., and Yoshida, T. (1995) Heme oxygenase-2. Properties of the heme complex of the purified tryptic fragment of recombinant human heme oxygenase-2. *J. Biol. Chem.* **270**, 6345-6350
15. Maines, M. D. (1997) The heme oxygenase system: a regulator of second messenger gases. *Annu Rev Pharmacol Toxicol* **37**, 517-554
16. Huang, T. J., McCoubrey, W. K., Jr., and Maines, M. D. (2001) Heme oxygenase-2 interaction with metalloporphyrins: function of heme regulatory motifs. *Antioxid Redox Signal* **3**, 685-696

17. Yi, L., and Ragsdale, S. W. (2007) Evidence that the heme regulatory motifs in heme oxygenase-2 serve as a thiol/disulfide redox switch regulating heme binding. *J. Biol. Chem.* **282**, 21056-21067
18. Yi, L., Jenkins, P. M., Leichert, L. I., Jakob, U., Martens, J. R., and Ragsdale, S. W. (2009) Heme regulatory motifs in heme oxygenase-2 form a thiol/disulfide redox switch that responds to the cellular redox state. *J. Biol. Chem.* **284**, 20556-20561
19. Varfaj, F., Lampe, J. N., and Ortiz de Montellano, P. R. Role of Cysteine Residues in Heme Binding to Human Heme Oxygenase-2 Elucidated by Two-dimensional NMR Spectroscopy. *J. Biol. Chem.* **287**, 35181-35191
20. Strobel, H. W., A. V. Hodgson, and S. Shen. . (1995) NADPH cytochrome P450 reductase and its structural and functional domains. *Cytochrome P 450*, 225-244
21. Tenhunen, R., Marver, H. S., and Schmid, R. (1969) Microsomal heme oxygenase. Characterization of the enzyme. *J. Biol. Chem.* **244**, 6388-6394
22. Yoshida, T., Noguchi, M., and Kikuchi, G. (1980) Inability of the NADH-cytochrome b5 reductase system to initiate heme degradation yielding biliverdin IX alpha from the oxygenated form of heme . heme oxygenase complex. *FEBS Lett.* **115**, 278-280
23. Kenaan, C., Zhang, H., Shea, E. V., and Hollenberg, P. F. Uncovering the role of hydrophobic residues in cytochrome P450-cytochrome P450 reductase interactions. *Biochemistry* **50**, 3957-3967
24. Higashimoto, Y., Sakamoto, H., Hayashi, S., Sugishima, M., Fukuyama, K., Palmer, G., and Noguchi, M. (2005) Involvement of NADPH in the interaction between heme oxygenase-1 and cytochrome P450 reductase. *J. Biol. Chem.* **280**, 729-737
25. Higashimoto, Y., Sugishima, M., Sato, H., Sakamoto, H., Fukuyama, K., Palmer, G., and Noguchi, M. (2008) Mass spectrometric identification of lysine residues of heme oxygenase-1 that are involved in its interaction with NADPH-cytochrome P450 reductase. *Biochem Biophys Res Commun* **367**, 852-858
26. Sugishima, M., Sato, H., Higashimoto, Y., Harada, J., Wada, K., Fukuyama, K., and Noguchi, M. (2014) Structural basis for the electron transfer from an open form of NADPH-cytochrome P450 oxidoreductase to heme oxygenase. *Proc Natl Acad Sci U S A* **111**, 2524-2529
27. Wang, J., and de Montellano, P. R. (2003) The binding sites on human heme oxygenase-1 for cytochrome p450 reductase and biliverdin reductase. *J. Biol. Chem.* **278**, 20069-20076
28. Danielson, P. B. (2002) The cytochrome P450 superfamily: biochemistry, evolution and drug metabolism in humans. *Curr Drug Metab* **3**, 561-597
29. Enoch, H. G., and Strittmatter, P. (1979) Cytochrome b5 reduction by NADPH-cytochrome P-450 reductase. *J. Biol. Chem.* **254**, 8976-8981
30. Williams, C. H., Jr., and Kamin, H. (1962) Microsomal triphosphopyridine nucleotide-cytochrome c reductase of liver. *J. Biol. Chem.* **237**, 587-595
31. Ono, T., and Bloch, K. (1975) Solubilization and partial characterization of rat liver squalene epoxidase. *J. Biol. Chem.* **250**, 1571-1579

32. Linnenbaum, M., Busker, M., Kraehling, J. R., and Behrends, S. Heme oxygenase isoforms differ in their subcellular trafficking during hypoxia and are differentially modulated by cytochrome P450 reductase. *PLoS One* **7**, e35483
33. Kutty, R. K., and Maines, M. D. (1981) Purification and characterization of biliverdin reductase from rat liver. *J. Biol. Chem.* **256**, 3956-3962
34. Maines, M. D., Ewing, J. F., Huang, T. J., and Panahian, N. (2001) Nuclear localization of biliverdin reductase in the rat kidney: response to nephrotoxins that induce heme oxygenase-1. *J Pharmacol Exp Ther* **296**, 1091-1097
35. Ahmad, Z., Salim, M., and Maines, M. D. (2002) Human biliverdin reductase is a leucine zipper-like DNA-binding protein and functions in transcriptional activation of heme oxygenase-1 by oxidative stress. *J. Biol. Chem.* **277**, 9226-9232
36. Tudor, C., Lerner-Marmarosh, N., Engelborghs, Y., Gibbs, P. E., and Maines, M. D. (2008) Biliverdin reductase is a transporter of haem into the nucleus and is essential for regulation of HO-1 gene expression by haematin. *Biochem J* **413**, 405-416
37. Miralem, T., Hu, Z., Torno, M. D., Lelli, K. M., and Maines, M. D. (2005) Small interference RNA-mediated gene silencing of human biliverdin reductase, but not that of heme oxygenase-1, attenuates arsenite-mediated induction of the oxygenase and increases apoptosis in 293A kidney cells. *J. Biol. Chem.* **280**, 17084-17092
38. Lerner-Marmarosh, N., Shen, J., Torno, M. D., Kravets, A., Hu, Z., and Maines, M. D. (2005) Human biliverdin reductase: a member of the insulin receptor substrate family with serine/threonine/tyrosine kinase activity. *Proc Natl Acad Sci U S A* **102**, 7109-7114
39. Lerner-Marmarosh, N., Miralem, T., Gibbs, P. E., and Maines, M. D. (2008) Human biliverdin reductase is an ERK activator; hBVR is an ERK nuclear transporter and is required for MAPK signaling. *Proc Natl Acad Sci U S A* **105**, 6870-6875
40. Liu, Y., and Ortiz de Montellano, P. R. (2000) Reaction intermediates and single turnover rate constants for the oxidation of heme by human heme oxygenase-1. *J. Biol. Chem.* **275**, 5297-5307
41. Aslanidis, C., and de Jong, P. J. (1990) Ligation-independent cloning of PCR products (LIC-PCR). *Nucleic Acids Res* **18**, 6069-6074
42. Marohnic, C. C., Panda, S. P., Martasek, P., and Masters, B. S. (2006) Diminished FAD binding in the Y459H and V492E Antley-Bixler syndrome mutants of human cytochrome P450 reductase. *J. Biol. Chem.* **281**, 35975-35982
43. Dawson, R. M. C. (1986) *Data for biochemical research.* 3rd ed. Oxford: Clarendon Press, New York, NY.
44. Delaglio, F., Grzesiek, S., Vuister, G. W., Zhu, G., Pfeifer, J., and Bax, A. (1995) NMRPipe: a multidimensional spectral processing system based on UNIX pipes. *J Biomol NMR* **6**, 277-293
45. T. D. Goddard and D. G. Kneller, S., University of California, San Fransico. SPARKY 3.
46. Andresen, C., Helander, S., Lemak, A., Fares, C., Csizmok, V., Carlsson, J., Penn, L. Z., Forman-Kay, J. D., Arrowsmith, C. H., Lundstrom, P., and

Sunnerhagen, M. Transient structure and dynamics in the disordered c-Myc transactivation domain affect Bin1 binding. *Nucleic Acids Res* **40**, 6353-6366
47. Cavanagh, J., Fairbrother, W., Palmer, A.G., 3rd, Rance, M., Skelton, N.J., *Protein NMR Spectroscopy: principles and practise.* 2nd ed.; Elsevier Academic Press: Amsterdam. (2007).
48. Quenouille, M. H. (1956) Notes on bias in estimation. *Biometrika* **43(3/4)**, 353-360
49. Ishikawa, K., Matera, K. M., Zhou, H., Fujii, H., Sato, M., Yoshimura, T., Ikeda-Saito, M., and Yoshida, T. (1998) Identification of histidine 45 as the axial heme iron ligand of heme oxygenase-2. *J. Biol. Chem.* **273**, 4317-4322
50. Huber, W. J., 3rd, Marohnic, C. C., Peters, M., Alam, J., Reed, J. R., Masters, B. S., and Backes, W. L. (2009) Measurement of membrane-bound human heme oxygenase-1 activity using a chemically defined assay system. *Drug Metab Dispos* **37**, 857-864
51. Dam, J., Velikovsky, C. A., Mariuzza, R. A., Urbanke, C., and Schuck, P. (2005) Sedimentation velocity analysis of heterogeneous protein-protein interactions: Lamm equation modeling and sedimentation coefficient distributions c(s). *Biophys J* **89**, 619-634
52. Schuck, P. (2000) Size-distribution analysis of macromolecules by sedimentation velocity ultracentrifugation and lamm equation modeling. *Biophys J* **78**, 1606-1619
53. Sambrook, J., and Russell, D. (2001) *Molecular Cloning: a Laboratory Manual,* 3rd Ed., Cold Spring Harbor Laboratory, Cold Spring Harbor, NY.
54. Pervushin, K., Riek, R., Wider, G., and Wuthrich, K. (1997) Attenuated T2 relaxation by mutual cancellation of dipole-dipole coupling and chemical shift anisotropy indicates an avenue to NMR structures of very large biological macromolecules in solution. *Proc Natl Acad Sci U S A* **94**, 12366-12371
55. Bianchetti, C. M., Yi, L., Ragsdale, S. W., and Phillips, G. N., Jr. (2007) Comparison of apo- and heme-bound crystal structures of a truncated human heme oxygenase-2. *J. Biol. Chem.* **282**, 37624-37631
56. Baker, J. M., Hudson, R. P., Kanelis, V., Choy, W. Y., Thibodeau, P. H., Thomas, P. J., and Forman-Kay, J. D. (2007) CFTR regulatory region interacts with NBD1 predominantly via multiple transient helices. *Nat Struct Mol Biol* **14**, 738-745
57. Carrington, A., and MacLachlan, A. (1967) *Introduction to Magnetic Resonance with Applications to Chemistry and Chemical Physics*, Harper & Row, New York
58. Tanford, C. (1963) *Physical Chemistry of Macromolecules,* Wiley, NY.
59. McCoubrey, W. K., Jr., and Maines, M. D. (1994) Site-directed mutagenesis of cysteine residues in biliverdin reductase. Roles in substrate and cofactor binding. *Eur J Biochem* **222**, 597-603
60. Zuiderweg, E. R., Hamers, L. F., Rollema, H. S., de Bruin, S. H., and Hilbers, C. W. (1981) 31P NMR study of the kinetics of binding of myo-inositol hexakisphosphate to human hemoglobin. Observation of fast-exchange kinetics in high-affinity systems. *Eur J Biochem* **118**, 95-104
61. Zuiderweg, E. R. (2012). in *Recent Developments in Biomolecular NMR* (Clore, G., and Potts, J. ed.), The Royal Society of Chemistry, Cambridge. pp 216-252

62. Matsui, T., Iwasaki, M., Sugiyama, R., Unno, M., and Ikeda-Saito, M. Dioxygen activation for the self-degradation of heme: reaction mechanism and regulation of heme oxygenase. *Inorg Chem* **49**, 3602-3609

Chapter 3 An analysis of the role of cysteine residues in biliverdin reductase substrate inhibition

3.1 Abstract

Biliverdin reductase (BVR) catalyzes the second step of heme degradation; the conversion of biliverdin to bilirubin. Rat BVR possesses three cysteine residues (C73, C280, and C291). Reports conflict regarding the requirement of C73 for enzymatic activity. Also, BVR is subject to strong substrate inhibition under conditions of high biliverdin concentration. Cysteine residues 280 and 291 of rat BVR are implicated in substrate (biliverdin) and cofactor (NADPH) binding and may have a role in mediating BVR substrate inhibition. In this chapter, the requirement for the cysteines of human BVR in catalysis and substrate inhibition are determined by assessing the effect of cys to ala substitutions on BVR catalysis and substrate inhibition. Human BVR possesses 5 cysteine residues with amino acid numbering increased by 1 as compared with rat BVR (C74, C204, C281, C292, and C293). Alanine substitution of C74 results in a large (~80%) reduction in specific activity, establishing that this residue is important for BVR catalysis. The C74A variant is also less sensitive to the addition of biliverdin, indicating a relief of substrate inhibition for this variant. Alanine substitution of additional residues (C281, C292, C293 and the double substitution C292/C293) does not effect steady state catalysis or substrate inhibition, indicating that these residues are not required to mediate either aspect of BVR.

3.2 Introduction to Biliverdin Reductase

As described in Chapter 1 of this thesis, the heme degradation pathway consists of two enzymatic steps mediated by heme oxygenase (HO) and biliverdin reductase (BVR). In the first step, HO converts heme to biliverdin by cleavage of heme at the α-*meso* carbon bridge (Figure 1.2) [Equation 1]. The two major isoforms of HO, HO-1 and HO-2, share a high degree of homology (55% identity and 76% similarity) and possess similar enzymatic activity (1). The HO isoforms HO-1 and HO-2 are 32 and 36 kDa

respectively, and both possess a C-terminal membrane spanning region which tethers the protein to the cytoplasmic side of the endoplasmic reticulum. The HO isoforms differ in their expression and regulation; while HO-1 is transcriptionally regulated and expressed in most tissues, HO-2 is expressed constitutively, primarily in the brain and testes (2,3)

Biliverdin reductase (BVR) mediates the second step of heme degradation, in which biliverdin is converted to bilirubin by the reduction of biliverdin at the γ-meso bridge (4-6). BVR is a soluble ~33 kDa protein that is predominantly cytosolic. As shown in Equation 2, BVR catalysis requires 2 reducing equivalents. BVR is unique in that it utilizes reducing equivalents from either NADH or NADPH, and has distinct pH optima for the two cofactors (pH ~6.75 for NADH and pH ~8.7 for NADPH) (6,7). NADPH is likely the most biologically relevant cofactor as at physiologic pH the K_m for NADPH is ~100-fold lower than the Km for NADH (8). Furthermore, in the cytosol where the majority of BVR is located, the $NADP^+$:NADPH couple is predominately reduced, while NAD^+:NADH is mostly oxidized (9).

$$\text{Heme} + 7e^- + 3O_2 \rightarrow \text{biliverdin} + CO + Fe(II) + 3H_2O \qquad \text{[Equation 1]}$$

$$\text{Biliverdin} + 2e^- \rightarrow \text{Bilirubin} \qquad \text{[Equation 2]}$$

Because bilirubin is less soluble than biliverdin, and high levels of bilirubin are neurotoxic, there has been some question as to why bilirubin is produced (10,11). Normal levels of bilirubin, however, are biologically beneficial for a number of reasons (12). In some mammals, the reduction of biliverdin to bilirubin facilitates the elimination of heme catabolites from the fetus, as the placenta is impermeable to biliverdin but permeable to bilirubin (13). In the bloodstream bilirubin is normally bound by albumin to enhance its solubility. It is transported to the liver where it is conjugated with glucoronic acid to increase solubility and facilitate excretion from the body (14). A balance between BR production and excretion is crucial as the accumulation of bilirubin leads to hyperbilirubinimia, a common medical complication in newborns that can result in neural impairment if not treated promptly (15). Common causes for hyperbilirubinimia are excessive bilirubin production, impaired glucuronidation, or acidosis which reduces the binding of BR to albumin (16).

While high levels of bilirubin are toxic, low levels confer protection against reactive oxygen species (ROS) (17-19). The bilirubin antioxidant system may be particularly important in the brain, as low levels of bilirubin (10 nM) protect neuronal cells from oxidation by 10,000-fold greater concentrations of hydrogen peroxide (20). Also, mice with a deletion of the brain specific HO-2 ($HO\text{-}2^{-/-}$) have reduced bilirubin levels and exhibit higher sensitivity to neurologic damage such as cerebral ischemia and traumatic brain injury (20,21).

In addition to its catalytic activity, additional functions have been ascribed to BVR. BVR is a transcriptional regulator of genes involved in the oxidative stress response. *In vitro* studies show that dimeric BVR binds activator protein (AP-1) DNA binding sites while monomeric BVR fails to bind DNA (22,23). AP-1 sites are DNA binding sites for regulatory proteins containing bzip dimerization motifs (such as BVR, c-Jun and c-Fos) and are involved in the regulation of oxidative stress responsive genes such as HO-1 (24-26).

Studies in cells demonstrate a role for BVR in HO-1 transcriptional regulation. While under normal conditions BVR is primarily cytosolic, in cells treated with hematin BVR translocates to the nucleus and is required for hematin-induced expression of HO-1 (23,27). Consistent with this observation, BVR is a heme binding protein *in vitro* (23). BVR possesses both nuclear localization and nuclear export signals (NLS and NES) and the NLS is required for HO-1 transcriptional activation (23).

In addition to its role in transcriptional activation, BVR is involved in a number of signaling pathways via its kinase activity. BVR is a rare dual specificity (Ser/Thr and Tyr) kinase (28,29) and functions in cell signaling pathways important for regulating glucose uptake gene expression. In the insulin signaling pathway, BVR is a target for insulin-activated insulin receptor tyrosine kinase (IRK). In cells, a reduction in BVR protein levels results in increased uptake of glucose in response to insulin (30). Furthermore, exposure of cells to peptides based on the C-terminus of BVR (KYCCSRK) modulate glucose uptake and IGF-1 stimulation for those cells (31). BVR also plays a role in the mitogen-activated protein kinase (MAPK) signaling pathway, which is involved in the transcriptional response to stress (32). BVR possesses MAPK binding sites and binds to the MAPK regulators mitogen-activated protein kinase kinase

(MEK) and extracellular signal-regulated kinase (ERK) and can activate these regulators via its kinase activity. There are many targets for activated ERK, including oxidative-stress responsive genes such as HO-1 and inducible nitric oxide synthase (iNOS) (32).

As described above, BVR and its product bilirubin are involved in various processes important for cellular function and health including heme catabolite excretion, antioxidant protection, transcriptional regulation, and cellular signaling. Thus, understanding the regulatory mechanisms of BVR is important for understanding these cellular mechanisms that are important in human health and disease.

Early studies characterizing BVR reveal a major mechanism of regulation for the enzyme; BVR is strongly substrate inhibited. Also, cysteine residues of BVR are implicated in substrate and cofactor binding and may be required for catalytic activity. This chapter further addresses the role of cysteine residues in BVR substrate inhibition.

BVR undergoes inhibition by thiol-reactive reagents, which inhibit catalytic activity for both rat and human BVR, suggesting that cysteine residues play an important role in catalytic function (4,8,33). Human BVR possesses five cysteines; C74 is present in the enzymatic cleft, C204 is found on the surface of the protein, and C281 is not surface exposed, as shown on the BVR crystal structure in Figure 3.1. C292 and C293 are near the C-terminus, however the BVR crystal structure contains residues 6-291, therefore C292 and C293 are not visible in Figure 3.1. Cysteines C74, C281, and C292 are highly conserved across multiple species (Figure 3.2). Rat BVR contains only the three highly conserved cysteines, and one fewer amino acid compared with human BVR, resulting in slightly differing numbering for the residues (C73, C280 and C291, rat numbering) (Figure 3.3).

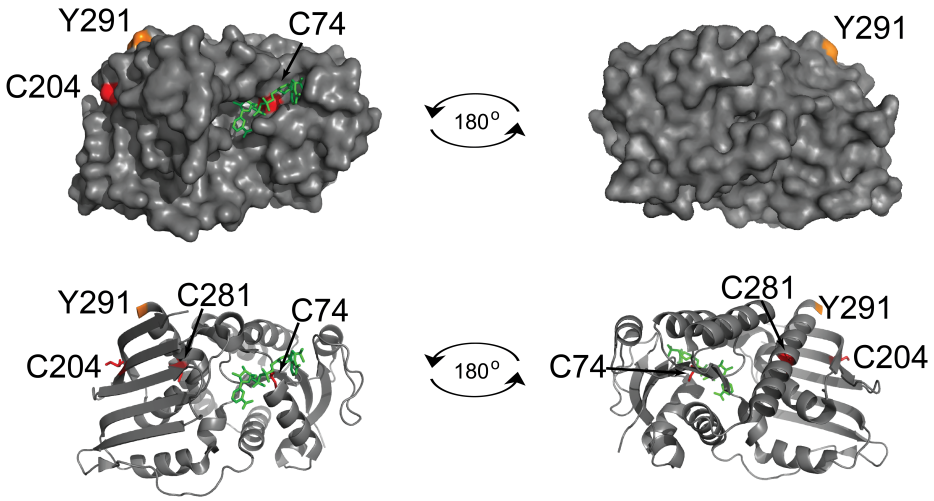

Figure 3.1. **Human BVR contains 5 cysteines.** The crystal structure of human BVR residues 6-291 (PDB 2H63) is shown as a space filled model (*top*) and as a cartoon (*bottom*). Cysteine side chains are red, while Y291, the most C-terminal BVR residue visible, is shown in orange. NADP+ is in green. C292 and C293 are not visible in this structure.

```
                1                                74                                204                               281       292/293
Human           MNAEPERKFGVVVVGVGRAG SSQEVEVAYICSESSSHEDYI KEDQYMKMTVCLETEKKSPLS LAAEKKRILHCLGLAEEIQKYCCSRK----
Chimp           MNTEPERKFGVVVVGVGRAG SSQEVEVAYICSESSSHEDYI KEDQYMKMTVCLETEKKSPLS LAAEKKRILHCLGLAEEIQKYCCSRK----
Rhesus          MNTEPERKFGVVVVGVGRAG SSQEVEVAYICSESSSHEDYI KEDQYMKMTVCLETEKKSPLS LAAEKKRILHCLGLAEEIQKYCCSRK----
Horse           MNAEPERKFGVVVVGVGRAG SSQEVEVAYICSENSSHEDYI KEDQYMKMTVCLETENKRPLT LAAEKKRILHCLWLAEEIQKHCYSKE----
Dog             MNAEPERKFGVVVVGVGRAG SSQEVEVAYICSESSSHADYI KEDQYMKMTVCLETENKRPLT LAAEKKRILHCLWLAEEIQKYCYSKK----
Cow             MNTEPERKFGVVVVGVGRAG SSQEVEVAFICSESSSHEDYI KEDQYMKMTVCLETENKSPLT LAAEKKRILHCLWLAGEIQKHCCSKQ----
Pig             MDAEPQRRFGVVVVGVGRAG SSQEVEVAFICSESSSHEDYI KEDQYMKMTVCLETENKSPLT LAAEKKRILHCLWLAGEIQKHCCSKK----
Rat             MDAEPKRKFGVVVVGVGRAG RSQEIDVAYICSESSSHEDYI KEDQYMKMTVQLETQNKGLLS LAAEKKRIMHCLGLASDIQKLCHQKK----
Mouse           MSTEPKRKFGVVVVGVGRAG RSQEVDVAYICTESSSHEDYI KEDQYMKMTVQLETQNKSPLS LAAEKKRILHCLELASDIQRLCHRKQ----
Zebrafish       -------MLGSVVVGIGIAG SRDDIHVAFICTENTSHEENI KENKYMKMTAHLLTQQHKPLT LQAERNRILHCLELADRIQQITENTHA---
Chicken         -------MFGTVVVGVGIAG RSKEIHAAFISTENRSHEETI KDKNYSRMTVHFQTANKKPLT LAAEKWRILRCLDLAGMIQQQCEQPEKICS
Xenopus         -------MFGAVVVGIGIAG KSKDIDAAFICTDNQNHEESV KELNYSKLTAHFLTAENRPLT LLAEKQRILKCIDLAEEIKKKCEH------
```

Figure 3.2. **Multiple species alignment of cysteines in BVR.** Sequence alignment (ClustalW2) of BVR from 12 species focusing on sequence encompassing cysteine residues. Numbering corresponds to the human sequence. Gaps represent sequence omitted for clarity.

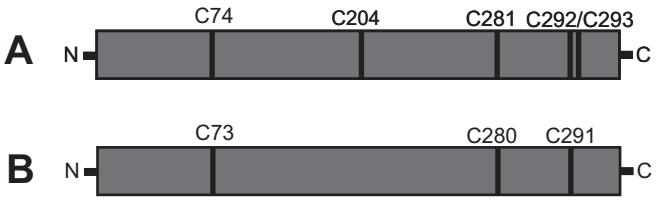

Figure 3.3. **Cysteines in rat BVR are conserved in human BVR.** Human BVR **(A)** and rat BVR **(B)** are highly conserved with 83.1% identity and 94.9% similarity. Cysteines are shown as black bars in their relative locations on the protein. hBVR contains an additional amino acid compared to rBVR.

Additional reports address the role of specific cysteines in rat BVR catalysis by determining the effect of cysteine to alanine substitutions at positions C73, C280, and C291 (rat BVR numbering). However these studies report conflicting results. One study finds the C73A substitution ablates enzymatic activity, suggesting C73 is required for catalysis (34). The same study reports the alanine substitution C280A has ~70% catalytic activity compared with wild type. However, a second group reports that the catalytic activities of both C73A and C280A variants are identical to that of the wild type enzyme (35). Thus the requirements for C73 and C280 for BVR catalysis are not clear.

Cysteine residues C280 and C291 of rat BVR are proposed to participate in substrate (biliverdin) and cofactor (NADPH) binding (34). Alanine substitution for C280 increases the K_m for biliverdin by 3-fold, while the K_m for NADPH is unaffected, suggesting a role for C280 in biliverdin binding. Substitution of C291 by Ala increases the K_m for NADPH 4.6-fold, while the K_m for biliverdin is unaffected, suggesting that C291 plays a role in binding NADPH (34). Both substrate and cofactor binding are important for catalysis, as a disruption in either substrate or cofactor binding could result in a reduction or loss of catalytic activity. As mentioned above, the C280A substitution causes reduced catalytic function (loss of 30% activity), further supporting that this residue may be important for BVR activity. While structural perturbations could also result in impaired enzymatic function, circular dichroism results demonstrate that the structures of the C280A and C291A variants are similar to wild type and that the alanine substitutions do not cause large structural changes (34).

BVR exhibits substrate inhibition; rat BVR shows dramatic concentration dependent inhibition with increasing concentrations of biliverdin (8,36,37). Kinetic studies suggest that the formation of the BVR-BV-NADP+ complex is inhibitory and that, at high biliverdin concentrations, product release from this complex is the rate limiting catalytic step (36). Supporting the existence of a BVR-BV-NADP+ complex, the fluorescence of the NADP+ analog etheno-NADP is enhanced in the presence of BVR,

but quenched and shifted in the presence of biliverdin, indicating that etheno-NADP and biliverdin are in close proximity (36).

Because BVR is strongly substrate inhibited and the inhibitory complex is reported to be BVR-BV-NADP+, we hypothesize that residues important for substrate or cofactor binding are important for mediating BVR:substrate inhibition. To test the importance of cysteine residues in human BVR substrate inhibition, we constructed alanine substitutions for these cysteine residues and determined the effects on substrate inhibition.

The analysis described in this Chapter focuses on the highly conserved cysteines C74A, C281A, and C292A (hBVR numbering). We determined the effect of Cys-to-Ala substitutions on catalytic activity and substrate inhibition. These studies also address the conflicting reports regarding the enzymatic requirement for C73 and C280 (or C74 and C281 in human BVR). In addition to examining the roles of the three highly conserved cysteines in hBVR (C74, C281, and C292), we also address the importance of C293A, which is not highly conserved but is located adjacent to C292. We find that human BVR, like rat BVR, is strongly substrate inhibited. We find little evidence to support a major regulatory role for C281, C292 or C293 in human BVR for either catalytic activity or substrate inhibition. However, consistent with the previous report by Mccourbrey and Maines (1994) we find that C74 of hBVR, equivalent to C73 of rat BVR, is important for BVR catalytic activity.

3.3 Materials and methods

3.3.1 Cloning, expression, and purification of human BVR

3.3.2 Materials

Ampicillin, isopropyl-β-D-thiogalactopyranoside (IPTG), NADPH, and bovine serum albumin (BSA) were purchased from Sigma (St Louis, MO). OneShot® BL21(DE3) chemically competent cells were purchased from Invitrogen/Life Technologies (Grand Island, NY). Glutathione Sepharose was purchased from GE Healthcare (Piscataway, NJ). Biliverdin (BV) was purchased from Frontier Scientific (Logan, UT). CompleteMini EDTA free protease inhibitor tablets were purchased from Roche (Indianapolis, IN).

3.3.3 Enzyme purification

The human *BVR* gene was purchased from American Type Culture Collection (Manassas, VA) and subcloned into the pGEX4T2 plasmid. This vector contains a glutathione s-transferase affinity purification tag to facilitate purification of BVR from bacterial homogenate. BL21(DE3) cells were transformed with plasmid containing the BVR gene, plated on Luria Broth (LB)/Agar with ampicillin (100 μg/ml) and incubated for 16h at 37°C. 100 mL LB with ampicillin (100 μg/mL) was inoculated with a single colony and incubated at 37°C for 16 h with agitation at 250 rpm. For BVR induction, 1 L LB with ampicillin (100 μg/mL) was inoculated with 10 mL stationary culture and incubated at 37°C, 250 rpm until growth reached an OD_{600} of ~0.8. BVR expression was induced with the addition of 300 mM IPTG and cells incubated at 20°C for 16 h, 250 rpm. Cells were harvested by centrifugation in a Sorvall© RC5B at 6,000 rpm, 4C for 10 min. Cell pellets were frozen in liquid nitrogen and stored at -80°C.

Cells were thawed and resuspended in lysis buffer (PBS with 0.5 mg/ml lysozyme, 0.4% Triton x-100, 0.5 mg/ml RNase, 2.5 μg/ml DNase, 1 CompleteMini EDTA free protease inhibitor tablet (Roche)) by stirring at 4°C for 30 min. Following sonication, the homogenate was centrifuged at 30,000 x g for 30 min at 4°C. The supernatant was loaded onto 5 mL Glutathione S-Transferase (GST) sepharose and washed extensively with 200 mL PBS. BVR was eluted with a linear gradient to 10 mM reduced glutathione and the GST purification tag was removed from BVR by limited thrombin proteolysis. The affinity tag was then separated from the protein by chromatography using glutathione sepharose affinity resin. Purified BVR was snap frozen in liquid nitrogen and stored at -80°C. All purification steps were performed at 4°C.

3.3.4 Site-directed mutagenesis of hBVR

Point mutations of hBVR were constructed using the QuickChange site-directed mutagenesis protocol (Stratagene, La Jolla, CA). Oligonucleotides were synthesized by Integrated DNA Technologies (Coralville, Iowa). Positive transformants were enriched by antibiotic selection and confirmed using DNA sequence analysis. All of the variants were purified as described above for the wild type enzyme.

3.3.5 BVR activity assay

BVR activity was assayed as previously described with some modifications (8). The assay was conducted in a double beam Shimadzu UV-2600 spectrophotometer at 20°C. The reaction cuvette contained 0.2 μM BVR, 1 mg/ml bovine serum albumin (BSA), 0.5 μM Mg Cl_2, 0.1 mM Tris pH 8.0 with varying amounts of biliverdin (BV) in a total volume of 1 ml. The reference cuvette contained an identical reaction. The reaction was initiated with the addition of 100 μM NADPH. Bilirubin production was monitored by the increase in absorbance at A_{468} and the milimolar difference extinction coefficient between bilirubin and biliverdin of 46.0 mM^{-1} cm^{-1} was used to determine the specific activity of BVR (mM BV/mg BVR/min) (8).

3.4 Experimental results

3.4.1 The role of cysteines in hBVR steady state enzyme activity

To address the requirement for highly conserved Cys residues at positions 74, 281, and 292 in the catalytic mechanism of hBVR, we replaced each of them with alanine and determined the effect on catalytic activity (Figure 3.4). The C74A construct is strongly impaired and exhibits only ~20% activity compared with the wild type enzyme. This result is consistent with a study with rat BVR that reports a requirement for C74 (34). On the other hand, the C281A, C292A, C293A variants had greater than 95% activity compared with the wild type enzyme, and substitution of both Cys292 and 293 led to a specific activity that was 78% of that of wild type BVR (Figure 3.4).

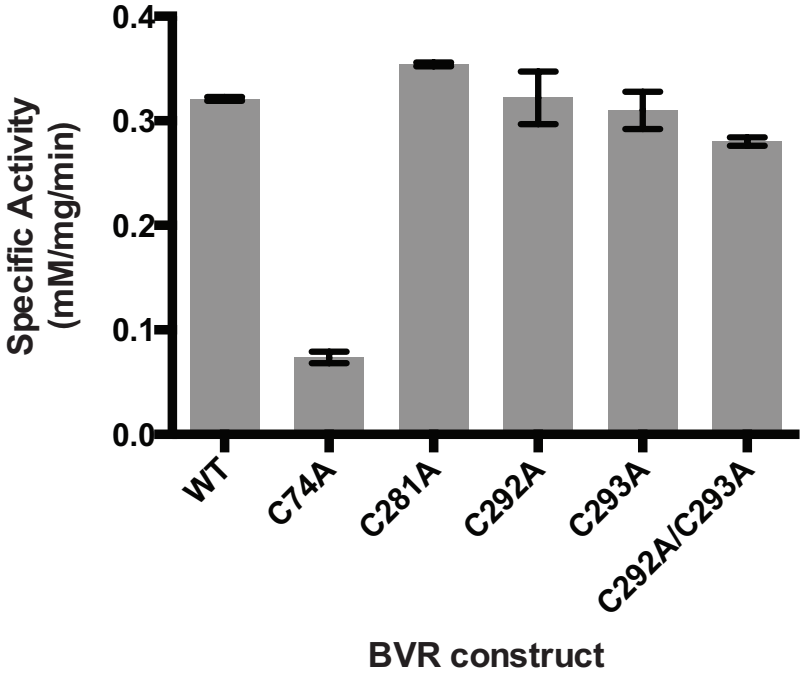

Figure 3.4. **The effect of alanine substitutions of cysteines on BVR activity.** Specific activity for various BVR constructs monitored by bilirubin production at 468 nm (Σ = 46 mM^{-1} cm^{-1}) for 0.2 μM BVR with 1.5 μM BV as described in methods. Data represent the mean of at least three independent experiments and error bars represent the standard deviation of the mean.

3.4.2 The role of cysteines in hBVR substrate inhibition

Catalytic activity of human BVR is strongly impaired as concentrations of biliverdin exceed BVR by 10-fold or more (Figure 3.5). C281A, C292A, C293A, and C292A/C293A exhibit similar sensitivity to increasing concentrations of biliverdin, suggesting these residues are not required for mediating BVR substrate inhibition. C74A is somewhat less sensitive to increasing biliverdin concentrations as compared to the other BVR constructs, however catalytic activity for this construct is also dramatically impaired (Figure 3.5).

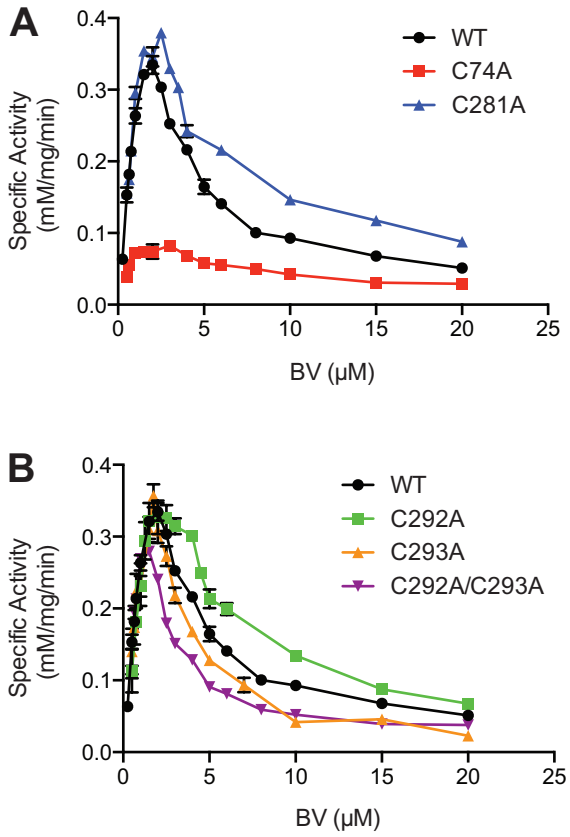

Figure 3.5. **The effect of alanine substitutions of BVR cysteines on BVR substrate inhibition.** Specific activity for various BVR mutants with various concentrations of BV as described in methods. Activity is expressed as mM BR/mg BVR/min. Bilirubin production is monitored at 468 nm (Σ = 60 mM^{-1} cm^{-1}). **(A)** Alanine substitutions of BVR constructs: wild type, C74A and C281A. **(B)** Alanine substitutions of BVR constructs: wild type, C292A, C293A and C292A/C293A. For clarity, the alanine variants are divided into the two groups as described, while WT is shown on both **(A)** and **(B)**. Data represent the mean of at least three independent experiments and error bars represent the standard deviation of the mean.

3.5 Discussion

Because earlier studies implicate specific cysteine residues in substrate and cofactor binding for rat BVR, we tested the conserved Cys residues in human BVR to determine their potential role(s) in steady-state catalysis and in mediating substrate inhibition. Alanine substitution at C281, C292, or C293 had little effect on hBVR catalytic activity (Figure 3.4), in contrast with results obtained with rat BVR (34). On the other hand, we find that catalytic activity is strongly impaired for the C74A construct,

consistent with a study conducted with rat BVR (34). This result clarifies a requirement for an intact cysteine at C74 in hBVR (C73 in rat BVR) that, until now, had been controversial.

It is not clear why Kikuchi *et al* observe no loss of catalytic activity for the C73A BVR construct as their reported methods are almost identical to those of Mccourbrey *et al* who report impaired activity for the same construct (34,35). One difference in the methods is that Kikuchi *et al* used purified enzyme whereas McCoubrey *et al* used bacterial lysates that were expressing BVR. However in the present study purified BVR is used, and we observe a similar loss of activity for the C73A mutant as McCourbrey *et al*, suggesting that the degree of purity for BVR is not a reason for the dissimilar results of the two previous studies.

The physiologic relevance of substrate inhibition for BVR is not known, however substrate inhibition is a regulatory mechanism observed in about 20% of enzymes and can be important for regulation of those enzymes (38). Substrate inhibition of BVR could regulate enzymatic activity under conditions when cells experience high levels of biliverdin levels. For example, after trauma that results in a bruise, the accumulation of biliverdin is evident in the greenish color of the bruise (39). Under hemolytic conditions such as bruising, large amounts of heme must be degraded due to the breakdown of red blood cells. Both HO and BVR require NADPH (HO receives electrons from NADPH via cytochrome P450 reductase), and, under conditions where high levels of heme must be degraded, competition for NADPH could occur. The K_m of BVR for NADPH is ~3 μM (8), while the K_m of CPR for NADPH is ~5 μM (40). Because free heme is toxic, substrate inhibition of BVR could be a mechanism to decrease competition for NADPH and favor the HO reaction over the BVR reaction under hemolytic (and perhaps other conditions) that result in an accumulation of heme.

We observed no major effect on BVR substrate inhibition for the BVR Cys to Ala variants C281A, C292A, C293A, and C292A/C293A. These variants all exhibit strong substrate inhibition with a very sharp inflection point at ~2 μM BV and at high concentrations (~20 μM) of BV exhibit less than 25% catalytic activity. On the other hand, the C74A variant does not exhibit a sharp inflection point at high BV concentrations, which demonstrates a relief of substrate inhibition for this construct.

Catalytic activity is also reduced for the C74A construct, and these results are consistent with weak NADP+ binding described for the rat BVR C73A construct (34).

3.6 Future directions

Under the conditions of the present study, C74 of human BVR is important for BVR catalytic activity. Studies utilizing rat BVR report alanine substitution of the analogous cysteine, C73, is unable to bind an NADP cofactor column, suggesting this cysteine is required for cofactor binding (34). The human BVR construct C74A is less sensitive to increasing concentrations of biliverdin compared to the other BVR constructs, and catalytic activity is reduced.

Previous studies suggest a role for C280 and C291 in binding BV and NADPH for rat BVR (34). If these residues do indeed play a role in substrate and cofactor binding, we would expect that alanine substitution of these residues would affect BVR substrate inhibition, which was not the case. Thus the role of C280 and C291 (C281 and C292 for human BVR) is unclear. Determining the effect of the alanine substitutions on the binding affinity of BVR for biliverdin and NADPH would clarify the role of these residues in BVR activity.

BVR catalysis does not require C281, C292, or C293 (Figure 3.4) and these residues are not required for mediating substrate inhibition (Figure 3.5). Many proteins contain cysteines that, under oxidizing conditions, form disulfide bonds which can modulate activity of those proteins (41,42). HO-2 posses a redox sensitive dithiol switch and the redox state of two C-terminal cysteines affect the affinity of HO-2 for heme (43). Given the redox sensitivity of HO-2 in the first step in heme degradation, and the role that BVR plays in protection against oxidative stress via production of bilirubin and in regulating genes responsible for mediating the oxidative stress response, it's likely that BVR may also be subject to redox regulation. Future studies testing the effects of oxidative conditions on BVR activity could help determine if BVR is subject to redox regulation. If BVR activity is affected by changes in the redox state, these effects may be mediated by the conserved cysteines addressed in the present studies and future studies testing requirements for those cysteines may be conducted.

3.7 References

1. Ishikawa, K., Takeuchi, N., Takahashi, S., Matera, K. M., Sato, M., Shibahara, S., Rousseau, D. L., Ikeda-Saito, M., and Yoshida, T. (1995) Heme oxygenase-2. Properties of the heme complex of the purified tryptic fragment of recombinant human heme oxygenase-2. *J. Biol. Chem.* **270**, 6345-6350
2. Maines, M. D. (1997) The heme oxygenase system: a regulator of second messenger gases. *Annu Rev Pharmacol Toxicol* **37**, 517-554
3. Ewing, J. F., and Maines, M. D. (1997) Histochemical localization of heme oxygenase-2 protein and mRNA expression in rat brain. *Brain Res Brain Res Protoc* **1**, 165-174
4. Kutty, R. K., and Maines, M. D. (1981) Purification and characterization of biliverdin reductase from rat liver. *J. Biol. Chem.* **256**, 3956-3962
5. P, O. C., and Colleran, E. (1971) Properties and kinetics of biliverdin reductase. *Biochem J* **125**, 110P
6. Singleton, J. W., and Laster, L. (1965) Biliverdin reductase of guinea pig liver. *J. Biol. Chem.* **240**, 4780-4789
7. Tenhunen, R., Ross, M. E., Marver, H. S., and Schmid, R. (1970) Reduced nicotinamide-adenine dinucleotide phosphate dependent biliverdin reductase: partial purification and characterization. *Biochemistry* **9**, 298-303
8. Noguchi, M., Yoshida, T., and Kikuchi, G. (1979) Purification and properties of biliverdin reductases from pig spleen and rat liver. *J Biochem* **86**, 833-848
9. Siess, E. A., Brocks, D. G., Lattke, H. K., and Wieland, O. H. (1977) Effect of glucagon on metabolite compartmentation in isolated rat liver cells during gluconeogenesis from lactate. *Biochem J* **166**, 225-235
10. Porter, M. L., and Dennis, B. L. (2002) Hyperbilirubinemia in the term newborn. *American family physician* **65**, 599-606
11. Shapiro, S. M. (2003) Bilirubin toxicity in the developing nervous system. *Pediatric neurology* **29**, 410-421
12. McDonagh, A. F. (2010) Controversies in bilirubin biochemistry and their clinical relevance. *Seminars in fetal & neonatal medicine* **15**, 141-147
13. McDonagh, A. F., Palma, L. A., and Schmid, R. (1981) Reduction of biliverdin and placental transfer of bilirubin and biliverdin in the pregnant guinea pig. *Biochem J* **194**, 273-282
14. Fevery, J. (2008) Bilirubin in clinical practice: a review. *Liver international : official journal of the International Association for the Study of the Liver* **28**, 592-605
15. Smitherman, H., Stark, A. R., and Bhutani, V. K. (2006) Early recognition of neonatal hyperbilirubinemia and its emergent management. *Seminars in fetal & neonatal medicine* **11**, 214-224
16. Stevenson, D. K., Vreman, H. J., and Wong, R. J. Bilirubin production and the risk of bilirubin neurotoxicity. *Semin Perinatol* **35**, 121-126
17. Stocker, R., Yamamoto, Y., McDonagh, A. F., Glazer, A. N., and Ames, B. N. (1987) Bilirubin is an antioxidant of possible physiological importance. *Science* **235**, 1043-1046
18. Sedlak, T. W., and Snyder, S. H. (2004) Bilirubin benefits: cellular protection by a biliverdin reductase antioxidant cycle. *Pediatrics* **113**, 1776-1782

19. Dore, S., Goto, S., Sampei, K., Blackshaw, S., Hester, L. D., Ingi, T., Sawa, A., Traystman, R. J., Koehler, R. C., and Snyder, S. H. (2000) Heme oxygenase-2 acts to prevent neuronal death in brain cultures and following transient cerebral ischemia. *Neuroscience* **99**, 587-592
20. Dore, S., and Snyder, S. H. (1999) Neuroprotective action of bilirubin against oxidative stress in primary hippocampal cultures. *Ann N Y Acad Sci* **890**, 167-172
21. Chang, E. F., Wong, R. J., Vreman, H. J., Igarashi, T., Galo, E., Sharp, F. R., Stevenson, D. K., and Noble-Haeusslein, L. J. (2003) Heme oxygenase-2 protects against lipid peroxidation-mediated cell loss and impaired motor recovery after traumatic brain injury. *J Neurosci* **23**, 3689-3696
22. Ahmad, Z., Salim, M., and Maines, M. D. (2002) Human biliverdin reductase is a leucine zipper-like DNA-binding protein and functions in transcriptional activation of heme oxygenase-1 by oxidative stress. *J. Biol. Chem.* **277**, 9226-9232
23. Tudor, C., Lerner-Marmarosh, N., Engelborghs, Y., Gibbs, P. E., and Maines, M. D. (2008) Biliverdin reductase is a transporter of haem into the nucleus and is essential for regulation of HO-1 gene expression by haematin. *Biochem J* **413**, 405-416
24. Lee, P. J., Camhi, S. L., Chin, B. Y., Alam, J., and Choi, A. M. (2000) AP-1 and STAT mediate hyperoxia-induced gene transcription of heme oxygenase-1. *Am J Physiol Lung Cell Mol Physiol* **279**, L175-182
25. Shaulian, E., and Karin, M. (2002) AP-1 as a regulator of cell life and death. *Nat Cell Biol* **4**, E131-136
26. Devary, Y., Gottlieb, R. A., Lau, L. F., and Karin, M. (1991) Rapid and preferential activation of the c-jun gene during the mammalian UV response. *Mol Cell Biol* **11**, 2804-2811
27. Maines, M. D., Ewing, J. F., Huang, T. J., and Panahian, N. (2001) Nuclear localization of biliverdin reductase in the rat kidney: response to nephrotoxins that induce heme oxygenase-1. *J Pharmacol Exp Ther* **296**, 1091-1097
28. Salim, M., Brown-Kipphut, B. A., and Maines, M. D. (2001) Human biliverdin reductase is autophosphorylated, and phosphorylation is required for bilirubin formation. *J. Biol. Chem.* **276**, 10929-10934
29. Kravets, A., Hu, Z., Miralem, T., Torno, M. D., and Maines, M. D. (2004) Biliverdin reductase, a novel regulator for induction of activating transcription factor-2 and heme oxygenase-1. *J. Biol. Chem.* **279**, 19916-19923
30. Lerner-Marmarosh, N., Shen, J., Torno, M. D., Kravets, A., Hu, Z., and Maines, M. D. (2005) Human biliverdin reductase: a member of the insulin receptor substrate family with serine/threonine/tyrosine kinase activity. *Proc Natl Acad Sci U S A* **102**, 7109-7114
31. Gibbs, P. E., Lerner-Marmarosh, N., Poulin, A., Farah, E., and Maines, M. D. (2014) Human biliverdin reductase-based peptides activate and inhibit glucose uptake through direct interaction with the kinase domain of insulin receptor. *FASEB J* **28**, 2478-2491
32. Lerner-Marmarosh, N., Miralem, T., Gibbs, P. E., and Maines, M. D. (2008) Human biliverdin reductase is an ERK activator; hBVR is an ERK nuclear transporter and is required for MAPK signaling. *Proc Natl Acad Sci U S A* **105**, 6870-6875

33. Maines, M. D., and Trakshel, G. M. (1993) Purification and characterization of human biliverdin reductase. *Arch Biochem Biophys* **300**, 320-326
34. McCoubrey, W. K., Jr., and Maines, M. D. (1994) Site-directed mutagenesis of cysteine residues in biliverdin reductase. Roles in substrate and cofactor binding. *Eur J Biochem* **222**, 597-603
35. Kikuchi, A., Park, S. Y., Miyatake, H., Sun, D., Sato, M., Yoshida, T., and Shiro, Y. (2001) Crystal structure of rat biliverdin reductase. *Nat Struct Biol* **8**, 221-225
36. Bell, J. E., and Maines, M. D. (1988) Kinetic properties and regulation of biliverdin reductase. *Arch Biochem Biophys* **263**, 1-9
37. Rigney, E., and Mantle, T. J. (1988) The reaction mechanism of bovine kidney biliverdin reductase. *Biochim Biophys Acta* **957**, 237-242
38. Reed, M. C., Lieb, A., and Nijhout, H. F. (2010) The biological significance of substrate inhibition: a mechanism with diverse functions. *BioEssays : news and reviews in molecular, cellular and developmental biology* **32**, 422-429
39. Randeberg, L. L., Haugen, O. A., Haaverstad, R., and Svaasand, L. O. (2006) A novel approach to age determination of traumatic injuries by reflectance spectroscopy. *Lasers in surgery and medicine* **38**, 277-289
40. Dignam, J. D., and Strobel, H. W. (1977) NADPH-cytochrome P-450 reductase from rat liver: purification by affinity chromatography and characterization. *Biochemistry* **16**, 1116-1123
41. Ryu, S. E. (2012) Structural mechanism of disulphide bond-mediated redox switches. *Journal of Biochemistry* **151**, 579-588
42. Hogg, P. J. (2003) Disulfide bonds as switches for protein function. *Trends Biochem Sci* **28**, 210-214
43. Yi, L., and Ragsdale, S. W. (2007) Evidence that the heme regulatory motifs in heme oxygenase-2 serve as a thiol/disulfide redox switch regulating heme binding. *J. Biol. Chem.* **282**, 21056-21067

Chapter 4 Ongoing Work and Future Directions

4.1 Characterization of the membrane binding HO-2/CPR electron transfer complex in vitro

Understanding protein-protein interactions between HO and CPR is important for understanding regulation of the heme degradation pathway, as electrons transferred via CPR are required for the HO reaction. Furthermore, in the cell, the availability of CPR could be a limiting factor for HO activity because of it provide electrons for various other proteins. In addition to HO, numerous other reactions require electrons via CPR and competition for CPR is likely to occur. For example, in mammals multiple cytochromes P450 also utilize electrons from CPR, and the ratio of CPR to P450s is ~1:20 (1-3). Therefore, the binding of CPR to its respective electron transfer partner is likely a critical point of regulation for enzymes that require CPR for catalysis. The first step towards understanding the competition among the electron acceptors (e.g. HO and P450s) is understanding the binding events that are required to produce a productive electron transfer complex. Characterization of the binding interface for soluble HO and CPR *in vitro* increases our understanding of the hydrophobic and electrostatic forces that drive the formation of a productive HO/CPR electron transfer complex and this information extends to other electron transfer complexes involving CPR.

The majority of studies characterizing HO-1 or HO-2 binding CPR have been conducted with soluble truncated proteins using a purified cell-free system. Previous work by other groups, and work herein, characterize a complex for soluble HO-1 and CPR (4-7) and soluble HO-2 and CPR (Chapter 2 of this thesis, Spencer *et al.*, manuscript in press). The interface for the HO isoforms and CPR is conserved, with the FMN region of CPR binding at an interface on HO-1 or HO-2 that involves K149 or K169, respectively, and the FAD domain of CPR binding at an HO interface involving L181 or L201 respectively (4-6); (Chapter 2, Spencer *et al*, manuscript in press).

Recent reports demonstrate that the membrane binding region of HO, and possibly the membrane bound environment for both HO and CPR, facilitate complex formation between these enzymes (8-11). However, a detailed characterization of the electron transfer complex between either full length HO-1 or HO-2 and CPR has not been performed and the requirements for the formation of the electron transfer complex for the full-length proteins have not been addressed either *in vitro* or in the cell. Therefore, while characterization of the soluble forms of HO and CPR provide valuable insight into the mechanisms that could control the HO system in the cell, it is important now to address the ability of HO and CPR to form a complex with the fully intact proteins that contain membrane anchors, and to understand cellular conditions that may promote such interactions. Furthermore, BVR contains a prenylation site and has been implicated in membrane binding, so this protein should also be included in studies of binary and ternary complexes with full-length HO's.

In Appendix 1 of this thesis, I have described a bifluorescence recombination (BiFC) system to address protein-protein interactions for HO-2 in a cellular context. HO-2 and BVR can form a fluorescent BiFC complex in mammalian cells, demonstrating that this method will be valuable in interrogating HO-2/CPR binding for full-length proteins in the cell. Future experiments in which the BiFC system is used to measure complex formation between full-length HO-2 and CPR could be valuable avenues to examine this binary complex within a cellular context. Specific residues of HO-2 are clearly implicated in binding CPR; L201 and K169 of HO-2 are important for the formation of a productive HO-2/CPR electron transfer complex for the soluble proteins *in vitro* (Chapter 2 of this thesis, Spencer *et al.* in press). Targeted mutagenesis studies using HO-2 and CPR BiFC constructs could determine the requirement of these residues for complex formation for the full-length proteins, in the context of the cell.

Understanding cellular conditions that may affect HO-2 catalytic activity is important as HO-2 is constitutively expressed and mechanisms for regulating its catalytic activity are not fully understood. Oxidative stress is likely to affect HO-2 catalytic activity in the cell. HO-2 possesses Cys-Pro heme regulatory motifs (HRMs) that modulate the enzyme's ability to bind heme. The disulfide state of the two C-

terminal HRMs is sensitive to the redox state of the cell, and under oxidizing conditions the affinity of HO-2 for heme is increased ~10-fold (12,13). Additionally, the end product of the heme oxygenase pathway, bilirubin, protects the cell against oxidative challenge (14-16).

Because oxidizing conditions affect the affinity of HO-2 for heme and increase the need for antioxidant bilirubin, I expect that oxidizing conditions would modulate the activity of HO-2 in the cell. Access to CPR is likely limiting for HO activity, and therefore I hypothesize that oxidative conditions would also increase protein-protein interactions for HO-2 and CPR. This hypothesis can be tested by determining the effects of the cellular redox state on the HO-2/CPR complex using an HO/CPR BiFC system, similar to what I have described for HO-2/BVR in Appendix 1.

Changes in heme levels in the cell may also result in altered activity of HO-2; increased HO activity would protect the cell from the cytotoxic effects of high heme concentrations (17). If CPR binding is a limiting factor for HO-2 activity in the cell, high heme levels would be expected to increase HO/CPR binding. Again, a BiFC system using HO and CPR can address the ability of intracellular heme levels to affect HO-2/CPR binding.

In conclusion, I have characterized the binding of soluble HO-2 with soluble CPR, which represents an important regulatory step in the HO pathway. Future studies to characterize these interactions with full-length proteins in the context of the cell will provide valuable insight into the nature of the full length HO/CPR electron transfer complex and how the heme degradation system responds to various cellular conditions such as oxidative stress or high levels of heme.

4.2 References

1. Cawley, G. F., Batie, C. J., and Backes, W. L. (1995) Substrate-dependent competition of different P450 isozymes for limiting NADPH-cytochrome P450 reductase. *Biochemistry* **34**, 1244-1247
2. Backes, W. L., and Kelley, R. W. (2003) Organization of multiple cytochrome P450s with NADPH-cytochrome P450 reductase in membranes. *Pharmacol Ther* **98**, 221-233
3. Estabrook, R. W., Franklin, M. R., Cohen, B., Shigamatzu, A., and Hildebrandt, A. G. (1971) Biochemical and genetic factors influencing drug metabolism. Influence of hepatic microsomal mixed function oxidation reactions on cellular metabolic control. *Metabolism* **20**, 187-199
4. Higashimoto, Y., Sakamoto, H., Hayashi, S., Sugishima, M., Fukuyama, K., Palmer, G., and Noguchi, M. (2005) Involvement of NADPH in the interaction between heme oxygenase-1 and cytochrome P450 reductase. *J. Biol. Chem.* **280**, 729-737
5. Higashimoto, Y., Sugishima, M., Sato, H., Sakamoto, H., Fukuyama, K., Palmer, G., and Noguchi, M. (2008) Mass spectrometric identification of lysine residues of heme oxygenase-1 that are involved in its interaction with NADPH-cytochrome P450 reductase. *Biochem Biophys Res Commun* **367**, 852-858
6. Sugishima, M., Sato, H., Higashimoto, Y., Harada, J., Wada, K., Fukuyama, K., and Noguchi, M. (2014) Structural basis for the electron transfer from an open form of NADPH-cytochrome P450 oxidoreductase to heme oxygenase. *Proc Natl Acad Sci U S A* **111**, 2524-2529
7. Wang, J., and de Montellano, P. R. (2003) The binding sites on human heme oxygenase-1 for cytochrome p450 reductase and biliverdin reductase. *J. Biol. Chem.* **278**, 20069-20076
8. Linnenbaum, M., Busker, M., Kraehling, J. R., and Behrends, S. Heme oxygenase isoforms differ in their subcellular trafficking during hypoxia and are differentially modulated by cytochrome P450 reductase. *PLoS One* **7**, e35483
9. Huber, W. J., 3rd, Marohnic, C. C., Peters, M., Alam, J., Reed, J. R., Masters, B. S., and Backes, W. L. (2009) Measurement of membrane-bound human heme oxygenase-1 activity using a chemically defined assay system. *Drug Metab Dispos* **37**, 857-864
10. Huber, W. J., 3rd, and Backes, W. L. (2007) Expression and characterization of full-length human heme oxygenase-1: the presence of intact membrane-binding region leads to increased binding affinity for NADPH cytochrome P450 reductase. *Biochemistry* **46**, 12212-12219
11. Huber Iii, W. J., Scruggs, B. A., and Backes, W. L. (2009) C-Terminal membrane spanning region of human heme oxygenase-1 mediates a time-dependent complex formation with cytochrome P450 reductase. *Biochemistry* **48**, 190-197

12. Yi, L., and Ragsdale, S. W. (2007) Evidence that the heme regulatory motifs in heme oxygenase-2 serve as a thiol/disulfide redox switch regulating heme binding. *J. Biol. Chem.* **282**, 21056-21067
13. Yi, L., Jenkins, P. M., Leichert, L. I., Jakob, U., Martens, J. R., and Ragsdale, S. W. (2009) Heme regulatory motifs in heme oxygenase-2 form a thiol/disulfide redox switch that responds to the cellular redox state. *J. Biol. Chem.* **284**, 20556-20561
14. Baranano, D. E., Rao, M., Ferris, C. D., and Snyder, S. H. (2002) Biliverdin reductase: a major physiologic cytoprotectant. *Proc Natl Acad Sci U S A* **99**, 16093-16098
15. Dore, S., and Snyder, S. H. (1999) Neuroprotective action of bilirubin against oxidative stress in primary hippocampal cultures. *Ann N Y Acad Sci* **890**, 167-172
16. Dore, S., Takahashi, M., Ferris, C. D., Zakhary, R., Hester, L. D., Guastella, D., and Snyder, S. H. (1999) Bilirubin, formed by activation of heme oxygenase-2, protects neurons against oxidative stress injury. *Proc Natl Acad Sci U S A* **96**, 2445-2450
17. Sassa, S. (2004) Why heme needs to be degraded to iron, biliverdin IXalpha, and carbon monoxide? *Antioxid Redox Signal* **6**, 819-824

Appendix 1 An analysis of HO-2/BVR protein-protein interactions in cells

A.1 Abstract

Heme oxygenase (HO) and biliverdin reductase mediate the first and second steps of heme degradation, respectively. HO exists as two major isoforms, HO-1 and HO-2. Other groups have previously described a complex between a soluble form of HO-1 (residues 1-265) and BVR using a variety of *in vitro* methods, however the ability of HO-2 and BVR to form a complex has not been addressed. Here we describe a bifluorescence recombination (BiFC) method to evaluate the ability of full length HO-2 to form a complex with other proteins in a cellular context. A split fluorophore with one half fused to the N-terminus of HO-2 and the complimentary half fused to the C-terminus of BVR is able to recombine to produce fluorescence when the complimentary BiFC constructs are coexpressed in mammalian cells. The membrane spanning region of HO-2 is not required for fluorescence reassembly, however the subcellular localization of the BiFC complex is determined by the subcellular localization of HO-2. Full length HO-2 is tethered to the endoplasmic reticulum while HO-2 that lacks the membrane-spanning region is cytosolic. The subcellular localization of the HO-2/BVR BiFC complex reflects the predicted subcellular localization of soluble and full length HO-2.

Chemical cross linking stabilizes an HO-2/BVR complex via the C-terminal cysteines of BVR (either C292 or C293). To determine if these cysteines are required for formation of the BiFC complex, BVR variants with serine substitutions at C292 or C293 were tested for their ability to form a BiFC complex with HO-2. BiFC complexes are observed for HO-2 and the BVR variants, indicating that the C-terminal cysteines of BVR are not required for the formation of the HO-2/BVR BiFC complex.

A.2 Introduction to Heme Oxygenase and Biliverdin Reductase

A.2.1 Protein-protein interactions between soluble HO and CPR or BVR

Full-length heme oxygenase (HO) contains a C-terminal membrane-spanning region that, in the cell, tethers the protein to the endoplasmic reticulum. The majority of *in vitro* studies involving HO have been conducted using the truncated forms of HO-1 and HO-2 in which the membrane anchor has been removed, using protein that was exogenously expressed and purified from *E. coli*. These forms of HO are more soluble and stable than the full length protein (1). The truncated versions of the proteins, HO-1(tn) and HO-2(tn), are comprised of residues 1-265 and 1-288, respectively. Full length cytochrome p450 reductase (CPR) possesses an N-terminal membrane spanning region that also tethers the reductase to the ER, however *in vitro* reports addressing soluble HO typically also use a soluble form of CPR (amino acid residues 66-680).

Protein-protein interactions between HO-1(tn) and the other enzymes involved in heme catalysis, CPR and biliverdin reductase (BVR), have been reported, primarily using *in vitro* studies in cell free systems with purified proteins. Surface plasmon resonance and fluorescence quenching studies report K_d values ranging from 0.4-2.0 μM for HO-1 and CPR, while an acetylation protection assay and SPR studies identify lysine residue 149 of HO-1 as important for binding CPR (2-4). Additionally, a recent crystal structure of a complex of HO-1(tn) with a CPR variant (ΔTGEE) has been reported (5). We find that an alanine substitution of K149 increases the K_m of CPR for HO-1(tn) by ~40-fold, consistent with a role for this residue in CPR binding HO-1 (Chapter 2 of this thesis, Spencer *et al*. manuscript in press).

Similar studies support that HO-1 and BVR may form a complex. Fluorescence quenching studies report K_d values ~0.2 μM for HO-1 and BVR (4). SPR studies indicate that BVR can compete with HO-1 for binding to immobilized CPR (2). Finally, in the presence of BVR, the rate limiting step for the HO-2 reaction is altered from biliverdin release to the conversion of Fe^{2+}-verdoheme to Fe^{3+}-biliverdin (6). However, in chemical modification studies in which HO-1 was subjected to acetylation, while the addition of CPR protected specific residues of HO-1 from chemical modification, no

protection from acetylation was observed upon addition of BVR (3). This suggests that, in contrast to CPR, BVR and HO-1 may not form a stable complex.

While complexes for HO-1 and CPR, and to a lesser extent HO-1 and BVR, have been described, little is known about the ability of HO-2 to form a complex with either CPR or BVR.

A.2.2 A role for the HO membrane spanning region in protein-protein interactions

While the majority of studies with HO have been performed with the truncated, soluble form, some recent reports suggest that the membrane-spanning region of HO enhances its interactions with CPR. A K_m value of 0.01 μM for CPR is reported for full length HO-1, (7) while we observe a K_m value 0.5 μM for the soluble proteins (Chapter 2 of this thesis, Spencer *et al.* manuscript in press). This value is ~50-fold lower than the K_m for CPR with the truncated form of HO-1, suggesting that the full length proteins bind more tightly than their soluble counterparts. Additionally, co-purification studies with both HO-1 and HO-2 demonstrate that CPR copurifies more efficiently with the full length HOs compared with the soluble forms (8).

Our results in Chapter 2 of this thesis indicate that BVR and the truncated soluble form of HO-2 do not form a high affinity complex. While the membrane-spanning regions or the membrane environment appears to facilitate HO/CPR interactions, the requirements of the HO transmembrane region has not been addressed for its interactions with BVR.

A.2.3 Fluorescence recombination to characterize protein-protein interactions in live cells

While a complex for soluble HO-1 and BVR has been described , less is known regarding the ability of HO-2 and BVR to form a complex. Because the membrane-spanning region has been to shown to facilitate protein-protein interactions, here we address the ability of full length HO-2 to form a complex with BVR in the physiologic context of the cell.

Green fluorescent protein fragment reassembly (GFPR) and bimolecular fluorescence complementation (BiFC) are methods in which non-fluorescent halves of a split fluorophore are fused to putative protein binding partners. Binding of the proteins of

interest brings the non-fluorescent fluorophore halves into close proximity permitting the reassembly of a fluorescent molecule (9-11). Thus protein-protein interactions can be monitored directly by fluorescence. These methods allow protein-protein interactions to be examined using proteins in their native cellular environment, an ideal scenario for membrane-bound proteins such as HO. Furthermore, the refolding of the fluorophore is essentially irreversible which can facilitate the detection of weak or transient interactions (9).

To address the ability of HO-2 and BVR to form a complex in the cell, fluorescence reassembly methods were therefore employed. The fluorescence recombination system described here can also be used to interrogate the ability of HO-2 to bind other proteins in the HO pathway such as CPR, and to define requirements for those interactions.

A.3 Materials and methods

A.3.1 Construction of chimeras for GFPR analysis of HO-2 and BVR

The HO-2 cDNA sequence encoding the full length protein (amino acid residues 1-316) was inserted into the GFPR expression vector pET11a-link-NGFP using polymerase chain reaction (PCR) amplification with 3' primers that introduced a XhoI site and 5' primers that introduced a BamHI site using PFU polymerase (Agilent; Santa Clara CA). The PCR product was then inserted into the ZeroBlunt TOPO vector according to the manufacturers instructions (Invitrogen/Thermo Fisher Scientific; Grand Island NY). Both HO-2 insert (from the TOPO subcloning vector) and vector (pET11a-link-NGFP) were subjected to restriction enzyme digestion with XhoI and BamHI and the subsequent insert or vector purified from 1% agarose gel using the QIAquick gel extraction kit according to the manufacturers instructions (Qiagen; Valencia CA). The HO-2 insert was ligated into the pET11a-link-NGFP vector using T4 DNA ligase according to the manufacturer's instructions (Promega; Madison WI). Ligation products were transformed into Top10 cells (Invitrogen/Thermo Fisher Scientific; Grand Island NY) and plated on Luria broth/agar plates with appropriate antibiotic selection (50 µg/ml

kanamycin). DNA constructs were screened using restriction digestion and the sequence confirmed by DNA sequencing.

The BVR cDNA sequence encoding residues 1-296 was inserted in frame into the GFPR expression vector pMRBAD-link-CGFP using the method described above, with restriction enzyme sites NcoI and AatII (3' and 5', respectively) using ampicillin selection (100 µg/ml).

GFPR expression vectors and positive controls (NZ and CZ) were a kind gift from Dr. Lynne Regan (Yale University, New Haven, CT).

A.3.2 Expression and visualization of GFPR by microscopy

The indicated GFPR constructs were transformed into BL21(DE3) cells according to the manufacturers protocol (Thermo Fisher Scientific; Grand Island NY) and cultured for 16 h at 37°C on Luria broth agar plates with the appropriate antibiotic selection: kanamycin (50 µg/mL) for pET11a-link-NGFP based constructs and ampicillin (100 µg/mL) for pMRBAD-link-CGFP based constructs. Individual colonies were used to inoculate 5 mL 2xYT (2 x yeast extract and tryptone) broth with the appropriate antibiotic resistance and cultures were incubated for 16 h at 37°C, 250 rpm. Protein expression was induced with 10 µM IPTG for pET11a-link-NGFP based constructs and 0.2% arabinose for pMRBAD-link-CGFP based constructs for 16 h at 20°C, 250 rpm.

To visualize fluorescence, 100 µl of the bacterial culture was concentrated by centrifugation at 5 x g for 2 min at 4°C and resuspended in 50 µl 1xPBS. 5 µl of concentrated bacterial culture was applied to a poly-l-lysine coated coverslip (BD Biosciences, San Jose, CA) and mounted to a slide with 5 µl prolong gold (Thermo Fisher Scientific; Grand Island NY).

Fluorescence images were acquired on an Olympus BX60 upright microscope (Olympus; Center Valley PA) in the Center for Live Cell Imaging at the University of Michigan Medical School. Illumination was provided from a 100 W halogen lamp for bright-field microscopy and by a BH@-RFL-T# 100W high pressure mercury lamp burner for fluorescent microscopy. Images were collected using a 100 x UPlanApo (oil-immersion) objective with a U-MWB2 filter for GFP fluorescence (Ex460-490 nm, Em520 nm). An Olympus DP70 CCD color camera (Olympus; Center Valley PA) using

DP70 controller/manager software v3.03 col was used to capture images. Identical conditions were used to collect images unless otherwise specified.

A.3.3 Construction of chimeras for BiFC analysis of HO-2 and BVR

The BiFC plasmids pBiFC-VN173, pBiFC-VC155 and pBiFC-CC155 were generously provided by Dr.Chang-Deng Hu (Purdue University, West Lafayette, IN) (10). These constructs encode amino acid residues 1-173 of Venus (VN173), residues 155-238 of Venus (VC155) and 155-238 of enhanced cyan fluorescent protein (CC155). Residues 155-238 of VC and CC are identical except for 2 amino acid changes - residues 145 and 146 are TA and AC for Venus and eCPF respectively. The fluorescence emission of the reassembled fluorophore is primarily determined by the nature of the N-terminal fragment, and reassembly of VN173 with either VC155 or CC155 produces fluorescent proteins with similar spectral characteristics (12,13).

To produce a soluble HO-2 BiFC construct, HO-2(tn), the HO-2 sequence lacking the C-terminal membrane spanning region (residues 1-288) was amplified by polymerase chain reaction (PCR) using a 5' primer pair that introduced a SalI site and a 3' primer pair which generated a BglII site with PFU polymerase (Agilent; Santa Clara CA). The PCR product was then inserted into the ZeroBlunt TOPO vector according to the manufacturers instructions (Invitrogen/Thermo Fisher Scientific; Grand Island NY). Both the HO-2(1-288) insert (from the TOPO subcloning vector) and vector (pBiFC-VC155) were subjected to restriction enzyme digest with SalI and BglII and the subsequent insert or vector was purified from a 1% agarose gel using the QIAquick gel extraction kit according to the manufacturers instructions (Qiagen; Valencia CA). The HO-2(1-288) insert was ligated into the pBiFC-VC155 vector using T4 DNA ligase according to the manufacturer-provided protocol (Promega; Madison WI). Ligation products were transformed into Top10 cells (Invitrogen/Thermo Fisher Scientific; Grand Island NY) and plated on Luria broth/agar plates with the appropriate antibiotic selection. DNA constructs were screened using restriction digestion and the sequence confirmed by DNA sequencing.

BVR was inserted into the pBiFC-VN173 and pBiFC-CC155 vectors following similar methods as described for HO-2 using BglII and XbaI restriction sites (5' and 3'

respectively) for pBiFC-VN173 and a SalI and BglII (5' and 3' respectively) for pBiFC-CC155.

To generate the full length HO-2 BiFC construct, HO-2(FL), residues 1-316 of HO-2 were inserted into the pBiFC-VN(1-173) vector according to the methods described above, using the restriction sites BglII and XbaI (5' and 3' respectively). The subsequent fusion protein results in the fluorophore fused to C-terminus of HO-2. Because full-length HO-2 is anchored to the ER with the catalytic core facing the cytosol and the C-terminus facing the ER lumen, this C-terminus fusion is therefore expected to be present in the ER lumen and not available to recombine with a cytosolic protein such as BVR. Therefore, another chimera was generated with the fluorophore fragment fused to the N-terminus of full length HO-2.

To generate the N-terminal VN(1-173) fluorophore, the full length HO-2 BiFC construct with a C-terminal fusion was modified as follows. The VN(1-173) sequence was PCR amplified with 5' and 3' primers containing compatible restriction sites (EcoRI and BglII, respectively) to insert the VN(1-173) sequence upstream of HO-2. The PCR product was subcloned into the TOPO vector, and insert and vector were prepared and ligated as described above. Then, to remove the fluorophore fused to the C-terminus of HO-2(FL), a stop codon was introduced after amino acid residue 316 of HO-2 using the QuickChange site directed mutagenesis protocol (Strategene; La Jolla CA). The resulting full length HO-2 fusion protein with the N-terminal fluorophore exhibited a molecular mass of ~44 kDa as determined by SDS-PAGE and Western blot analysis, consistent with the size of HO-2 and the VN1-173 fluorophore, confirming that the insertion of a stop codon was effective in eliminating expression of the C-terminal fluorophore.

To generate the BVR(C292S) and BVR(C293S) pBiFC-CC155 variants of BVR, site directed mutagenesis was conducted according to the QuickChange protocol (Stragegene; La Jolla CA).

DNA sequencing was used to confirm the sequence of all DNA constructs described.

A.3.4 Expression and visualization of BiFC by microscopy

HEK293 cells were maintained in Dulbecco's Modified Eagle Medium (DMEM; Gibco/Thermo Fisher Scientific; Grand Island NY) supplemented with 10% fetal bovine serum (FBS) and 2 mM L Glutamine at 37°C, 5% CO_2. Cells were transfected with 0.25 µg/mL of the indicated BiFC construct(s) using Lipofectamine2000 according to the manufacturer's protocol (Thermo Fisher Scientific; Grand Island NY). Briefly, cells were plated on poly-l-lysine coated glass bottom slides (Lab-Tek; Hatfield PA) 24 hours before transfection at a density of 500,000 cells/ml. Under these conditions cells were ~60% confluent at the time of transfection. Cells were then incubated for 24 hours post-transfection before visualization of BiFC. Immediately before BiFC visualization cells were incubated 1µM ER tracker and 5 µg/mL Hoechst for 20 min at 37°C, 5% CO_2. Cells were then washed with HBSS (Hanks Balance Salt Solution; GIBCO/Thermo Fisher Scientific; Grand Island NY) and visualized.

BiFC images were collected from live cells using a heated stage (Harvard Apparatus, Incl; Holliston MA) and an Olympus IX70 inverted microscope (Olympus; Center Valley PA) in the Center for Live Cell Imaging (CLCI) at the University of Michigan Medical School. Fluorescent microscopy images were illuminated with an X-Cite 120 metal halide light source (EXFP; Mississauga, OM, Canada) using a 100 x oil immersion objective. Filters used for the various fluorophores were: Venus: excitation 492 nm/BP18 and emission 535 nm/BP40; ER tracker: excitation 572 nm/BP23 and emission 630 nm/BP60; Hoechst: excitation 350 nm/BP50 and emission 465 nm/BP30.

Images were collected using a CoolSNAP HQ2 14-bit CCD camera (Photometrics; Tucson AZ). All devices were controlled through Metamorph Premier v6.3 software (Molecular Devices; Downington PA).

For colocalization studies, cells were prepared as described above and imaged using a TILL iMIC widefield inverted microscope (TILL Photonics; Graefelfing; Bavaria Germany) with a fully automated motorized travel stage and Z-axis control using a Plan Super Apochromat 100x oil immersion objective. Illumination for fluorescence images was provided by a Till Oligochrome 150W Xenon source (TILL Photonics; Graefelfing; Bavaria Germany). Images were acquired using an Andor iXO DU897 cooled EMCCD camera. Image acquisition was controlled by Till LA software (TILL Photonics;

Graefelfing; Bavaria Germany) and image processing and deconvolution of z-stacks was conducted using Imaris (Bitplane; South Windsor CT). Colocalization of the deconvoluted images was evaluated by determining the Pierce coefficient using JACoP (ImageJ) according to published methods (14).

A.3.5 Analysis of BiFC by flow cytometry

For flow cytometry, HEK293 cells were plated on 12 well flat bottom tissue culture plates (Corning® Costar®, Corning NY) and transfected with the indicated BiFC constructs as described for BiFC visualization by microscopy. Cells were prepared according to published methods (13). Briefly, cells were washed with PBS and lifted from the plate by incubation with 0.15 M KCl and 0.015 M Na-citrate in PBS for 5 min at 37°C, 5% CO_2. Cells were then collected, washed with PBS, and suspended in 250 µl 0.8% BSA in PBS. Flow cytometry analysis was conducted using a FACS Aria II cell sorting system (BDBiosciences; San Jose CA) at the University of Michigan Flow Cytometry Core in the Office of Research.

Analysis was restricted to live cells by gating cells that exhibited forward and side-scatter features typical of live cells. To analyze fluorescence events of transfected cells, threshold values were set for BiFC that excluded 99% of non-transfected cells and the fluorescence events were determined for 10,000 cells. Histogram and error bars represent the mean and standard deviation from 3 independent experiments.

A.3.6 Chemical cross-linking of HO and BVR or RNase

The reducible, heterobifunctional cross-linker (succinimidyl 6-(3-[2-pyridyldithio]-propionamido)hexanoate) (LC-SPDP) was used in a two-step reaction according to the manufacturer's instructions (Thermo Scientific/Pierce, Rockford, IL). HO-1 or HO-2 was activated as follows: a fresh 3 mM solution of LC-SPDP was prepared in DMSO. 10 μM HO-1 or HO-2 was prepared in conjugation buffer (0.1 M 4-(2-hydroxyethyl)-1-piperazineethanesulfonic acid (HEPES), pH 7.5, 30 mM ethylenediaminetetraacetic acid (EDTA), 150 mM NaCl) and incubated with 0.1 mM LC-SPDP for 30 min at room temperature. Unconjugated cross-linker was then removed by 3 rounds of buffer exchange using 10,000 MWCO Amicon microconcentrators (Millipore, Billerica, MA). 10 μM BVR, or RNase was then added to the activated protein and the reaction was

incubated at 4°C overnight. Cross-linking reactions were analyzed by 5-15% gradient sodium dodecyl sulfate polyacrylamide gel electrophoresis (SDS PAGE) (BioRad, Berkeley, CA) and visualized by staining the gel with Coomassie blue (15).

A.3.7 Co-purification of BVR with HO-2

For the co-purification of BVR with HO-2, the cross-linking reaction was performed exactly as described above, however HO-2 contained an N-terminal 6xHis tag (hisHO-2) that was absent in the other reactions. By SDS-PAGE, the cross-linked products of the reaction containing hisHO-2 and BVR migrated to identical positions as those in which the 6xHis tag had been removed from HO-2. Samples of hisHO-2 alone, BVR alone, or cross-linked hisHO-2/BVR were incubated with 100 μl of Ni NTA resin (50% slurry) for 2 hours at 4°C. Samples were rotated on a Boekel variable speed mini-tube rotator (Fisher Scientific; Pittsburgh PA). Affinity resin and associated proteins were harvested by centrifugation for 5 minutes at a setting of 2,400 x g at 4°C with an accuSpin Micro 17R refrigerated microcentrifuge (Fisher Scientific; Pittsburgh PA) and washed three times with 1 ml of wash buffer (50 mM Tris-HCl pH 8.0, 30 mM NaCl, 20 mM imidazole). Protein bound to the resin was eluted with 50 mM Tris-HCl, pH 8.0, 30 mM NaCl, 300 mM imidazole. Eluted fractions were boiled for 5 minutes in SDS-PAGE loading buffer (50 mM Tris-HCL, pH 6.8, 2% (w/v) SDS, 0.1% (w/v) bromophenol blue, 10% (v/v) glycerol, and 100 mM dithiothreitol) and separated by 10% SDS PAGE (15). Proteins were then transferred to a nitrocellulose membrane and detected using antibodies against either HO-2 (16) or BVR (Abcam, Cambridge, MA).

A.4 Experimental Results

A.4.1 A green fluorescent protein reassembly (GFPR) system for assessing protein-protein interactions between HO-2 and BVR

While protein-protein interactions have been described for HO-1 and BVR, the majority of these experiments were performed *in vitro* using the soluble form of HO-1 in a purified system (2-5). The ability of HO-2 and BVR to form a complex has not been addressed. While valuable information can be obtained from a purified system, more

recent data indicates that the HO-1 membrane-spanning region facilitates protein-protein interactions (7,8,17). The goal of our experiments is to address the ability of HO-2 and BVR to form a complex in the cellular context using full length HO-2.

Green fluorescent protein reassembly (GFPR), in which non-fluorescent halves of GFP are fused to the protein binding partners of interest, permits the direct detection of binding interactions via fluorescence (9,18,19). Binding of the GFPR fusion proteins brings the non-fluorescent GFP halves into close proximity, permitting the GFP fragments to reassemble into a fluorescent protein. Reassembled GFP has spectral properties identical to those of intact GFP (19). When the GFP halves are not fused to proteins that form a complex, the GFP halves fail to produce a reassembled fluorescent protein (19). In addition to permitting the analysis of protein-protein interactions in the more native context of a cell, GFPR can enhance the detection of weak/transient interactions by stabilizing or trapping the complex of interest. Protein complexes with K_d values ranging from 1 μM to 1 mM have been successfully detected using GFPR methods (9).

The GFPR protein constructs described here consist of a GFP molecule split into N- and C-terminal fragments between residues 157 and 158. The non-fluorescent GFP halves are fused to the N-terminus of HO-2 or C-terminus of BVR (Figure A.1). While the individual GFP halves are not fluorescent, the binding of BVR to HO-2 could bring their respective GFP fragments into close proximity, allowing the reassembly of a productive fluorescent molecule. Thus, HO-2/BVR binding can be directly monitored via fluorescence. As a positive control, GFPR constructs fused to leucine zipper motifs for which protein-protein interactions have been well characterized, are also used (19).

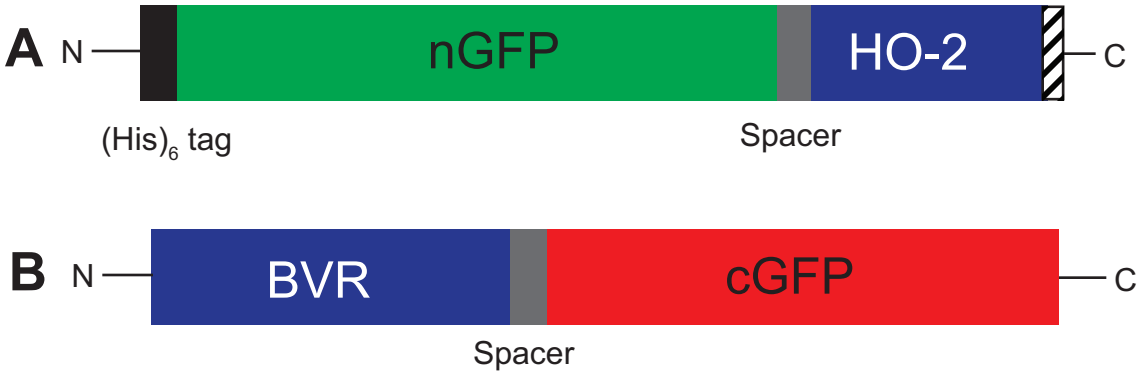

Figure A.1. **GFPR fusion proteins for HO-2 and BVR. (A)** Full length HO-2(1-316) was cloned into the GFPR expression vector pET11a-link-NGFP to produce a protein construct with an N-terminally fused GFP fragment as shown. The hatched rectangle represents the HO-2 membrane spanning domain. **(B)** BVR was cloned into the GFPR expression vector pMRBAD-link-CGFP to produce a protein construct with a C-terminally fused GFP fragment as shown.

To interrogate the ability of HO-2 and BVR to form a GFPR complex, BL21(DE3) cells were co-transformed with the indicated GFPR constructs and fusion protein expression was induced as described in the Methods section. The co-expression of HO-2 and BVR GFPR constructs, or the compatible leucine zipper fusion constructs, produces *E. coli* cell that exhibit green fluorescence, while transformation of cells with the individual GFPR constructs resulted in no detectable fluorescence (Figure A.2). The leucine zipper constructs NZ and CZ are reported to have high affinity and robust GFP reassembly and were used as a positive control (9,19). These results indicate that full length HO-2 and BVR are capable of forming a complex in cells and that the orientation of the GFP fragments fused to HO-2 and BVR is correct to permit visualization of HO-2/BVR binding.

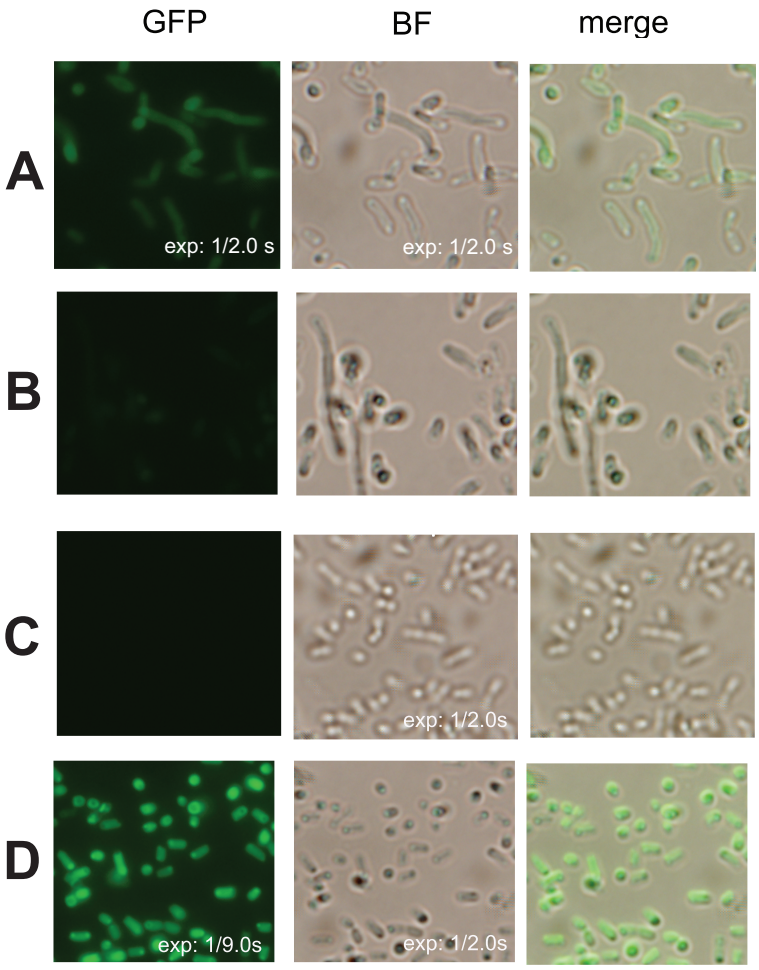

Figure A.2. **Coexpression of HO-2 and BVR GFPR constructs produces fluorescence. (A)** *E.coli* cells transformed with HO-2/BVR GFPR constructs are fluorescent. Cells transformed with only HO-2 **(B)** or BVR **(C)** GFPR constructs lack fluorescence. **(D)** Cells transformed with GFPR positive control constructs (NZ/CZ) also produce fluorescence. Exposure time is indicated in the lower right corner of the image.

A.4.2 A bifluorescent recombination system for interrogating HO-2 and BVR interactions in mammalian cell

While the GFPR results show that HO-2 and BVR can form a complex, similar to that described for HO-1 and BVR, the cellular context and architecture of a bacterium is quite distinct from that of a mammalian cell. While in the mammalian cell HO-2 is tethered to the endoplasmic reticulum, there is no analogous membrane in *E. coli.* To address the ability of HO-2 and BVR to form a complex in the more physiologic

mammalian cell, a bifluorescent recombination (BiFC) approach was utilized. Like GFPR, BiFC utilizes the reassembly of a split fluorophore fused to putative protein binding partners. While the fluorophore fragments individually exhibit no fluorescence, protein-protein binding of a BiFC pair can bring the fluorophore fragments into close proximity allowing reassembly of a fluorescent molecule. Similar to GFPR, protein-protein interactions can be monitored *via* fluorescence and the reassembled fluorophore can stabilize transient protein-protein interactions. However, the BiFC constructs are mammalian expression vectors and therefore protein-protein interactions can be interrogated in the more physiologic context of the mammalian cell.

HO-2, lacking the C-terminal membrane spanning region (residues 1-288) and full length HO-2 (residues 1-316) were inserted into the BiFC fusion vectors and BVR was inserted into expression vectors for the cognate half of the split fluorophore as described in the Methods (Figure A.3). C-terminal fluorophore fragments are derived from either Venus and eCFP, however residues 155-238 of these proteins are identical except for 2 amino acid changes - residues 145 and 146 are TA and AC for Venus and eCPF respectively, and the recombined fluorophores exhibit similar spectral properties (12,13).

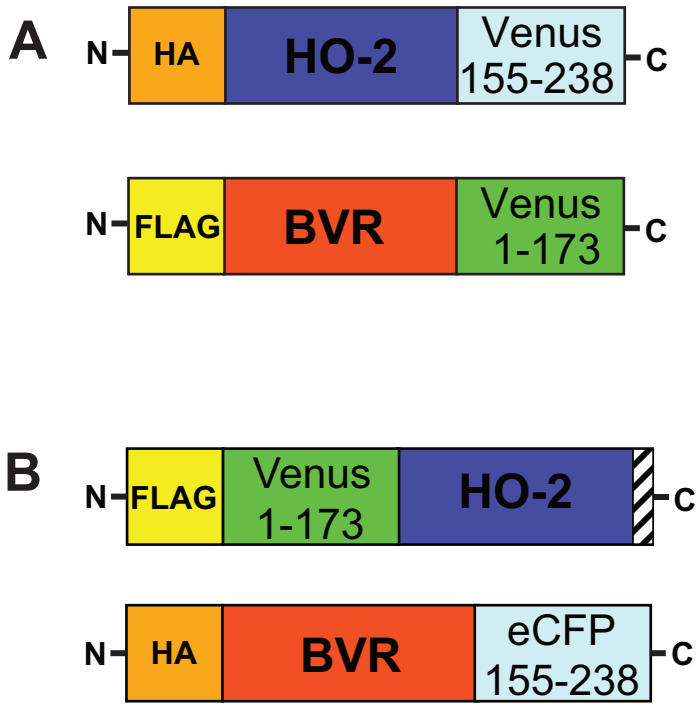

Figure A.3. **BiFC constructs to address HO-2 and BVR fluorescence reassembly. (A)** BiFC fusion proteins to address the ability of soluble HO-2(1-288) and BVR to produce fluorescence. **(B)** BiFC fusion constructs to address the ability of full length HO-2 (residues 1-316) to produce fluorescence. The hatched rectangle represents the HO-2 transmembrane region.

A.4.3 The requirement for the HO-2 membrane spanning region in HO-2/BVR BiFC

To test the ability of HO-2 and BVR to form a complex in mammalian cells and to test if the HO-2 membrane spanning region is required, full length and soluble HO-2 (HO-2(FL) and HO-2(tn)) were cotransfected into HEK293 cells with their cognate BVR BiFC construct (Figure A.4). Both soluble and membrane bound HO produce a fluorescent BiFC complex when coexpressed with the cognate BVR BiFC construct, however the localization of the BiFC complexes are distinct. The BiFC pair with full length HO-2 exhibits perinuclear localization, similar to what is observed for staining of the ER (Figure A.4*A*). The BiFC complex for soluble HO-2 and BVR is diffuse throughout the entire cell (Figure A.4*B*). The localization of the BiFC complexes is

consistent with the expected localization of the HO-2 forms. Full length HO-2(FL) is expected to be membrane bound at the ER while soluble HO-2(tn) is expected to exhibit cytosolic localization. This result shows that the membrane spanning region of HO-2 determines the subcellular localization of the HO-2/BVR BiFC complex, however the membrane spanning region of HO-2 is not required for the formation of an HO-2/BVR BiFC complex as BiFC fluorescence is apparent under both conditions.

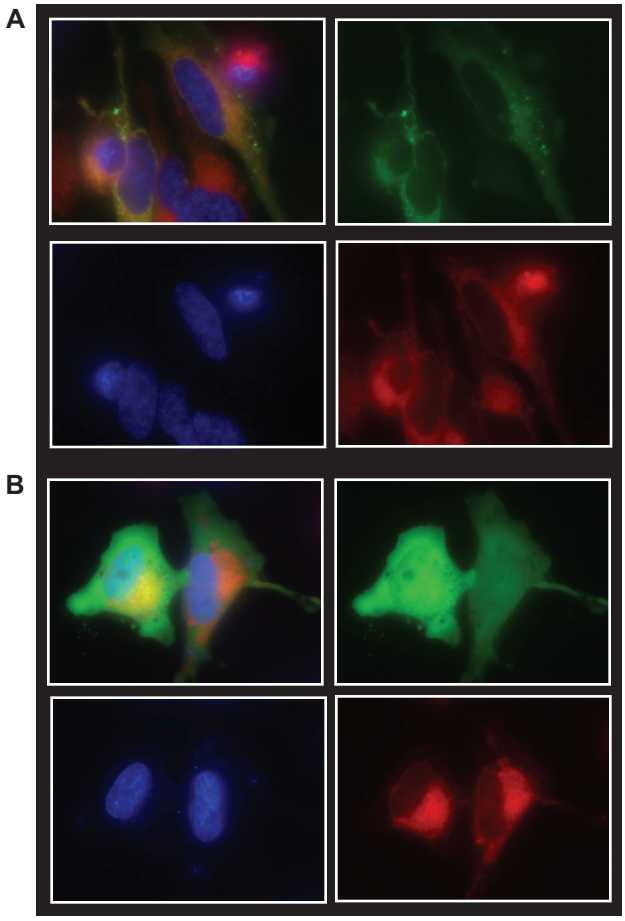

Figure A.4. **Subcellular localization of HO-2 and BVR BiFC complex is dependent on the HO-2 membrane spanning region.** Cells co-expressing HO-2(1-316).VN173 and BVR.Cc155 **(*A*)** or cells co-expressing HO-2(1-288).VC155 and BVR.VN173 **(*B*)** were stained with Hoechst (blue) and ER tracker (red). BiFC is shown in green.

To characterize the subcellular localization of the HO-2(FL)/BVR BiFC complex in greater detail, the colocalization of HO-2(FL)/BVR BiFC with various cell markers was determined (Figure A.5). The HO-2(FI)/BVR BiFC pair was transfected into HEK293 cells as described in the Methods section. Live cells were then stained with ER Tracker

(Biorad) and Hoechst nuclear stain. The fluorescence of live cells were imaged by collecting a series of z-stacks which were subjected to deconvolution using Imaris (Bitplane; South Windsor CT).

Figure A.5*A* shows representative images of two cells with a clear overlay of BiFC (green) and ER tracker (red) as yellow in the merged panel. To quantify the colocalizaton of the BiFC signal and ER, the Pearson's coefficient was determined using the ImageJ colocalization tool JACoP (14). Complete positive colocalization results in a Pearson's coefficient of 1, and no correlation results in a Pearson's coefficient of 0. The BiFC signal has a strong positive correlation with the ER stain (Pearson's coefficient = 0.966) supporting that the HO-2/BVR BiFC complex is located at the ER. As a positive control, the Pierce coefficient of BiFC with BiFC signal was determined (Pearson's coefficient = 1.0). These results support that the HO-2(FL)/BVR BiFC complex localizes to the ER, the expected localization for full length HO-2. Furthermore, because BVR is cytosolic, these results support that HO-2(FL) is oriented properly with the catalytic domain towards the cytosol where it is available for binding with BVR.

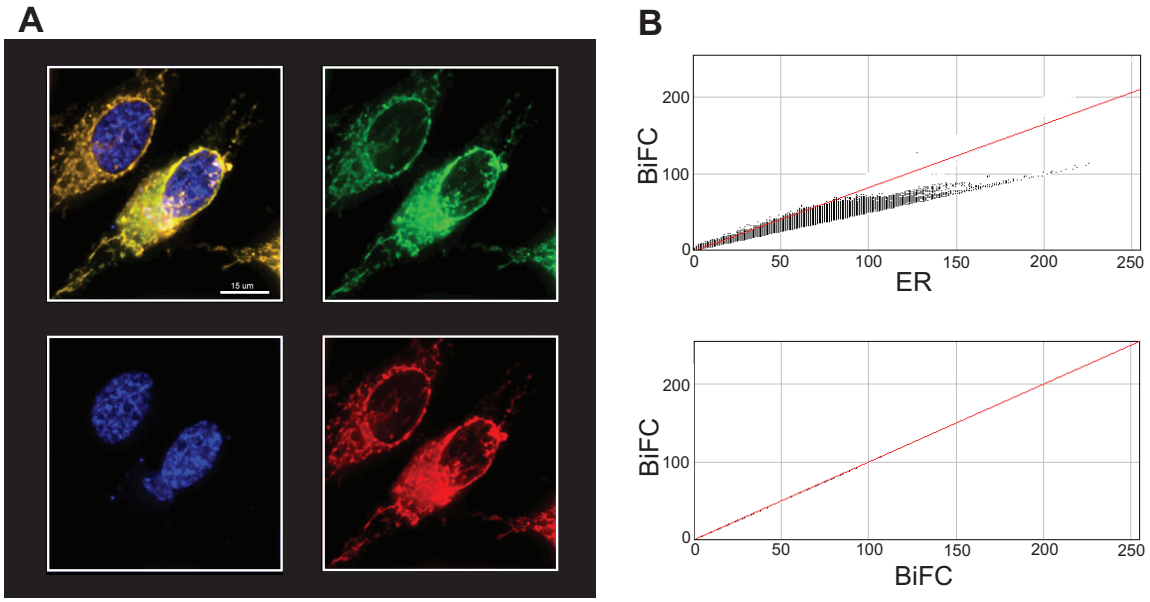

Figure A.5. **HO-2(1-316) and BVR BiFC colocalizes with the ER. (A)** Cells co-expressing HO-2(1-316).VN173 and BVR.CC155 were stained with Hoechst (blue) and ER tracker (red). BiFC is shown in green. The colocalization of BiFC (green) and ER tracker (red) is visible as yellow in the top left panel. Hoechst nuclear stain is blue. **(B)** Pearson's coefficient was determined for the colocalization of BiFC and ER (*top panel*), BiFC and BiFC (*lower panel*) using ImageJ JACoP (14).

Flow cytometry was conducted to quantify the differences in BiFC signal for HO-2(FL)/BVR and HO-2(tn)/BVR. Consistent with what is observed by microscopy, HO-2(FL)/BVR produces less BiFC signal (~70%) compared with the HO-2(tn)/BVR BiFC pair (Figure A.6*A*).

While differences in BiFC signal between HO-2(FL)/BVR and HO-2(tn)/BVR could be interpreted as BVR binding less efficiently to HO-2(FL), differences in protein expression levels could also produce similar results. To determine the expression levels of the various BiFC constructs, equivalent total protein from cells lysates that were co-transfected with the BiFC pairs was resolved by SDS-PAGE and subjected to Western blot analysis using antibodies specific for HO-2 or BVR. The relative expression of the HO-2 and BVR protein constructs was then determined by densitometry (ImageJ). HO-2 and BVR proteins are both expressed at lower levels in the HO-2(FL)/BVR expressing cells relative to cells expressing the HO-2(tn)/BVR constructs (53% and 83% expression for HO-2(FL) and BVR respectively) (Figure A.6*B*). Thus differences in expression

levels for the BiFC fusion proteins are the likely cause for the differences in the BiFC signal intensity between HO-2(tn)/BVR and HO-2(FL)/BVR expressing cells. These data demonstrate, however, that both soluble and full-length HO-2 produce robust BiFC signal with their cognate BVR BiFC partners and that the HO-2 transmembrane region is not required for the formation of HO-2/BVR BiFC complexes, and thereby establishes a context in which the requirements of HO-2/BVR binding can be addressed quantitatively.

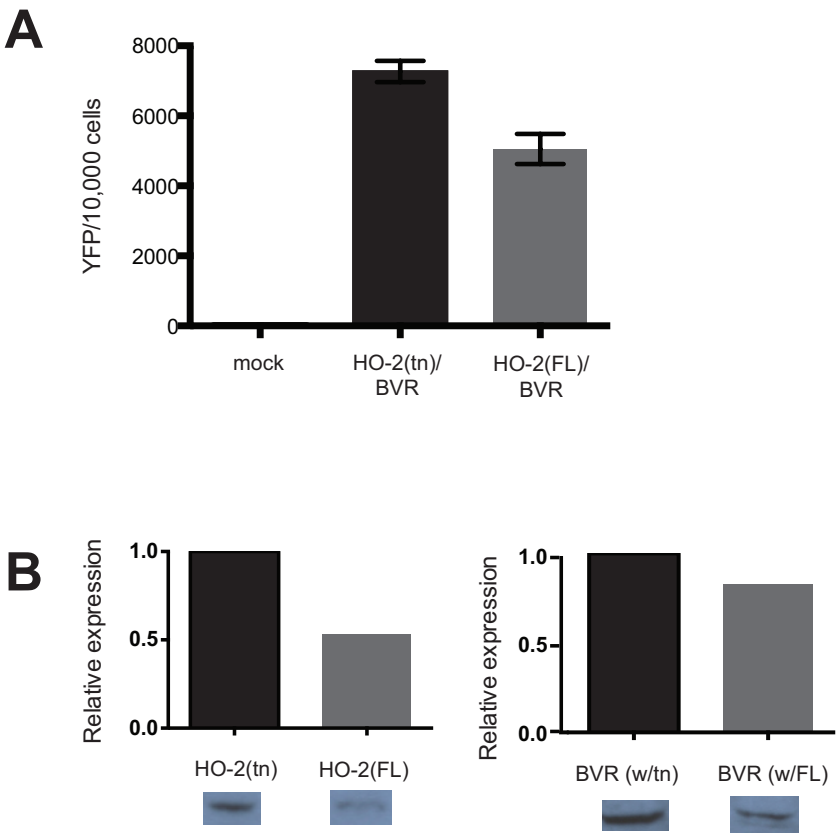

Figure A.6. **Membrane localization requirements for HO-2/BVR BiFC. (A)** HEK293 cells were transfected with the indicated BiFC constructs as described in the methods and YFP signal quantified by flow cytometry. **(B)** The relative expression of HO-2 or BVR constructs as determined by Western blot analysis of cellular lysates from HEK293 cells. The bottom panels show the Western blot band that was quantified for densitometry, as described in the Methods section.

A.4.4 An analysis of BVR C-terminal cysteines in binding HO-2

In vitro chemical cross-linking studies between soluble HO-2(tn) and BVR are described in Chapter 2 (Spencer *et al.,* manuscript in press). To briefly summarize, a complex between HO-2(tn) and BVR is stabilized by the heterobifunctional cross-linker LC-SPDP. These results are recapitulated from Figure 2.16 in this appendix as Figure A.7*A*. Because a complex between soluble HO-1(tn) (residues 1-265) and BVR is reported in the literature (2-5), cross-linking between HO-1(tn) and BVR was included as a positive control. In the HO-2 only sample, an HO-2 homodimer is also stabilized by the cross-linking reaction. Because HO-2(tn) and BVR are similar in size, a co-purification of BVR with HO-2(tn) was conducted to determine if BVR was directly linked to HO-2(tn) in the cross-linked product (Figure A.7*B*). Indeed, BVR copurifies with HO-2(tn) but not affinity resin alone, demonstrating that HO-2 and BVR are directly linked. The chemical cross-linker failed to stabilize a complex for an unrelated cysteine containing protein, RNase, and either HO-1(tn) or HO-2(tn) (Figure A.7*C*).

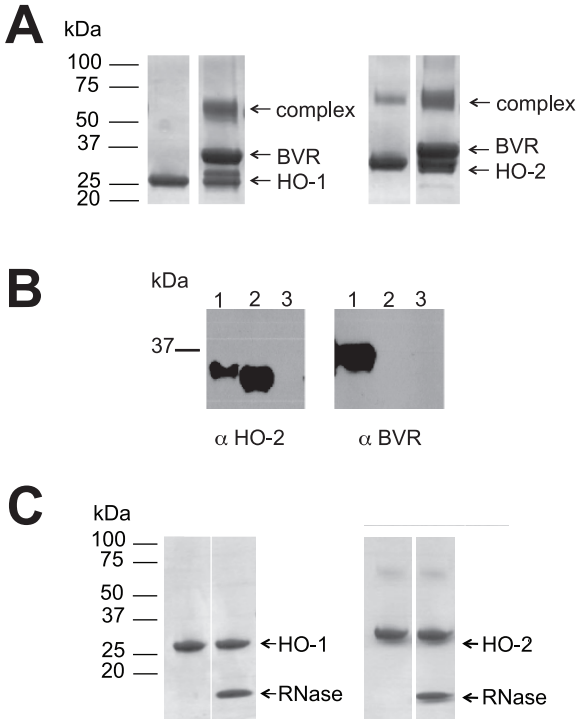

Figure A.7. **Chemical cross-linking stabilizes an HO/BVR complex. (A)** The heterobifunctional cross linker LC-SPDP stabilizes a complex between HO-1 or HO-2 and BVR. **(B)** Reducing SDS-PAGE and Western blot of HO-2 pull down and associated BVR. Lane 1: cross linking reaction, Lane 2: HO-2 only, Lane 3: BVR only. **(C)** No complex is trapped for HO-1 or HO-2 with RNAse. Crosslinking reactions contained 10 μM of the indicated protein.

Human BVR contains 5 cysteines that could be available for cross-linking with HO-2; C74, C204, C281, C292 and C293. Analysis of the HO-2(tn)/BVR complex by tryptic digest and LC-MS/MS identified C292 or C293 of BVR as being cross-linked to K264 of HO-2. The analysis was unable to distinguish between C292 and C293 as they occurred on the same peptide.

To determine if either C292 or C293 are required for BVR binding HO-2, C292 or C293 was substituted with a serine residue in the BVR BiFC expression construct. The HO-2(FL)/BVR, HO-2(FL)/BVR(C292S) and HO-2(FL)/BVR(C293S) BiFC pairs were cotransfected into HEK293 cells and BiFC signal quantified by flow cytometry (Figure A.8). A serine substitution at C292 or C293 has no effect on HO-2(FL)/BVR BiFC signal,

suggesting that neither of these residues are required for HO-2(FL)/BVR BiFC complex formation.

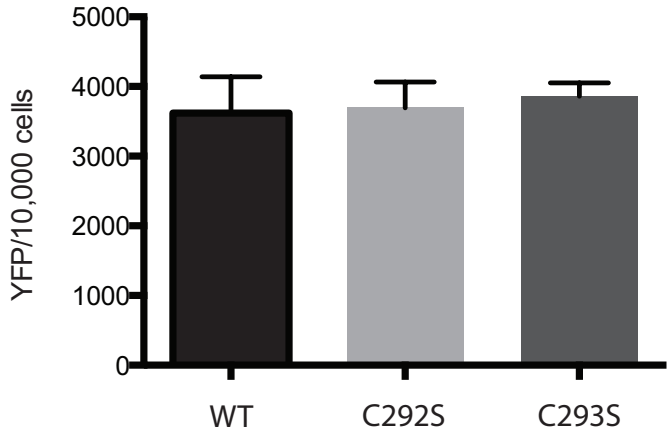

Figure A.8. **BVR cysteine requirements for HO-2/BVR BiFC.** HEK293 cells were transformed with HO-2(FL) and the indicated BVR construct and BiFC signal quantified by flow cytometry.

A.5 Discussion

In the current study we demonstrate that coexpression of HO-2 and BVR protein constructs that are fused with complementary halves of a split fluorophore results in fluorescence reassembly in both *E. coli* and mammalian cells. Co-expression of HO-2/BVR GFPR constructs results in robust fluorescence in *E. coli*. Furthermore, the expression of the HO-2/BVR GFPR complex displays a diffuse pattern throughout the cell (Figure A.2*A*) . In *E. coli*, the expression of some exogenous proteins can result in the aggregation of proteins in inclusion bodies that could drive the reassembly of the GFP fragments independent of HO-2 and BVR. Fluorescent proteins that are aggregated in inclusion bodies, however, typically display a highly localized and punctate distribution in the bacterium (20,21). The diffuse distribution of the HO-2/BVR GFPR signal suggests that reassembly is not driven by the aggregation of HO-2 and BVR in inclusion bodies (Figure A.2*A*).

The subcellular localization of the HO-2/BVR BiFC signal in mammalian cells is consistent with the expected diffuse (likely cytosolic) subcellular localization of HO-2(tn), which lacks the membrane spanning region, and localization of membrane-bound HO-2(FL) at the ER. BVR is predominantly present in the cytosol (22). These data demonstrate that the subcellular localization of HO-2 drives the localization of the BiFC complex.

These results demonstrate that BVR is capable of binding both soluble and membrane bound HO-2 in the mammalian cell and lacks a strict requirement for the HO-2 membrane spanning region or for the C-terminal cysteines of BVR for formation of the HO-2/BVR BiFC complex (Figure A.6 and Figure A.8).

Considering the high homology of HO-1 and HO-2 (55% identity and 76% similarity), the ability of HO-2 and BVR to form GFPR and BiFC complexes is consistent with reports that BVR binds HO-1 and may reflect a physiologically relevant event (2-4). However, split fluorophores can posses the ability to reassemble independent of the fusion binding partners (e.g. HO-2 and BVR) (11). To determine the degree of specificity for the BiFC reassembly, a binding interface for HO-2 and BVR must be identified. Disruption of the HO-2/BVR interface (e.g. mutagenesis), and subsequent loss of BiFC signal would support that the BiFC fluorescence observed in the current study is driven by HO-2/BVR binding rather than fluorophore reassembly. While various requirements for HO-2/BVR BiFC complex formation were tested (the HO-2 membrane spanning region, BVR C-terminal cysteines), these conditions did not markedly affect BiFC signal and are not required for the fluorescence observed. Additional mutations, such as truncation of the BVR C-terminus, could provide insight into the specificity of the HO-2/BVR BiFC complex; whether it reflects a physiologic complex between HO-2 and BVR, and if so, what the interface of that complex might be.

In vitro studies to identify the HO-2/BVR interface, described in Chapter 2 of this thesis (Spencer *et al*, in press) have been conducted with the hopes that the results might clarify a mutagenesis scheme to test the specificity of the HO-2/BVR BiFC complex. However, NMR binding studies suggest that BVR binds HO-2 with considerably weaker affinity than what was expected according to published results, and fail to identify an interface for the two enzymes. In fact, in the absence of an

irreversible step such as chemical cross-linking or fluorescent reassembly, we are unable to detect an HO-2/BVR complex. In light of these results, while the cellular context of HO-2 and BVR may promote complex formation, it is also possible that the fluorescent reassembly methods are trapping an extremely weak or transient event that may or may not have physiologic relevance.

A.6 Future directions

While at this time the existence and nature if the HO-2/BVR complex is unresolved, this work demonstrates HO-2 BiFC fusion proteins are capable of forming BiFC complexes with other BiFC fusion proteins (BVR) and this system could be used to address HO-2 protein interactions with additional proteins of the HO pathway, such as CPR. Both soluble and full-length HO-1 are reported to bind CPR, the electron transfer partner required for HO activity. Methods such as mutagenesis, lysine acetylation protection assays and crystallography have been used to define an interface for the HO-1/CPR complex (2-5,8,17,23). We have identified and characterized an HO-2/CPR complex that is similar to what is described for HO-1 and CPR (see Chapter 2 of this thesis; Spencer *et al*, in press). Furthermore, the C-terminal membrane-spanning region of HO-1 (and HO-2) is thought to facilitate HO/CPR binding (7,8).

Also, in Chapter 2 of this thesis we use NMR and gel filtration methods to determine that soluble HO-2 exits as homodimer, however the physiologic relevance of the HO-2 homodimer is unknown. The crystal structure of the HO-2 homodimer has also been determined (24). The BiFC method could be used to determine if HO-2 forms a homodimer in cells and provide insight into the physiologic relevance of the HO-2 dimer.

The BiFC method represents a powerful tool that could provide information regarding the molecular and cellular requirements for HO-2 protein-protein interactions in the cell. Additionally, a tripartite complex between HO, CPR, and BVR has been proposed (25). A multicolor BiFC system has been used to study protein-protein interactions among multiple proteins, such as the transcription factors MIX, MAD and MAX, and could be used to interrogate interactions of HO-2, CPR and BVR in their native context of the cell (26).

A.7 References

1. Ishikawa, K., Matera, K. M., Zhou, H., Fujii, H., Sato, M., Yoshimura, T., Ikeda-Saito, M., and Yoshida, T. (1998) Identification of histidine 45 as the axial heme iron ligand of heme oxygenase-2. *J. Biol. Chem.* 273, 4317-4322
2. Higashimoto, Y., Sakamoto, H., Hayashi, S., Sugishima, M., Fukuyama, K., Palmer, G., and Noguchi, M. (2005) Involvement of NADPH in the interaction between heme oxygenase-1 and cytochrome P450 reductase. *J. Biol. Chem.* 280, 729-737
3. Higashimoto, Y., Sugishima, M., Sato, H., Sakamoto, H., Fukuyama, K., Palmer, G., and Noguchi, M. (2008) Mass spectrometric identification of lysine residues of heme oxygenase-1 that are involved in its interaction with NADPH-cytochrome P450 reductase. *Biochem Biophys Res Commun* 367, 852-858
4. Wang, J., and de Montellano, P. R. (2003) The binding sites on human heme oxygenase-1 for cytochrome p450 reductase and biliverdin reductase. *J. Biol. Chem.* 278, 20069-20076
5. Sugishima, M., Sato, H., Higashimoto, Y., Harada, J., Wada, K., Fukuyama, K., and Noguchi, M. (2014) Structural basis for the electron transfer from an open form of NADPH-cytochrome P450 oxidoreductase to heme oxygenase. *Proc Natl Acad Sci U S A* 111, 2524-2529
6. Liu, Y., and Ortiz de Montellano, P. R. (2000) Reaction intermediates and single turnover rate constants for the oxidation of heme by human heme oxygenase-1. *J. Biol. Chem.* 275, 5297-5307
7. Huber Iii, W. J., Scruggs, B. A., and Backes, W. L. (2009) C-Terminal membrane spanning region of human heme oxygenase-1 mediates a time-dependent complex formation with cytochrome P450 reductase. *Biochemistry* 48, 190-197
8. Linnenbaum, M., Busker, M., Kraehling, J. R., and Behrends, S. Heme oxygenase isoforms differ in their subcellular trafficking during hypoxia and are differentially modulated by cytochrome P450 reductase. *PLoS One* 7, e35483
9. Wilson, C. G., Magliery, T. J., and Regan, L. (2004) Detecting protein-protein interactions with GFP-fragment reassembly. *Nat Methods* 1, 255-262
10. Hu, C. D., and Kerppola, T. K. (2003) Simultaneous visualization of multiple protein interactions in living cells using multicolor fluorescence complementation analysis. *Nat Biotechnol* 21, 539-545
11. Kerppola, T. K. (2006) Design and implementation of bimolecular fluorescence complementation (BiFC) assays for the visualization of protein interactions in living cells. *Nat Protoc* 1, 1278-1286
12. Shyu, Y. J., Liu, H., Deng, X., and Hu, C. D. (2006) Identification of new fluorescent protein fragments for bimolecular fluorescence complementation analysis under physiological conditions. *Biotechniques* 40, 61-66
13. Robida, A. M., and Kerppola, T. K. (2009) Bimolecular fluorescence complementation analysis of inducible protein interactions: effects of factors affecting protein folding on fluorescent protein fragment association. *J Mol Biol* 394, 391-409
14. Bolte, S., and Cordelieres, F. P. (2006) A guided tour into subcellular colocalization analysis in light microscopy. *J Microsc* 224, 213-232

15. Sambrook, J., and Russell, D. (2001) *Molecular Cloning: a Laboratory Manual,* 3rd Ed., Cold Spring Harbor Laboratory, Cold Spring Harbor, NY.
16. Yi, L., Jenkins, P. M., Leichert, L. I., Jakob, U., Martens, J. R., and Ragsdale, S. W. (2009) Heme regulatory motifs in heme oxygenase-2 form a thiol/disulfide redox switch that responds to the cellular redox state. *J. Biol. Chem.* 284, 20556-20561
17. Huber, W. J., 3rd, Marohnic, C. C., Peters, M., Alam, J., Reed, J. R., Masters, B. S., and Backes, W. L. (2009) Measurement of membrane-bound human heme oxygenase-1 activity using a chemically defined assay system. *Drug Metab Dispos* 37, 857-864
18. Magliery, T. J., Wilson, C. G., Pan, W., Mishler, D., Ghosh, I., Hamilton, A. D., and Regan, L. (2005) Detecting protein-protein interactions with a green fluorescent protein fragment reassembly trap: scope and mechanism. *J Am Chem Soc* 127, 146-157
19. Ghosh, H., Regan. (2000) Antiparallel Leucine Zipper-Directed Protein Reassembly: Application to the Green Fluorescent Protein. *J. Am. Chem. Soc.* 122, 5658-5659
20. Garcia-Fruitos, E., Gonzalez-Montalban, N., Morell, M., Vera, A., Ferraz, R. M., Aris, A., Ventura, S., and Villaverde, A. (2005) Aggregation as bacterial inclusion bodies does not imply inactivation of enzymes and fluorescent proteins. *Microbial cell factories* 4, 27
21. Raghunathan, G., Munussami, G., Moon, H., Paik, H. J., An, S. S., Kim, Y. S., Kang, S., and Lee, S. G. (2014) A variant of green fluorescent protein exclusively deposited to active intracellular inclusion bodies. *Microbial cell factories* 13, 68
22. Kikuchi, A., Park, S. Y., Miyatake, H., Sun, D., Sato, M., Yoshida, T., and Shiro, Y. (2001) Crystal structure of rat biliverdin reductase. *Nat Struct Biol* 8, 221-225
23. Huber, W. J., 3rd, and Backes, W. L. (2007) Expression and characterization of full-length human heme oxygenase-1: the presence of intact membrane-binding region leads to increased binding affinity for NADPH cytochrome P450 reductase. *Biochemistry* 46, 12212-12219
24. Bianchetti, C. M., Yi, L., Ragsdale, S. W., and Phillips, G. N., Jr. (2007) Comparison of apo- and heme-bound crystal structures of a truncated human heme oxygenase-2. *J. Biol. Chem.* 282, 37624-37631
25. Yoshinaga, T., Sassa, S., and Kappas, A. (1982) The occurrence of molecular interactions among NADPH-cytochrome c reductase, heme oxygenase, and biliverdin reductase in heme degradation. *J. Biol. Chem.* 257, 7786-7793
26. Grinberg, A. V., Hu, C. D., and Kerppola, T. K. (2004) Visualization of Myc/Max/Mad family dimers and the competition for dimerization in living cells. *Mol Cell Biol* 24, 4294-4308